©2019

Atreju Ian Lackey

THE ROLE OF ENTEROCYTE FATTY ACID-BINDING PROTEINS IN THE INTESTINE AND
WHOLE-BODY ENERGY HOMEOSTASIS

By

ATREJU IAN LACKEY

A dissertation submitted to the

School of Graduate Studies

Rutgers, The State University of New Jersey

In partial fulfillment of the requirements

For the degree of

Doctor of Philosophy

Graduate Program in Nutritional Sciences

Written under the direction of

Dr. Judith Storch

And approved by

_____

_____

_____

_____

_____

New Brunswick, New Jersey

October, 2019

ABSTRACT OF THE DISSERTATION

The Role of Enterocyte Fatty Acid-Binding Proteins in the Intestine and Whole-Body Energy

Homeostasis

By Atreju Ian Lackey

Dissertation Director:

Dr. Judith Storch

The fatty acid binding protein (FABP) family consists of 14-15 kDa cytoplasmic proteins which are

abundantly expressed in various mammalian tissues. In the proximal small intestinal enterocyte,

at least three FABPs are highly expressed: liver FABP (LFABP; FABP1), which is also expressed

in the liver, intestinal FABP (IFABP; FABP2), which is only expressed in the small intestine, and

cellular retinoid binding protein 2 (CRBP2), which is also only expressed in the small intestine.

Previous studies in high fat (HF) fed mice null for either LFABP or IFABP revealed a divergent

phenotype, with LFABP$^{-/-}$ mice displaying a metabolically healthy obese (MHO) phenotype, while

IFABP$^{-/-}$ mice remained lean. Conditional knock out LFABP mice (LFABP-cKO) were generated

to assess what role intestinal-LFABP may have in the MHO phenotype. Like HF fed whole-body

LFABP$^{-/-}$ mice, intestine-specific LFABP$^{-/-}$ (LFABP$^{int-/-}$) were found to have better capacity for

endurance exercise when compared to their wild-type (WT) "floxed" controls (LFABP$^{fl/fl}$).

Additionally, female LFABP$^{int-/-}$ were found to be more obese after the HF feeding challenge,

having greater BW gain and increased fat mass. Thus, the ablation of intestine-specific ablation

of LFABP is enough to induce the MHO phenotype in female mice, and improved exercise

capacity in male and female mice. To assess the intestinal phenotypic changes that might explain

their lean phenotype, HF feeding studies were performed in IFABP$^{-/-}$ mice. Additionally, as it was observed that HF fed IFABP$^{-/-}$ mice had a more fragile small intestine, we hypothesized that the ablation of IFABP may result in alterations in intestinal morphology and structure. IFABP$^{-/-}$ mice were found to have reduced energy absorption, taking in fewer calories while excreting the same amount of calories as their WT counterparts. Additionally, IFABP$^{-/-}$ mice had more rapid intestinal transit, partly explaining the reduction in energy absorption. IFABP$^{-/-}$ mice were observed to have a shortened average villus length, a thinner muscularis layer, reduced goblet cell density, and reduced Paneth cell abundance. The ablation of IFABP also resulted in alterations in tissue retinoid levels, and mucosal vitamin A-related gene expression. Although IFABP$^{-/-}$ mice were found to have a drastic reduction in mucosal CRBP2 gene expression, no changes were observed in CRBP2 protein abundance. Taken together, this work has demonstrated a role for enterocyte lipid binding proteins in efficient uptake and trafficking of not only dietary lipid, but nutrients in general. These studies have also revealed a role for the enterocyte FABPs in modulating intestinal physiology, intestinal morphology, and the whole-body ramifications of such alterations.

Acknowledgements

Table of Contents

Page

List of Tables

List of Figures

Appendix

List of Abbreviations

2-AG	2-arachidinoylglycerol
5-HT	5-hydroxytryptamine
ACSL	Long chain acyl-CoA synthetase
AEA	Anandamide
AFABP	Adipocyte fatty acid binding protein
AJ	Adheren junction
ATF	Activating transcription factor
AUC	Area under the curve
BBM	Brushborder membrane
BLM	Basolateral membrane
BrdU	Bromodeoxyuridine
BW	Body weight
Cas	CRSIPR-associated
CB1R	Cannabinoid receptor 1
CBC	Crypt base columnar
CBR	Cannabinoid receptor
CCK	Cholecystokinin
CD36	Cluster of differentiation 36
CDH1	Cadherin 1
Chop	CCAAT-enhancer-binding protein homologous protein
cKO	Conditional knock out
CLDN	Claudin

CNS	Central nervous system
COX	Cyclooxygenase
CRBP	Cellular retinol binding protein
CRBP2	Cellular retinol binding protein 2
CRISPR	Clustered regulatory interspaced short palindromic repeats
CVD	Cardiovascular disease
DG	Diacylglycerol
DGAT	Diacylglycerol acyltransferase
DIO	Diet induced obesity
DNA	Deoxyribonucleic acid
DSB	Double strand breaks
EC	Endocannabinoid
ECS	Endocannabinoid system
eIF2	Eukaryotic initiation factor
ER	Endoplasmic reticulum
FA	Fatty acid
FAAH	Fatty acid amide hydrolase
FABP	Fatty acid binding protein
FABPpm	Plasma membrane fatty acid binding protein
FAT	Fatty acid translocase
FATP	Fatty acid transport protein
FITC	Fluorescein isothiocyanate
GI	Gastrointestinal
GIP	Gastric inhibitory peptide
GLP	Glucagon-like peptide

GPAT	Glycerol-3-phosphase acyl transferase
GPCR	G-protein coupled receptor
GTT	Glucose tolerance test
H&E	hematoxylin and eosin
HF	High fat
HFABP	Heart fatty acid binding protein
HFD	High fat diet
HNF	Hepatic nuclear factor
HPLC	High performance liquid chromatography
IFABP	Intestinal fatty acid binding protein
IHC	Immunohistochemistry
ILBP	Ileal fatty acid binding protein
IMTG	Intramuscular triacylglycerol
iNOS	Inducible nitric oxide synthetase
JAMA	Junctional adhesion molecule A
KFABP	Keratinocyte fatty acid binding protein
KO	Knock out
LCFA	Long chain fatty acid
LF	Low fat
LFABP	Liver fatty acid binding protein
LFD	Low fat diet
LPS	Lipopolysaccharide
LRAT	Lecithin retinol acyltransferase
LRC	Label retaining cell
MCP1	Monocyte chemoattractant protein 1

MG	Monoacylglycerol
MGAT	Monoacylglycerol acyl transferase
MGL	Monoacylglycerol lipase
MHO	Metabolically healthy obese
MUC	Mucin
NAE	N-acylethanolamine
NAFLD	Non-alcoholic fatty liver disease
NHR	Nuclear hormone receptor
OEA	Oleoylethanolamide
PAM	Protospacer adjacent motif
PAS	Periodic acid-Schiff
PCR	Polymerase chain reaction
PCTV	Prechylomicron transport vesicles
PFA	paraformaldehyde
pIF	Purified IFABP
PL	Phospholipids
pLF	Purified LFABP
PPAR	Peroxisome proliferator-activated receptor
PPRE	Peroxisome proliferator response element
PYY	Peptide tyrosine tyrosine
RAR	Retinoic acid receptor
RER	Respiratory exchange ratio
RNA	Ribonucleic acid
ROS	Reactive oxygen species
RXR	Retinoid X receptor

SCFA	Short chain fatty acid
SEM	Standard error of the mean
SFA	Saturated fatty acid
sgRNA	Guide RNA
SR-B2	Scavenger receptor CD36
SREBP	Sterol regulatory element binding protein
ssDNA	Single strand DNA
T2DM	Type 2 diabetes mellitus
TBP	TATA-binding protein
TG	Triacylglycerol
TJ	Tight junction
UFA	Unsaturated fatty acid
UPR	Unfolded protein response
Vcre	Villin Cre
VLCFA	Very long chain fatty acid
VLDL	Very low density lipoprotein
VN	Vagus Nerve
WT	Wild-type
XBP1	X-box-binding protein1
Xbp1s	Spliced X-box-binding protein1
ZO1	Zonnula occludens 1

Chapter 1

Introduction and Review of the Literature

Introduction

Lipids are a broad class of biomolecules that are soluble in non-polar solvents [1]. This class of biomolecule includes, but is not limited to, fatty acids (FA), triglycerides (TG), cholesterol, fat-soluble vitamins, and phospholipids (PL). While they vary in numerous properties, such as hydrophobicity, they can all be extracted by organic solvents [1]. Such diversity allows for lipids to participate in an array of physiological processes, with lipids playing roles in energy storage, cell signaling, and the modulation of cellular structures via alterations is cell membranes [2]. In the context of human health, it is particularly important to point out that lipids are an important source of energy in the diet, since they have a higher caloric density (kcal per gram) when compared to carbohydrates and protein [3].

Obesity is a multifaceted disease that is characterized by excessive fat storage, and is often accompanied by metabolic dysfunction in multiple tissues [4]. In 2005 it was estimated that obesity and obesity-derived illnesses cost the United States 190.2 billion dollars, representing 20.6% of all medical expenses [5]. Data from the third National Health and Nutrition Examination Survey (NHANES III) has demonstrated that as of 2008 two thirds of US adults are considered overweight or obese [6]. Obesity is now considered to be the leading cause of preventable death around the world [7]. Dietary lipid quantity and quality have been found to be related to obesity and obesity-related comorbidities such as cardiovascular disease (CVD), type 2 diabetes mellitus (T2DM), and several types of cancer [8–10]. Dietary fat is important to human health, and its ingestion has downstream effects on metabolically active tissues, such as the liver and the gastrointestinal (GI) tract. Therefore, it is of integral importance to understand how dietary lipids are absorbed and processed by the human body, allowing for better informed attempts at nutritional and/or pharmacological interventions.

The overall aim of the research in this dissertation is to elucidate the function of the enterocyte fatty acid-binding proteins (FABPs), liver-FABP (LFABP or FABP1) and intestinal-FABP (IFABP),

in the small intestine. LFABP, which is also expressed in the liver, and IFABP, which is solely expressed in the small intestine, are members of the FABP family, a family of intracellular lipid binding proteins that have high affinities for FAs [11,12]. While these two proteins only share about 29% amino acid sequence homology, their tertiary structures are very similar and they are both highly expressed **(Fig 1-1)** [11]. However, it is unusual for proteins with identical functions to be expressed within the same cell type; thus, it is generally believed that LFABP and IFABP play different roles relating to intestinal lipid metabolism. In these studies, transgenic mice that do not express LFABP or IFABP in the intestine were used to help elucidate their individual functions.

A

Human LFABP (PDB: 2F73)

B

Human IFABP (PDB: 3IFB)
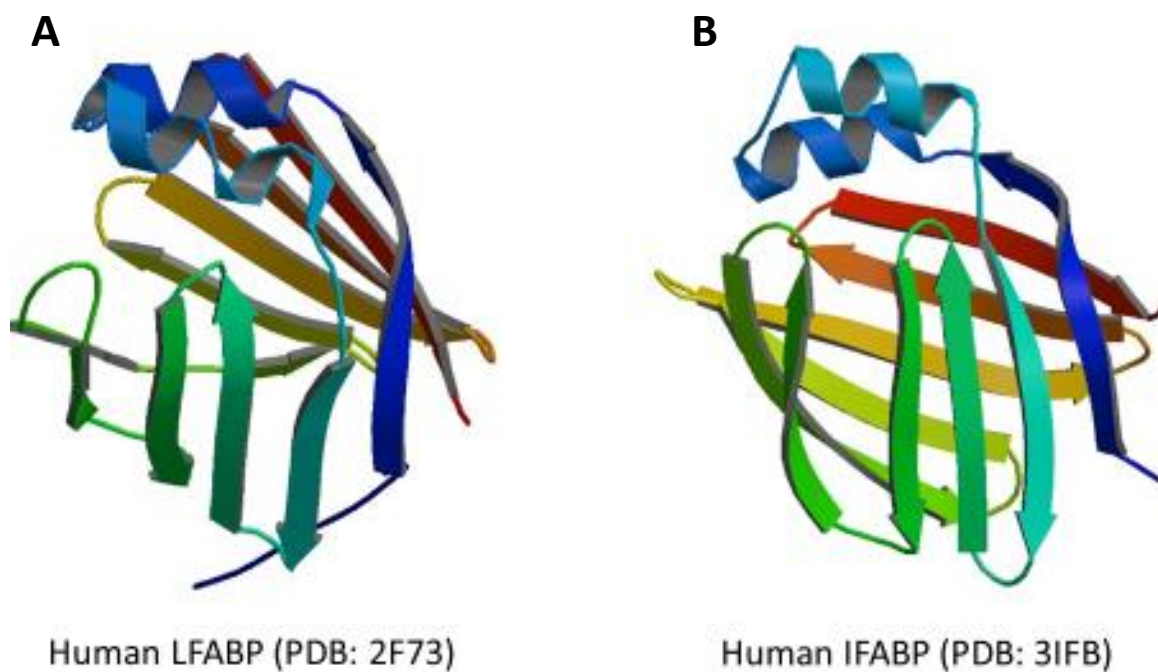
Figure 1-1: **LFABP and IFABP structure.** The ribbon diagrams of lowest-energy solutions structures for *A*, apo-LFABP [13] and *B*, apo-IFABP [14]. Tertiary structural features of the FABP family include 2 antiparallel β-helix sheets with 5 strands that form the "clam shell" ligand binding pocket.

Previously, comparative studies using IFABP^{-/-} and whole-body LFABP^{-/-} mice revealed only modest differences when mice were fed a chow diet [15]. However, subsequent studies performed using mice challenged with 45% Kcal high fat (HF) diets revealed dramatic whole-body phenotypic differences, with IFABP^{-/-} mice being resistant to diet induced obesity (DIO), while LFABP^{-/-} mice became more obese, but remained relatively healthy [16]. The present work involved the same HF feeding protocol. For the IFABP^{-/-} mice, phenotypic changes in the intestine that could alter whole-body phenotypes were assessed. Additionally, we developed a novel tissue-specific knock out strain of the LFABP^{-/-} mice, allowing us to assess how the ablation of LFABP specifically in the small intestine may lead to alterations at the whole-body level in response to a HF challenge. The overall goal of this work is to uncover the individual effects of these two highly expressed small intestinal FABPs that are similar in structure, but appear to have different functions. More specifically, it is of importance to understand the mechanisms of intracellular lipid assimilation and trafficking in the small intestine so that appropriate nutritional and/or pharmaceutical interventions can be developed to eliminate or ameliorate lipid-related chronic diseases, such as obesity, type 2 diabetes mellitus, and CVD. In the following introductory sections, an overview of lipid consumption, digestion, and absorption will be presented, with emphasis placed on the morphological and cellular structures of the small intestine. This will be followed by a review of the current knowledge about the FABP family, and the previous studies that assessed mice null for either LFABP or IFABP.

Dietary Triglycerides

In the United States, dietary lipid represents 32-37% of caloric intake in adults [17,18]. The main challenge related to the digestion and absorption of dietary lipid is that without modulation, they would be insoluble in the aqueous environment that they would encounter within the intestinal lumen and within the absorptive enterocytes. In order for the absorption of lipid to be efficient, the body has a complex set of mechanisms that that allow for dietary lipid to be processed, packaged,

and transported [19]. These processes are initiated in the stomach but continue in the small intestine. The efficient digestion of dietary lipid depends on the combination of enzymes, transport proteins, and bile acids that allow the non-polar and aqueous components to mix more readily.

While many types of lipids are present in the diet, triglycerides (TG) are the major source of dietary lipid, representing greater than 90% of the lipid consumed [20]. TGs consist of three FAs esterified to a glycerol backbone. In the human diet, that majority of TGs that are consumed are rich in long chain FAs (LCFA), which contain 14 or more carbons in the chain [19]. Additionally, the FAs that make up the TG molecule are either saturated FAs (SFA) or unsaturated FAs (UFA). Animal products, such as lard or butter, tend to be rich in SFAs, while plant oils, such as olive oil and soybean oil, are rich in UFAs. The United States and other Western populations are known to consume diets that are rich in saturated LCFAs, such as palmitate (C16:0) and stearate (C18:0). Chronic consumption of high levels of long chain SFAs has been linked to higher risk of cardiovascular disease (CVD), an obesity-related comorbidity that has had increasing prevalence in Western societies [21]. Conversely, diets rich in long chain UFAs, such as the Mediterranean diet, seem to be associated with a more healthy cardiovascular profile [22–24].

Digestion of Triglycerides

Most food components, including dietary lipid, are ingested in a form that is not readily available for use by the body. In order for the body to access these components, they need to be broken down into smaller components that can then be absorbed, assimilated, and moved into circulation [25]. The gastrointestinal (GI) tract is responsible for carrying out the functions of ingestion, digestion, and absorption. Components of the GI tract include the oral cavity, pharynx, esophagus, small intestine, large intestine, and rectum **(Fig 1-2A)** [26]. Additionally, accessory organs such as the liver, gallbladder, and pancreas provide secretions that are necessary for processing the nutrients within the GI tract [26]. Digestion of dietary TG beings in the stomach, where the mechanical mixing of the stomach contents, in the form of grinding and peristaltic

movement, helps to emulsify the lipids in the food bolus, forming chyme [1,19]. Some of the TG is hydrolyzed to diacylglycerol (DG) and FA via gastric lipase, an enzyme that is secreted by chief cells of the gastric mucosa [26,27]. While gastric lipase has an optimal pH of around 4, the enzyme is still active at pH 6 to 6.5, allowing this lipase to process TG as the chyme moves from the stomach, through the pyloric sphincter, and into the duodenum [27]. Overall, the digestion of dietary fat in the stomach is relatively limited, but the processing that occurs is integral to its subsequent digestion in the lumen of the small intestine.
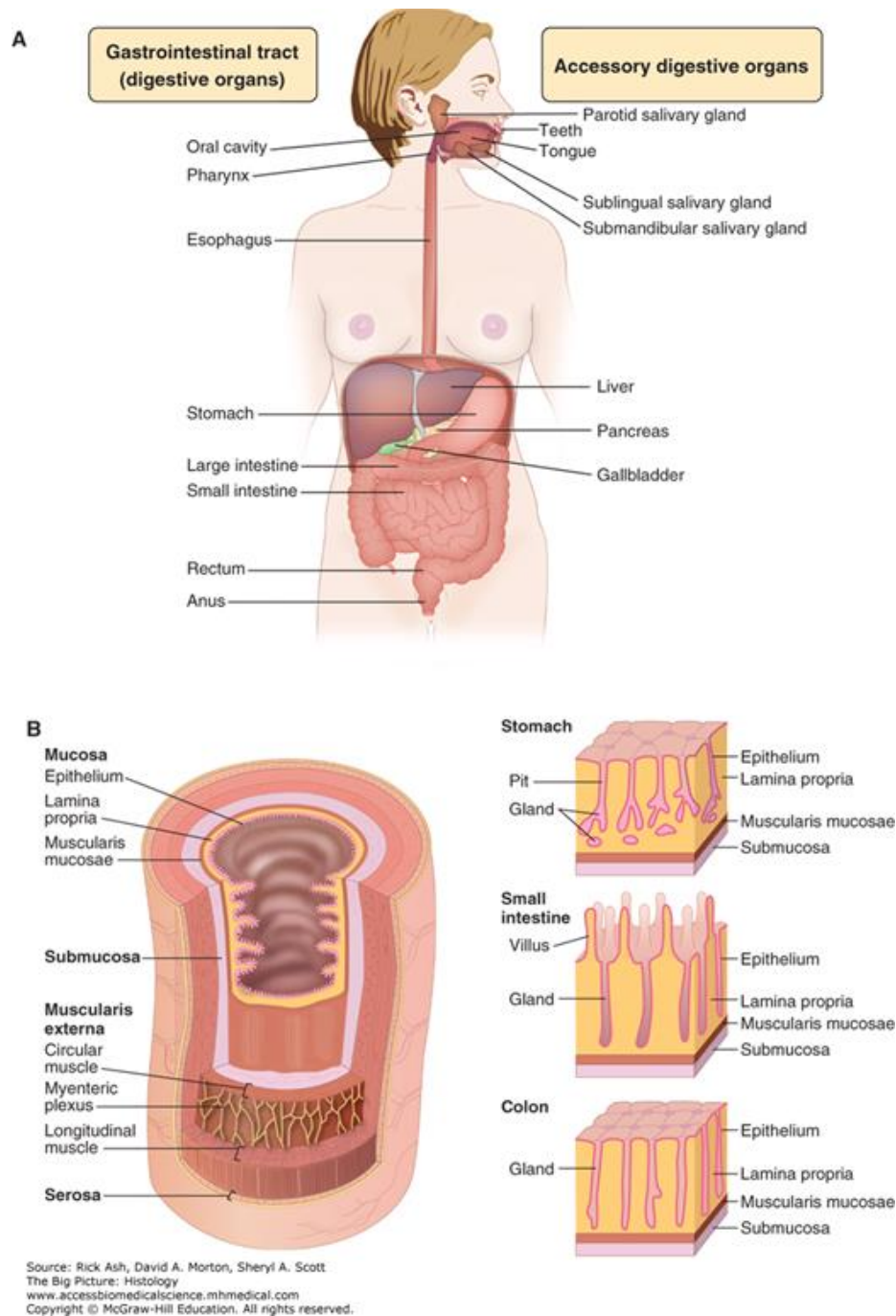
Figure 1-2: **Components and histological organization of gastrointestinal tract-related organs.** *A*, location of GI tract and accessory digestive organs. *B*, overall organization of the physiological layers of the organs for different regions of the GI tract. Adapted from Ash, Morton, and Scott [28]. Reprinted with permission from McGraw-Hill Education © 2013.

As the acidic chyme moves into the duodenum, it triggers the release alkaline secretions from the Brunner glands and bicarbonate-rich secretions from the pancreas, resulting in the neutralization of the gastric acid that the chyme has been exposed to [27]. The pancreas also secretes pancreatic lipase and colipase into the intestinal lumen, allowing pancreatic lipase to facilitate the hydrolysis of the remaining TG and DG in the chyme, forming 2-monoacylcerols (2-MG) and FAs [27]. For efficient absorption of the lipophilic MGs and FAs in the lumen to occur, these digestion products must be solubilized. Micellar solubilization by bile salts allows these lipid digestion products to cross the barrier that is present in the form of the "unstirred water layer" that surrounds the epithelial surface [27]. Bile salts are detergents that are synthesized in the liver and stored in the gallbladder. As the chyme initially moves into the duodenum, in addition to the pancreatic secretions and the secretions of the Brunner glands, bile, which contains bile salts, bilirubin, phospholipids, water, cholesterol, amino acids, and steroids is also secreted [29]. This combination of secretions allows for the emulsification of dietary lipids via micelle formation [30,31]. Once formed, these micellular lipid products are able to easily cross the unstirred water layer, resulting in significantly increased aqueous concentrations of FAs, MGs, and other lipid species [30].

Small Intestine Composition and Structure

In the GI tract, the small intestine is major site of dietary lipid absorption and assimilation. The small intestine of an adult human is about 500 to 700 cm in length, while the average mouse small intestine length is about 35 cm [26,32]. Starting at the pyloric sphincter and ending at the ileocecal valve, the small intestine forms a long tube that can be divided anatomically intro three sections: the duodenum, jejunum, and the ileum [1]. These regions vary in length, with the duodenum , jejunum, and ileum consisting of approximately 5, 38, and 57% of the total length, respectively [26]. There are no clear morphological distinctions between connecting sections. However, certain characteristics, such as the prevalence of certain cell types or size of specific morphological

structures, are gradually altered depending on the intestinal region. Lipid absorption primarily occurs in the jejunum, while bile acid reuptake mainly occurs in the ileum [27].

Like other regions of the GI tract, the small intestine contains several layers of cells. These layers include the mucosa, submucosa, muscularis, and serosa **(Fig 1-2B)** [26]. The mucosal layer contains cells that are integral for luminal nutrient absorption and modulation of immune function. The mucosa forms small finger-like folds, known as villi, which function to increase the surface area of the luminal nutrient contact for enhanced absorption. These villi are lined with a specialized type of epithelial cell called enterocytes, which are the most abundant cell type of the small intestine, and are primarily involved with the uptake and processing of dietary nutrients [33]. These villi are covered in small hair-like projections on the apical (lumen-facing) surface of the enterocyte called microvilli [26,33]. When magnified, these microvilli resemble the hairs of a paint brush, which has led to the apical surface of the enterocytes also being described as the "brush border membrane" [34]. The combination of the mucosal folds, villi, and microvilli leads to a small intestinal structure with a surface area that is about 600 times greater than that of a similar length simple cylinder, which enhances nutrient absorption [26].

In addition to enterocytes, the small intestinal mucosa contains several other types of cells **(Fig 1-3A)** [35]. An array of enteroendocrine cells are present throughout the GI tract, assisting with processes that involve nutrient sensing and alterations in intestinal motility **(Fig 1-3B)** [26,36]. Within the small intestine, some of the types of enteroendocrine cells that are present include I cells, S cells, M cells, and K cells; like many other intestinal epithelia cell types, the relative abundance of different cell types is influenced by the region of the small intestine [36]. The small intestinal epithelium also contains a secretory cell type, called goblet cells, which secrete mucus that acts as an initial defensive barrier, providing protection from physical and chemical challenges[37–41]. The mucus layer can be divided into two functional components: the top layer, or loosely adherent layer, which is able to trap bacteria and prevent them from interacting with the epithelium, and the

A
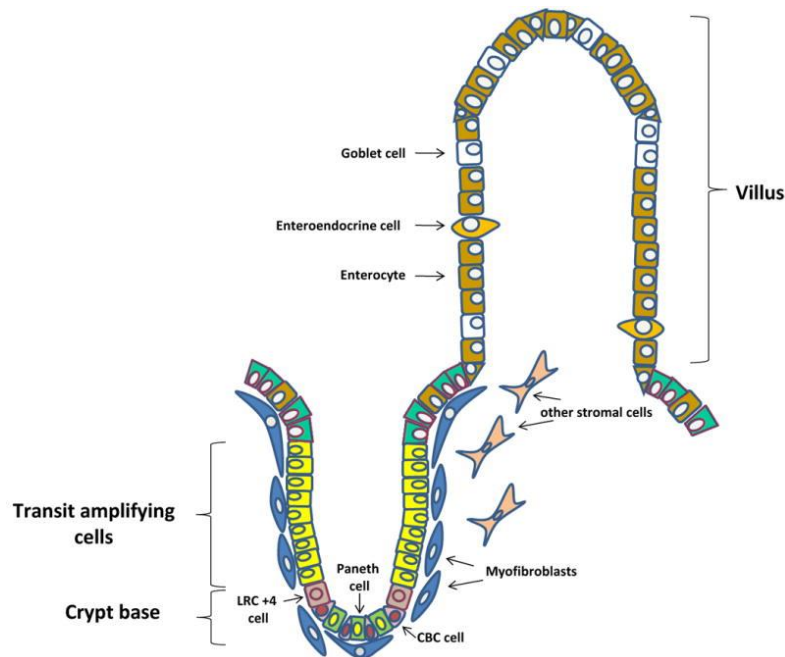
B
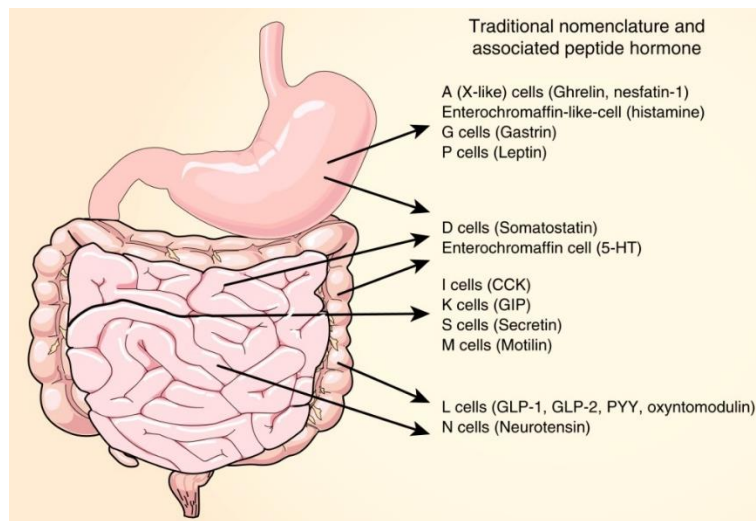
Figure 1-3: **Cells of the gastrointestinal tract that are present in the small intestine.** *A*, The intestinal crypt-villus axis. Stem cells in the crypt base give rise to transit amplifying cells. These cells differentiate into enterocytes, enteroendocrine cells, Paneth cells, and goblet cells. *LRC, label retaining cells; CBC Cell, crypt base columnar cell.* Graphic by Shaker and Rubin [35]. Adapted by permission from Elsevier: Translational Research © 2010. *B*, the enteroendocrine cell types of the GI tract, and the peptide hormones that each cell has been traditionally associated with. *5-HT, 5-hydroxytryptamine; CCK, Cholecystokinin; GIP, Gastric inhibitory polypeptide; GLP-1,*

Glucagon-like peptide-1; GLP-2, Glucagon-like peptide-2; PYY, Peptide tyrosine tyrosine. Graphic by Worthington, Reimann, and Gribble [36]. Adapted by permission from Springer Nature: Mucosal Immunology © 2018.

bottom layer, or firmly adherent layer, which provides structural support and provides a critical barrier for preventing bacterial adhesion to the epithelium[38,42,43]. The amount of goblet cells present in the small intestine increases from the duodenum to the ileum, and reaches maximal abundance in the distal colon [37].

The epithelial cells of the villi have a relatively rapid turnover period, with the average lifespan ranging from approximately 3 to 5 days [26,44]. As they age, these cells travel towards the tip of the villi, and are eventually sloughed off into the lumen [45]. In between villi, new epithelial cells are produced by stems cells located in the crypts [44]. Paneth cells, another hypersecretory cell type of the small intestine, are also located in the crypts, where the secrete antimicrobial peptides and proteins that influence cell differentiation [44]. Unlike the other cell types of the small intestine, Paneth cells appear to have a longer lifespan, lasting about 15 to 17 days [44].

The various cell types of the SI connect with one another by macromolecular protein structures that are called tight junctions (TJs) [46,47]. Several transmembrane proteins, such as claudins, occludins, and junctional adhesion molecules (JAMs) form TJs that can either induce the formation of tightening gate-like structures, or loosening pore-like structures [46,48–50]. The relative proportion and distribution of specific TJ proteins will influence whether a tighter or looser structure forms, which in turn will impact the overall permeability of the small intestine. A small intestine that has relatively high permeability can lead to the translocation of various bacterial products, such as lipopolysaccharide (LPS), which can then lead to chronic inflammation and tissue damage [48,50]. However, it is important for the small intestine to be at least semi-permeable, as this permeability allows for the paracellular uptake of small nutrients and water [51–53]. During the course of these studies it was observed that HF fed mice lacking IFABP appear to have an intestinal fragility phenotype, with the intestine breaking easily upon removal. It was hypothesized that the IFABP$^{-/-}$ mice may have alterations in intestinal permeability that could predispose their small intestine towards being more fragile. Thus, one of the aims of this work focuses on

assessing aspects intestinal morphology and physiology that might influence the durability of small intestinal tissue.

The basolateral side of the enterocytes more directly interacts with the other layers of the small intestine. In the submucosal region, the lymphatic capillaries transport the chylomicrons that have been formed by the enterocytes (to be discussed below), allowing for these TG-rich lipoproteins to be delivered into circulation [24,54]. The submucosal layer provides structural support, and access to the blood supply. Underneath the submucosal layer, the muscularis layer provides additional structural support, and plays an important role in the transit of nutrients [26]. Peristaltic contractions along with signaling from enteroendocrine cells have great influence over the muscular contractions that push the digesta forward [27]. The rate of the muscular contractions is important, since efficient uptake of dietary nutrients depends on how long the nutrients in the lumen are exposed to digestive enzymes. Below the muscularis layer is the serosal layer, which provides an additional layer of protection for the small intestine through secretions that lubricate its movement within the peritoneal cavity [26].

Enterocyte FA and MG Uptake

After the hydrolysis of a TG molecule in the intestinal lumen, two FAs and one 2-MG are present in the intestinal lumen. Unlike TG, these lipid species can be absorbed across the apical side of the intestinal enterocyte through transcellular processes. Yet, the exact mechanism of uptake of these lipids is not fully understood. It is known that the dietary lipid products can be taken up via passive diffusion, where the mixed micelles, containing the solubilized dietary lipid products, are thought to move dietary FAs and MGs through the unstirred water layer to the brush border membrane, for subsequent uptake [27]. This process, which depends on the concentration of intracellular FA and 2-MG remaining low when compared to luminal FA and 2-MG, is facilitated by the rapid intracellular re-esterification of these lipids back into TG [19,27]. Although passive diffusion of dietary lipid products is known to occur, kinetic studies have shown that the uptake of

FA is saturable, which supports the involvement of transport proteins [55,56]. However, uptake of FA can still occur after proteolytic treatment of the brush border membrane, which also supports a role for passive diffusion as well [27,55–58].

Enterocyte processing of FA depends on the site of entry, with exogenous FAs entering from the apical side, while endogenous FA enters from the basolateral side [59]. Though both sides of the enterocyte express membrane bound transport proteins that are thought to be involved in FA uptake, it is important to note that intestinal lumen free FA concentration is estimated to be in the low micromolar (µM) range [56,60], while estimated concentration in circulation is proposed to be in the low nanomolar (nM) range [61]. This difference in luminal FA versus FA in circulation concentrations indicates that the relative contribution of FA transporters to total FA uptake *in vivo* is likely to be relatively small compared to their contribution to FA uptake in other tissues [55,57]. Instead, bulk uptake of apical FA likely occurs through passive diffusion, while FA transporters likely play a more important role in the uptake of basolateral FA and/or nutrient sensing [19,55,58].

There have been several proteins that have an affinity for binding FA that are thought to play a role in the carrier-mediated uptake of dietary FA. Initially fatty acid transport protein 4 (FATP4) was thought to play a role in apical FA uptake [62,63]. However, it was observed that FATP4 is localized to the endoplasmic reticulum (ER), and functions to catalyze the conversion of FA into fatty acyl CoAs [57,62,63]. Additionally, FATP4-null mice do not develop steatorrhea, and do not have reduced intestinal FA uptake, further suggesting that this protein does not play a large role in the efficient uptake of dietary FA [62].

Cluster of Differentiation 36 (CD36), also known as scavenger receptor CD36 (SR-B2) and FA translocase (FAT), is another enterocyte membrane protein that is thought to play a role in dietary FA uptake. Scavenger receptors are membrane proteins that are characterized by being able to recognize similar molecular patterns in their ligands, rather than a specific epitope [58]. CD36 is highly expressed in throughout the small intestine, though its expression is highest in the most

proximal portion, where the bulk of dietary lipid uptake occurs [57,64]. While its relative contribution to FA uptake in the small intestine is thought to be relatively low, CD36 meditated uptake of FA exerts a regulatory effect, inducing increased chylomicron production and increased secretions from enteroendocrine cells [65,66]. Aside from very long chain FA (VLCFA), which have carbon chains that are greater than or equal to 22 carbons in length, CD36^{-/-} mice do not appear to malabsorb dietary lipid [65,67]. However, in response to high fat (HF) feeding, CD36^{-/-} mice appear to have a shift in the region of lipid absorption, with more lipid being taken up in the more distal regions of the small intestine [65–67]. Thus, intestinal CD36 does not appear to be necessary for bulk uptake of dietary lipid, but rather acts as a lipid sensor in the proximal portion of the small intestine, regulating the enteroendocrine cell responses to various types of lipid challenges while also modifying chylomicron production in enterocytes [58,65].

Other putative FA transport proteins are highly expressed in the small intestine, though relative to CD36, less work has been performed to examine their influence on luminal FA uptake. The scavenger receptor class B type 1 (SR-B1) is another member of the CD36 family this is abundantly expressed in the small intestine [68,69]. Like CD36^{-/-} mice, SR-B1^{-/-} mice do not have reduced intestinal FA absorption [67]. The small intestine also expresses the plasma membrane FA binding protein (FABPpm), and antibody inhibition of this protein has been shown to lead to reduced uptake of FA *in vitro* [58]. While no additional work has examined its role in intestinal FA uptake, other studies using skeletal muscle have revealed that FABPpm plays an important role in response to physiological states in which skeletal muscle is actively taking up plasma FA, such as fasting or endurance exercise [70,71].

Similar to FAs, 2-MGs are also hypothesized to be taken up into the enterocyte through both passive diffusion and active transport mechanisms. Just like FAs, *in vitro* studies using Caco-2 cells revealed that uptake of MG is saturable [55,56]. Interestingly, the addition of excess FA, but not

DG, to the medium of Caco-2 cells led to reduced uptake of 2-MG, suggesting that the same transport proteins may be involved in the uptake of both FA and 2-MG into the enterocyte [55,72].

Intestinal Lipid Processing

One of the main tasks of enterocytes is to process dietary lipids to be packaged and eventually exported to other tissues for use, meaning that enterocytes are periodically and consistently exposed to lipid challenges that many other cell types would not normally be exposed to. Additionally, inside of the enterocyte, like other cell types, the excessive buildup of FA can induced cytotoxicity [73–75]. Thus, the cell must process the FAs in order to prevent their accumulation as well as to provide lipid substrates to other tissues. Dietary FAs and 2-MGs are mainly reconstituted back into TG. First, FAs must be activated by being converted into fatty acyl CoA. This reaction is catalyzed by acyl-CoA synthetase long chain family members 3 and 5 (ACSL3, ACSL5) [76], or FATP4 [77]. The formation of fatty acyl-CoA from FA ensures that the concertation gradient favors the continued uptake of FA from the lumen into the enterocyte. After activation, fatty acyl-CoA is able to be incorporated into TGs. These TGs are primary packaged into large ApoB48-containing lipoprotein particles called chylomicrons, which are subsequently secreted from the basolateral side of the enterocyte into the lymph, and then eventually to the general circulation [24,54].

In enterocytes, TG synthesis can occur via 2 different pathways. The predominant pathway uses monoacylglycerol acyl transferase-2 (MGAT2), which is located in the ER, to catalyze the acylation of MGs into DGs [78]. The resultant DG can be further acylated by diacylglycerol acyl transferase (DGAT) to reform TG [79,80]. Unlike other tissues, due to the high abundance of MGs formed from dietary TG in the intestinal lumen, the MGAT pathway is the predominant route for TG formation in the intestinal enterocyte, accounting for approximately 75% of the TG that is synthesized [80–82].
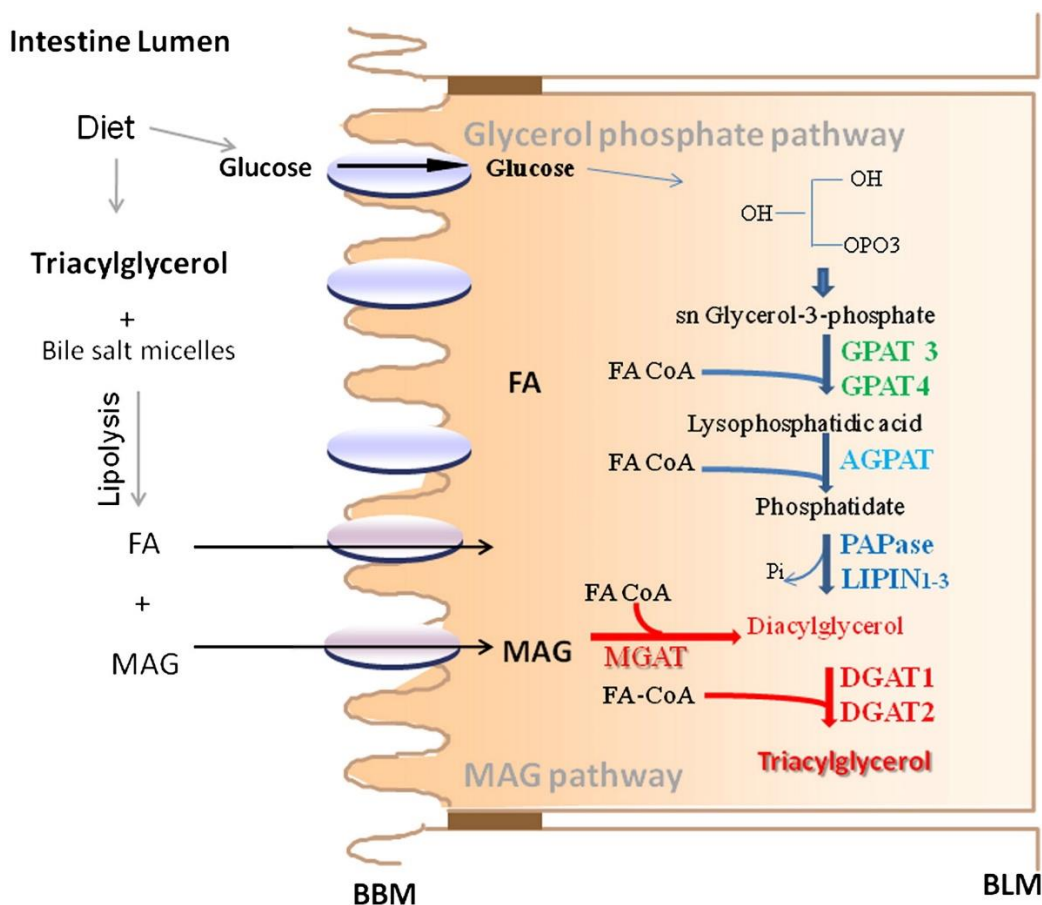
Figure 1-4: **Uptake and re-esterification of dietary FA and MG in the intestinal enterocyte.** In the lumen, TGs are hydrolyzed by lipases, forming FAs and 2-MGs. Re-esterification of FAs and MGs primary occurs via the MGAT pathway, though GPAT pathway is alternative route for TG synthesis. FA; Fatty acid; FA CoA, Fatty acid acyl coenzyme A; GPAT, glycerol-3-phosphate acyltransferase; AGPAT, 1-acylglycerol-3-phosphate acyltransferase.; PAPase, phosphatidic acid phosphatase, MGAT, Acyl-CoA:monoacylglycerol acyl transferase-2; DGAT, diacylglycerol acyltransferase; MAG, monoacylglycerol, BBM, brushborder membrane; BLM, basolateral membane. Figure from Pan and Hussein [83]. Adapted by permission from Elsevier: Biochimica et Biophysica Acta © 2012.

When there is low MG available, an alternative pathway for TG synthesis, known as the glycerol-3-phosphate acyl transferase (GPAT) pathway exists [84,85]. This pathway involves the acylation of glycerol 3-phosphate to form phosphatidic acid, which is subsequently hydrolyzed to release inorganic phosphate and form DG [84]. This DG can then be esterified by DGAT to form TG.

In the enterocyte, in addition to being used for TG synthesis and subsequent release into circulation in the form of chylomicrons, FAs and MGs can be utilized for other cellular functions. Some FAs and 2-MGs that are reincorporated into TGs can be stored in intracellular lipid droplets for future use [86–88]. Fatty acyl-CoAs formed from FA can also be incorporated into membrane phospholipids, with the type of acyl chain that is incorporated having an influence on various membrane properties [89,90]. FAs may also be used by the mitochondria or peroxisomes for oxidation, though this process does not represent a major component FA use in enterocytes. Additionally, FAs and MGs can play roles in the regulation of gene expression and cell signaling by servings as ligands for nuclear hormone receptors (NHRs) and G-protein coupled receptors (GPCRs) [91–93].

Lipid Sensing and Signaling in the Intestine

In addition to being the major site of dietary lipid absorption, the small intestine also plays an important role in nutrient sensing. Throughout the small intestine enteroendocrine cells are present, secreting important peptide hormones in response to the presence or lack of specific nutrients, leading to the alteration of GI enzyme secretion, motility, and satiety [94–98]. Enteroendocrine cells only comprise about one percent of the epithelial cells that line the gut, but when taken together, they form the largest endocrine organ system [36,97]. In response to stimulation from luminal nutrients enteroendocrine cells secrete an array of peptide hormones, including glucagon-like peptide 1 and 2 (GLP-1, GLP2), cholecystokinin (CCK), peptide tyrosine tyrosine (PYY), and leptin [36,97]. Historically it was hypothesized that specific differentiated enteroendocrine

cells were specialized, being mainly responsible for secreting individual peptide hormones for specific biological functions. For example, I cells were thought to only secrete CCK, a peptide hormone that is responsible for inducing gall bladder contraction and the secretion of pancreatic enzymes [99,100]. Likewise, K cells were thought to secrete GIP, stimulating insulin secretion, while M cells were shown to secrete motilin, a hormone responsible for inducing gastric movement [97,101]. Enterochromaffin cells secrete 5-hydroxytryptamine (5-HT), which in turn can modulate appetite and increase GI motility [36,97]. D cells and S cells secrete somatostatin and secretin, respectively, leading to reduced pancreatic secretion reduced secretion of gastric acid [36,97]. While the dogma has been that one type of enteroendocrine cell secretes a specific peptide hormone, more recent *in vitro* and *in vivo* studies have revealed that specific enteroendocrine cells are able to secrete an array of peptide hormone types, and that the relative abundance of hormones that are secreted, now referred to as the enteroendocrine "secretome", is likely to be based on tissue location rather than specific cell lineage [99,102–104]. Indeed, ileal and colonic L cells have been shown to secrete GLP-1, GLP-2, and PYY, which in turn, can modulate food intake, GI motility, and insulin secretion [36,97,104,105]. Interestingly, mice that lack neurogenin 3 specifically in the intestine, which leads to elimination of all enteroendocrine cell subtypes, experience reduced lipid absorption and reduced weight gain, demonstrating that enteroendocrine cells are necessary for the efficient uptake of dietary lipid [106].

The vagus nerve (VN) plays an integral role in the bidirectional communication that occurs between the central nervous system (CNS) and the GI tract. In the intestine, the afferent endings of the VN express receptors that bind the gut peptide hormones that are released from enteroendocrine cells of the GI tract [107]. For example, ghrelin stimulates increased food intake by inhibiting vagal afferent firing [107]. Exogenous administration of ghrelin to rodents acutely stimulates increased food intake, while rodents that have undergone a vagotomy do not respond to ghrelin administration [107]. Vagal tone can be altered by chronic nutritional challenges, with

components of the enteroendocrine cell secretome being modulated by alterations in food intake and body composition [108,109]. Thus, altered vagal tone is commonly observed in chronic metabolic diseases such as obesity and type 2 diabetes mellitus [107].

In addition to the gut peptides secreted by the enteroendocrine cells, specific lipids can also act as signals to influence alterations in GI gene expression, appetite, and motility. This "message-modulator" function allows these lipids to amplify, diminish, or modify signals transmitted by other molecules [110]. N-acylethanolamines (NAEs) are a group of lipids that can be synthesized by the intestine, and they have been shown to influence food intake in response to a dietary lipid challenge [111]. Oleoylethanolamide (OEA) is a NAE that promotes satiety, and it can act as a potent agonist for the nuclear hormone receptor (NHR) peroxisome proliferator-activated receptor α (PPARα) [112,113]. Additionally, duodenal infusion of lipid, but not carbohydrates or protein, induces OEA mobilization, suggesting that OEA may be part of a negative feedback system that promotes reduced consumption of lipid [114].

Anandaminde (AEA) is an endocannabinoid (EC) that is also part of the NAE family of lipid signaling molecules. The EC system plays a critical role in energy homeostasis, including modulating food intake through a complex signaling system that is used by both the CNS and peripheral tissues [115]. The EC system consists of the EC agonists, 2-arachidinoylglycerol (2-AG) and AEA, the cannabinoid receptors (CBRs), and the synthetic and degradative enzymes that are responsible for EC anabolism and catabolism, respectively [115,116]. Increased levels of 2-AG and AEA can result in the overstimulation of the EC system via cannabinoid receptor 1 (CB1R) in both the CNS and peripheral tissues, promoting increased food intake [115–117]. In the VN, CB1R activation induced slower GI transit, while chemical inhibition or genetic silencing results in more rapid intestinal transit [118–120]. Chronic activation of the EC system in many organs and organ systems has been associated with obesity in both rodent models and humans [116,117,121,122]. Additionally, intestinal levels of 2-AG have been shown to increase in response to dietary lipids,

but not carbohydrates [123]. Taken together, these data support a vital role for intestinal lipids in the regulation of food intake and systemic energy balance in response to nutrient availability.

Fatty Acid Binding Proteins

Intracellular carrier proteins are thought to be required for the efficient trafficking of hydrophobic lipid species within the hydrophilic cytoplasmic milieu, although this has not been definitively shown. In the 1970s, members of the fatty acid-binding protein (FABP) family were initially identified as proteins within the cytosol that are able to bind FA [124,125]. These 14-15 kDa proteins have highly conserved tertiary structures, consisting of 10 β-strands that form a ligand binding barrel, and 2 small α-helices [12]. The FABP family consists of 9 FABPs and 4 cellular retinol-binding proteins (CRBPs). These FABPs are present in high abundance (~1-5% of total soluble protein) in the cytosol of most tissues, with some tissues expressing more than one type **(Table 1-1)** [126]. Interestingly the small intestine, a major site of lipid processing, expresses at least 4 members of the FABP family in high abundance, with the distribution of these proteins varying in different regions of the small intestine **(Figure 1-5)**.

Table 1-1: **The tissue location for the expression of FABP family members.** Adapted from Storch and Corsico [12], and Napoli [127].

FABP	Tissue Expression
Liver-FABP (FABP1)	Liver, **small intestine (jejunum>duodenum>>ileum)**, kidney
Intestine-FABP (FABP2)	**Small intestine (jejunum>ileum>duodenum)**
Heart-FABP (FABP3)	Cardiac muscle, skeletal muscle, brain, kidney, brown adipose tissue
Adipocyte-FABP (FABP4)	Adipocyte, macrophage, dendritic cell
Epidermal-FABP (FABP5)	Skin, esophagus, adipocyte, macrophage, dendritic cell, mammary gland, brain, kidney, lung, heart, skeletal muscle, testis, retina, lens, spleen
Ileal-FABP (FABP6)	**Small intestine (ileum)**
Brain-FABP (FABP7)	Brain, skin
Myelin-FABP (FABP8)	Peripheral nervous system
Testis-FABP (FABP9)	Testis, adipose tissue
Cellular Retinol Binding Protein 1	Most tissues
Cellular Retinol Binding Protein 2	**Small intestine (duodenum, jejunum > ileum)**

Though many members of the FABP family were initially shown to bind FA with high affinity, some members of the family also bind other hydrophobic ligands. Recently, it has been demonstrated that several FABPs are able to bind AEA and 2-AG [128,129]. It has been hypothesized that these FABPs act to enhance uptake and subsequent hydrolysis of these lipid species by their degradative enzymes, fatty acid amide hydrolase (FAAH) or monoacylglycerol lipase (MGL)[129–134]. Since it is known that AEA and 2-AG modulate food intake, it is possible that members of the FABP family may play an important role in the regulation and maintenance of energy balance.

Enterocyte FABPs

The intestinal enterocyte expresses at least two members of the FABP family simultaneously **(Fig 1-5A)**: liver-FABP (LFABP or FABP1), which is also expressed in the liver, and intestinal-FABP (IFABP or FABP2), which is solely expressed within the intestine [11,15,16]. While these proteins only share about 29% amino acid sequence homology, their tertiary structures are very similar. However, it is unusual for proteins with identical functions to be expressed within the same cell type; thus, it is generally believed that LFABP and IFABP play different roles relating to intestinal lipid metabolism. In humans, IFABP is less abundant than LFABP [135,136], while mice express similar levels of LFABP and IFABP within the SI mucosa [135–137].

In addition to LFABP and IFABP, the proximal small intestinal enterocytes also express cellular retinol binding protein 2 (CRBP2), representing 0.4-1.0% of total soluble protein **(Fig 1-5B)** [127]. CRBP2 binds retinol with a high affinity, and is thought to act as a chaperone to bring it to lecithin retinol acyltransferase (LRAT) so that LRAT may catalyze the conversion of retinol into retinyl ester [127,138]. In the distal small intestine another FABP, the ileal bile acid binding protein (ILBP or FABP6), is also present **(Fig 1-5A)**. This protein is also able to bind FA, but has a higher affinity for bile acids [139], and a lower affinity for FA when compared to LFABP and IFABP [140,141], suggesting that ILBP plays a larger role in bile acid metabolism than FA metabolism.

A

B

CRBP2 (~16kDa)→
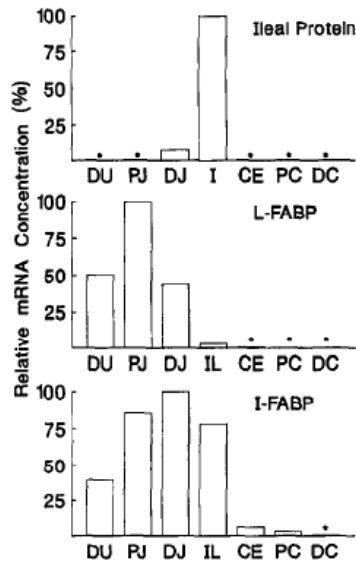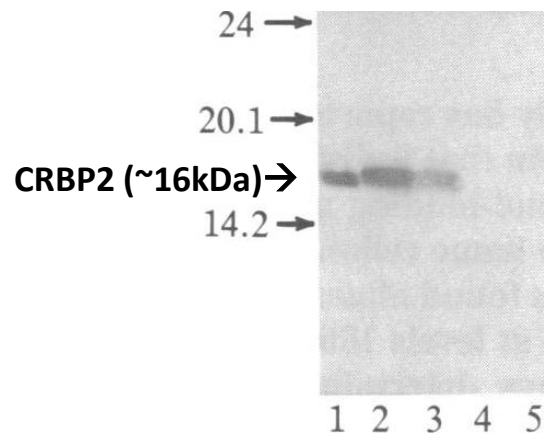
Figure 1-5: **Small intestinal location of enterocyte FABPs**. *A*, RNA blotting mouse small (I need to eliminate the word "small") intestine that was divided into 7 sections. The mRNA distribution of LFABP, IFABP, and ileal protein (ILBP) is shown, with LFABP having higher expression in the duodenum and jejunum, IFABP being most highly expressed in the jejunum, and ILBP being most highly expressed in the ileum. *DU, duodenum; PJ, proximal jejunum; DJ, distal jejunum; IL, ileum; CE, cecum; PC, proximal colon; DC, distal colon.* Figure from Sacchettini et al [142]. Adapted by

permission from American Society for Biochemistry and Molecular Biology: Journal of Biological Chemistry © 1990. *B,* Western blotting for CRBP2. Lane 1 is purified CRBP2. Lanes 2, 3 and 4 are extracts of jejunal mucosa, ileum mucosa, and colonic mucosa, respectively. Lane 5 is purified CRBP1. Figure from Crow and Ong [143]. Adapted by permission from the Proceedings of the National Academy of Sciences of the United States of America © 1993.

LFABP

As mentioned above, LFABP is an intracellular protein that is abundantly expressed in the intestinal enterocyte. It is present throughout the small intestine, but it most abundant in the duodenum and jejunum, where the majority of dietary lipid is absorbed [11]. Previous *in vitro* studies have demonstrated that LFABP is able to bind FA with a high affinity, with K_d values in the nanomolar range [144,145]. LFABP is an atypical member of the FABP family in that it is able to bind two FA ligands instead of one [146]. LFABP is also a unique FABP in that it transfers ligands to phospholipid (PL) membranes via an aqueous diffusion mechanism rather than the typical collisional mechanism [147]. Additionally, LFABP has been shown to be able to bind other types of lipid, including but not limited to monoacylglycerols (MG), prostaglandins, and lysophospholipids [146]. The cytosolic distribution of LFABP seems to be influenced by fasting and feeding cycles. During the fed state, LFABP is distributed throughout the cytosol, while during the fasted state it localizes to the apical membrane [148]. LFABP has been shown to play an important role in the budding of prechylomicron transport vesicles (PCTVs) from the ER [58,88,149–151]. These PCTVs are processed in the Golgi to form mature chylomicrons, which subsequently leave the enterocyte to enter lymphatic and then general circulation [58]. This process allows for dietary lipid to be delivered to the rest of the body, and demonstrates that LFABP plays a role in influencing dietary lipid availability for other tissues, in addition to the small intestine and liver where it is expressed.

Several studies have been performed to investigate the role of LFABP in the regulation of lipid metabolism-related genes. It has been hypothesized that LFABP is able to act as a lipid

chaperone, carrying ligands to the lipophilic binding pockets of NHRs. For example, the LFABP gene has been shown to contain a peroxisome proliferator response element (PPRE), allowing for increased LFABP gene expression to be induced upon PPARα activation [152]. PPARα is a NHR that is highly expressed in the liver and small intestine, and is typically associated with the induction of genes involved with FA oxidation [112,113]. In the liver it has been shown that LFABP is able to transfer FAs to the nucleus and co-localize with PPARα [153–155], that LFABP directly interacts with PPARα, and that expression of LFABP enhances the transcription of many PPARα target genes [154–156]. It has also been recently demonstrated that LFABP is able to bind synthetic PPARα agonists, resulting in LFABP translocation to the nucleus [157]. In addition to PPARα, LFABP has also been shown to interact with hepatocyte nuclear factor 4 α (HNF4α), a NHR that regulates a wide array of physiological processes such as lipid metabolism, cell differentiation, and cell-cell structural interactions [152,158–160]. FA oxidation in the liver and intestine is reduced in the absence of LFABP, further supporting its role in the regulation of gene expression [15,16,161,162]. The expression of LFABP appears to also be in influenced by the intake of dietary lipid, with increased lipid intake being associated with increased expression of LFABP in both the small intestine and liver [125,163–165]. Gender also appears to influence LFABP expression, with female rats having increased hepatocyte LFABP expression when compared to male rats [137,166]. Interestingly, estradiol treatment of castrated male rats resulted in hepatic LFABP levels similar to that of intact female rats, while testosterone treatment of ovariectomized female rats resulted in hepatic LFABP levels similar to that of intact males, showing sex steroids play a role in the regulation of LFABP expression[167].

While there have been no reported cases of deletion of the LFABP gene in humans, a human polymorphism has been described [168–171]. This polymorphism, which is a substitution of an alanine for a threonine at position 94 (T94A), is associated with increased plasma TG and free FA levels, and non-alcoholic fatty liver disease (NAFLD) [171–173]. Chang liver cells transected with the T94A

LFABP variant were shown to have reduced uptake of FA, increased accumulation of cholesterol, and no change in TG accumulation when compared to cells transfected with the wild-type (WT) variant [174]. However, it is important to note that "Chang liver" cells are not liver cells, but are instead derived from human cervical cancer cells, meaning that these cells are likely to not have the same physiological responses that cultured primary hepatocytes would.

The T94A allele results in LFABP with altered conformational structure and function [168,169,171]. Expression of the T94A LFABP variant in human hepatocytes impairs ligand-induced PPARα transcription of β-oxidative enzymes [168]. Interestingly fenofibrate, an activator of PPARα, is less effective at lowing plasma TG in humans that have the T94A variation, when compared to subjects that express the WT variation of LFAP [171,172]. It is thought that the impaired activation of PPARα in response to the presence of the T94A LFABP variant is due to the altered protein structure of the variant, leading to alteration in ligand/protein interactions.

IFABP

While LFABP is abundantly expressed in both the liver and the intestine, IFABP is only expressed in the intestine. IFABP is present throughout the small intestine, though it is most highly abundant in the jejunum. Like LFABP, IFABP is also found distributed throughout the cytosol in the fed state, but localizes to the apical membrane during the fasted state [148]. Unlike LFABP, IFABP does not appear to be involved in chylomicron formation [149–151]. Instead, IFABP is thought to play a role in the efficient uptake and trafficking of luminal FA to various enterocyte organelles [64]. Both of the enterocyte FABPs are also hypothesized to serve as cytosolic reservoirs for FAs, helping to prevent lipotoxicity while eventually directing the FAs to be converted into TGs, converted into PLs, or oxidized [11].

Like other members of the FABP family, IFABP has a high affinity for both saturated and unsaturated LCFAs, though compared to LFABP it has a lower affinity for unsaturated FAs

[144,145,175]. Unlike LFABP, *in vitro* studies have shown that IFABP transfers FAs to membranes via a collisional mechanism that is typical of most members of the FABP family [147]. Intestinal expression of IFABP is influenced by PYY, with greater IFABP expression being observed in response to PYY release [105]. In mice, the ablation of LFABP does not induced compensatory upregulation of IFABP at the levels of gene expression and protein abundance; there is no compensatory upregulation of LFABP in response to IFABP ablation as well [11,15,16]. Unlike LFABP, the IFABP gene does not contain a PPRE, and is likely not regulated by PPARα [176]. The lack of compensatory upregulation in gene knockout mice, and differences in its regulation in response to NHRs and signaling peptides, provides additional indirect evidence that LFABP and IFABP have different functions with this small intestine.

Like LFABP, deletion of the IFABP gene has not been reported in humans, though a polymorphism has been identified involving a threonine to alanine substitution at amino acid 54 (A54T) [177]. This amino acid substitution results in an increased affinity for FA relative to the alanine-containing proteins [177,178]. Individuals with the A54T variant were found to have higher rates of insulin resistance, elevated plasma TG, and atherosclerosis [177,179–181]. *In vitro* and *ex vivo* studies have demonstrated that the A54T variant is associated with increased TG synthesis and secretion, which is consistent with the hyperlipidemia that is observed in human subjects [182,183].

LFABP and IFABP in Intestinal Lipid Metabolism

It has been proposed that the LFABP and IFABP are both involved in directing lipids towards the synthesis of either PL or TG within the enterocyte. Dietary lipids, such as FA and MG are delivered via the apical side of the enterocyte, and are mainly incorporated into TG and later secreted from the basolateral side of the enterocyte in the form of TG-rich lipoproteins known as chylomicrons. Conversely, bloodstream derived FA are transported into the enterocyte through the basolateral surface, and are primarily used for either PL synthesis or oxidation [19]. Several *in vitro* and *ex vivo* studies have suggested that the enterocyte FABPs are involved in efficient uptake of FA from

both the intestinal lumen and the bloodstream [148,184]. In a series of experiments performed by Alpers and colleagues [148], an intestinal explant system was used to study the roles of IFABP and LFABP in response to either an apical or basolateral FA challenge. It was observed that, regardless of the site of FA entry, LFABP was able to bind more FA than IFABP. Interestingly, IFABP bound more apically administered FA than basolateral FA, suggesting that IFABP plays a bigger role in the transport of dietary-derived FA rather than FA from the bloodstream. Additionally, immunohistochemistry (IHC) was used to observe the subcellular localization of IFABP and LFABP in rat enterocytes [148] . It was observed that in the fed state, both enterocyte FABPs were distributed throughout the cytosol. However, in the fasted state, IFABP and LFABP both localized to the apical surface of the enterocyte. These series of experiments contributed to the hypothesis that the enterocyte FABPs are necessary for efficient uptake, assimilation, and trafficking of dietary FA.

LFABP$^{-/-}$ and IFABP$^{-/-}$ Mice

To study the enterocyte FABPs in a more physiologically relevant *in vivo* system, whole-body knockout mouse models were generated. For LFABP, two independent laboratories generated LFABP$^{-/-}$ mice on the C57BL/6 background [161,162,185]. The St. Louis LFABP$^{-/-}$ mice [113,186,187] were generated using mice from the Jackson Laboratory (BL6J), while the Texas LFABP$^{-/-}$ mice [188,189], from which our LFABP$^{-/-}$ mice are derived, were generated using Taconic mice (BL6N), and backcrossed to C56BL/6J mice to generate another line of LFABP$^{-/-}$ on the BL6 background (BL6J/N 0.6/0.4). The St. Louis LFABP$^{-/-}$ mice gain less weight than WT mice upon high fat feeding, while the Texas mice and our mice become obese [11,16,113,186,188]. It is worth mentioning, however, that that the St. Louis LFABP$^{-/-}$ and Texas LFABP$^{-/-}$ lines share many similarities, including defective hepatic FA uptake, oxidation, and VLDL secretion [161,185,187,190].

One line of IFABP$^{-/-}$ mice has been generated on the C56BL/6J background by Vassileva and colleagues [191]. There appeared to be a sexually dimorphic phenotype in response to HF feeding,

where male IFABP^{-/-} mice fed 35% Kcal fat HF diet with 1.25% cholesterol for 19 weeks, or fed 41% Kcal fat diets containing beef tallow of safflower oil for 14 days, were found to have increased BW relative to male WT mice, while female IFABP^{-/-} mice on the 35% Kcal fat HF diet with 1.25% cholesterol did not have significantly different BW when compared to female WT mice [191]. Our IFABP^{-/-} mice are a substrain derived from the original line, and have been maintained on the C56BL/6J background.

In recent years, our lab has conducted direct comparative studies using both LFABP^{-/-} and IFABP^{-/-} mice. The initial studies, performed by Lagakos et al made use of chow fed male mice for baseline phenotypic evaluations [15]. Previously it had been hypothesized that since both proteins are highly expressed within the small intestine, it is possible that ablating one may cause compensatory upregulation of the remaining enterocyte FABP. However, as previously reported by others [185,191], it was observed that mucosal expression of IFABP or LFABP, was not upregulated in mice null for LFABP or IFABP, respectively [15], lending credence to the hypothesis that these two proteins serve distinct functions within the small intestine. Additionally, Lagakos and colleagues observed that the BW of chow-fed LFABP^{-/-} and IFABP^{-/-} mice did not differ from WT mice[15]. While it was initially hypothesized that the enterocyte FABPs were necessary for efficient uptake of dietary lipid, an analysis of fecal lipid content revealed that the ablation of LFABP or IFABP did not result in increased fecal lipid percentage in chow fed mice[15]. Some modest phenotypic changes were observed during and at the end of the chow feeding protocol: IFABP^{-/-} mice were found to lose more fat mass, and LFABP^{-/-} mice lost less fat-free mass than WT mice, in response to fasting. Additionally, intraduodenally administered [14C] FA revealed that IFABP^{-/-} mice recovered more of the radiolabel in the form of PL in the mucosa, relative to WT mice, suggestion that IFABP may play a role in directing dietary FA towards the synthesis of TG[15]. While LFABP^{-/-} mice did not differ from WT mice in terms of [14C] FA partitioning, intraduodenal delivery of [3H] monoolien resulted in increased incorporation of the label in mucosal PL, MG, and

DG, while incorporation of label into mucosal TG was decreased[15]. This suggests that LFABP plays a role in directing dietary MG away from PL synthesis and towards TG synthesis. Interestingly, the ablation of LFABP resulted in reduced oxidation of intraduodenally administered [^{14}C] FA [15]. As has been shown in the liver [161], it appears that that LFABP plays a role in trafficking FA towards oxidative pathways within the enterocyte.

While no dramatic whole-body phenotypic differences were noted in either IFABP$^{-/-}$ mice or LFABP$^{-/-}$ mice fed a low fat (LF) chow diet [15], it was hypothesized that the lipid load of the chow diet was not high enough to sufficiently stress the mice lacking only one enterocyte FABP, especially since the single knockout mice still express high levels of the remaining enterocyte FABP. Thus, HF feeding studies were commenced and the findings of Gajda et al were quite dramatic: HF fed LFABP$^{-/-}$ mice gained more weight and fat mass, relative to WT mice, while IFABP$^{-/-}$ remained lean, gaining less weight and fat mass [16]. It was also found that LFABP$^{-/-}$ mice had lower respiratory exchange ratios (RERs) than WT mice, indicating that these mice primarily utilize lipid as an energy source [16]. Conversely, the leaner HF fed IFABP$^{-/-}$ mice were found to have higher RERs than WT mice, suggesting that these mice preferentially oxidize carbohydrate as an energy source [16]. LFABP$^{-/-}$ mice were found to have increased food intake, and IFABP$^{-/-}$ mice were observed to have decreased food intake, relative to WT mice [16]. However, an assessment of feeding efficiency revealed that the leanness of the IFABP$^{-/-}$ mice and the increased BW and fat mass of the LFABP$^{-/-}$ could not be fully explained by alterations in food intake [16]. Most interestingly, an assessment of fecal lipid content revealed that even when challenged with chronic HF feeding, the amount of lipid in the feces did not differ between the three groups of mice [16], suggesting that the ablation of LFABP or IFABP does not result in malabsorption of dietary lipid. Thus, the prevailing idea that the enterocyte FABPs are critical for bulk dietary lipid assimilation requires further examination.

Summary

The intestinal enterocytes are thought to be integral to the absorption and assimilation of dietary lipid from the intestinal lumen. With dietary TG accounting for >90% of the lipid in the human diet, its hydrolysis products, MGs and FAs, are of particular importance in terms of what lipids the enterocytes are exposed to. LFABP and IFABP are both highly abundant lipid binding proteins that have high affinities for FAs, and they are hypothesized to be necessary for the efficient uptake and trafficking of lipids within intestinal enterocytes. While these proteins are from the same family and have similar structures, differences in ligand binding, specificities, affinities, and mechanisms of delivery have been observed, suggesting that these proteins play different roles within the small intestine in regards to the modulation of lipid transport and metabolism. Furthermore, *in vivo* studies in mice have shown that LFABP$^{-/-}$ and IFABP$^{-/-}$ mice respond drastically differently to chronic high fat feeding, with LFABP$^{-/-}$ mice becoming more obese, while IFABP$^{-/-}$ mice remain lean. This profound phenotypic divergence has provided further evidence that these have difference function within the small intestine. It is important to keep in mind that LFABP is also expressed in the liver, meaning that the phenotypes observed in the HF fed LFABP$^{-/-}$ can be a result of the response to lacking liver-LFABP, lacking small intestinal-LFABP, or some combination of the two. In regards to the IFABP$^{-/-}$ mice, it is important to note that while these mice remain lean on a HF diet, it was observed that the lean phenotype could not be fully explained by reductions in food intake. Since IFABP is only expressed in the small intestine, it is imperative to assess other aspects of intestinal physiology that might induce alterations in body weight and body composition. Therefore, the aims of this thesis project are:

Specific Aims

SPECIFIC AIM 1: To assess what the contribution of intestinal LFABP is to the obese phenotype that has been observed in HF-fed LFABP^{-/-} mice.

As mentioned above, feeding LFABP^{-/-} mice a HF diet resulted in increased BW, fat mass, and food intake relative to WT mice [16]. Surprisingly, although LFABP^{-/-} mice became obese they remained relatively healthy, being normoglycemic, normoinsulinemic, and also displaying reduced hepatic steatosis, and intestinal TG secretion rates similar to that of lean mice [16,113,187,192,193]. Further, despite their obesity, the LFABP^{-/-} mice were found to be more active [16], and our recent studies show that LFABP^{-/-} mice have greater exercise endurance than WT mice [194]. It has been recognized that a subset of the obese population is still found to be healthy, not displaying various comorbidities that are commonplace amongst obese people; this phenomenon has become known as the "metabolically healthy but obese" (MHO) state [195,196]. The LFABP^{-/-} mice thus appear to be a model of MHO. In order to understand the underlying causes of the LFABP^{-/-} phenotype, it is critical to know whether it is dependent on the ablation of LFABP in the intestine or in the liver, or if simultaneous ablation is necessary. Thus, one of our aims focuses on generating LFABP conditional knockout (cKO) mice so as to assess the role of LFABP specifically within the small intestine that may influence the whole-body phenotypic changes in the LFABP^{-/-} mice. To this end, body weight gain, body composition, food intake, indirect calorimetry, and other metabolic indicators will be used to assess whole-body energy homeostasis in the LFABP-cKO mice.

SPECIFIC AIM 2: To assess what changes are occurring within the small intestine of IFABP^{-/-} mice that may explain the resistance to diet-induced obesity and the fragility of the small intestine.

As the enterocyte FABPs have long been thought to be involved in dietary lipid uptake and assimilation [11], it is tempting to speculate that HF fed IFABP^{-/-} might malabsorb lipid in addition to

having a decreased food intake, explaining the observed lean phenotype. As noted above, however, the fecal lipid content did not vary between IFABP^{-/-} and WT mice when challenged with either LF chow or 45% Kcal fat HF diets, suggesting that the IFABP^{-/-} mice were not malabsorbing lipid [15,16]. It is possible that the lipid content of the 45% Kcal HFD is not sufficient to stress the absorptive capacity of the SI enterocytes, thus, as part of the second aim, we will examine the fecal fat content of mice fed a supraphysiological 60% Kcal fat diet. In addition, we will determine not only fecal lipid content, but also total fecal excretion, and the intestinal transit time of mice fed the 45% Kcal HF diet.

During organ collection, it was observed that the intestinal tissue of the HF fed IFABP^{-/-} mice seemed to be more fragile than that of WT mice, with the tendency to easily break upon removal. We, therefore, also hypothesized that the ablation of IFABP may lead to alterations in intestinal structure and, perhaps, inflammation. Thus, part of the second aim will focus on gene expression, histological, and immunohistochemical analyses to assess SI integrity, morphology, and inflammatory status.

Chapter 2

The Generation and Whole-Body Phenotyping of Intestine-Specific Liver Fatty Acid-Binding Protein Knockout Mice

Abstract

Liver fatty acid-binding protein (LFABP or FABP1) is a highly abundant intracellular lipid binding protein that is expressed in liver and small intestine of mice. High fat (HF) feeding of male whole-body LFABP^{-/-} mice resulted in animals that appeared to be obese, yet metabolically healthy. LFABP^{-/-} mice gained more weight and had higher fat mass, but displayed better exercise capacity when compared to their wild-type (WT) controls. Intestine-specific ablation of LFABP (LFBAP[int-/-]) resulted in male mice that did not differ from WT-LFABP floxed (LFABP^{fl/fl}) controls in body weight or body composition. On the other hand, female LFABP[int-/-] mice were more obese than their LFABP^{fl/fl} counterparts. Both male and female LFABP[int-/-] mice were found to have better exercise capacity. It appears that the ablation of both liver- and intestinal-LFABP, or perhaps ablation in liver only, may be necessary to induce the metabolically healthy obese (MHO) phenotype observed in whole body male LFABP knockout mice, but that intestine-specific ablation is sufficient to induce the improvement in exercise capacity.

Introduction

Obesity, a disease state that is characterized by excessive fat storage and is often accompanied by an array of metabolic comorbidities, is considered to be the leading cause of preventable death around the world [7]. In addition the physical burdens placed on individuals, obesity and obesity-related illnesses represent a substantial financial burden economically [5]. Prevalence has increased over the years, with two thirds of US adults are considered overweight or obese [10]. With increased fat storage being integral to the development of obese phenotypes, dietary lipid quantity and quality are thought to play important roles in the etiology of obesity and its related comorbidities [8–10].

The absorptive enterocytes of the small intestine are primary responsible for the absorption and subsequent processing of dietary lipid. The abundance of triacylglycerol (TG), the primary component of dietary lipid, is elevated in Western diets. Absorption of dietary TG, after its luminal hydrolysis to fatty acid (FA) and monoacylglycerol (MG), is highly efficient, with greater than 95% of dietary lipid taken up [11,33]. Once absorbed, it is thought that these hydrophobic lipid species require intracellular lipid binding proteins to be efficiently transported within the hydrophilic cytoplasmic milieu.

The intestinal enterocyte expresses at least two members of the FABP family simultaneously: liver-FABP (LFABP or FABP1), which is also expressed in the liver, and intestinal-FABP (IFABP or FABP2), which is solely expressed within the intestine [11,15,16]. Two independent laboratories have generated LFABP^{-/-} mice on the C57BL/6 background [161,162,185]. The St. Louis LFABP^{-/-} mice [113,186,187] were generated using mice from the Jackson Laboratory (BL6J), while the Texas LFABP^{-/-} mice [188,189], from which our LFABP^{-/-} mice are derived, were generated using Taconic mice (BL6N), and backcrossed to C56BL/6J mice to generate another line of LFABP^{-/-} on the BL6 background (BL6J/N 0.6/0.4). The St. Louis LFABP^{-/-} mice gain less weight than WT mice upon high fat feeding, while the Texas mice and our mice become obese [11,16,113,186,188]. It is worth

mentioning, however, that that the St. Louis LFABP^{-/-} and Texas LFABP^{-/-} lines share many similarities, including defective hepatic FA uptake, oxidation, and very low density lipoprotein (VLDL) secretion [161,185,187,190].

In our hands, feeding LFABP^{-/-} mice a HF diet results in increased body weight, fat mass and food intake relative to WT mice [16]. Although LFABP^{-/-} mice become obese they appear to be relatively healthy, being normoglycemic, normoinsulinemic, and also displaying reduced hepatic steatosis, and intestinal triglyceride (TG) secretion rates similar to that of lean mice [16,113,187,192]. Further, despite their obesity, the LFABP^{-/-} mice are more active[16], and additional studies show that LFABP^{-/-} mice have greater exercise endurance than WT mice.   It has been recognized that a subset of the obese population is still found to be healthy, not displaying various comorbidities that are commonplace amongst obese people; this phenomenon has become known as the "metabolically healthy but obese" (MHO) state [195,196]. The LFABP^{-/-} mice thus appear to be a model of MHO. In order to understand the underlying causes of the LFABP^{-/-} phenotype, it is critical to know whether it is dependent on the ablation of LFABP in the intestine or in the liver, or if simultaneous ablation is necessary. In this study, LFABP conditional knockout (cKO) were generated to assess the role of LFABP specifically within the small intestine, and to determine how much the intestinal LFABP contributes to the phenotype of the whole body LFABP null.

To generate the LFABP-cKO mice, the type II bacterial clustered regulatory interspaced short palindromic repeats (CRISPR)/CRISPR-associated (Cas) system was used as an efficient gene-targeting technology **(Fig 2-1A)** [197,198]. Traditionally, mice that have a gene flanked by loxP sites ("floxing" of a gene) were generated by targeting in embryonic stem cells and subsequently producing germline chimeric mice [199,200]. However, this process is time consuming, and inducing precise modifications can be unreliable. More recently, genome editing using direct microinjection of synthetic RNA-guided nucleases into zygotes has accelerated the production of gene-modified animals with precise alterations. The CRISPR/Cas system makes use of guide RNAs (sgRNAs)

that contain a targeting sequence (crRNA), and a Cas9 nuclease-recruiting sequence (tracrRNA) [201]. The Cas9 nuclease, when recruited, induces double-strand breaks (DSBs) at the sites of recognition. In order for specific alterations to DNA to be induced, single stranded (ss) DNA donors must be introduced so that they can be incorporated into the host organisms' DNA via homology driven repair (HDR). To generate a cKO mouse using the CRISPR/Cas system, two separate sgRNAs must be used to introduced loxP sites upstream and downstream of a critical exon for a gene of interest. The resultant "floxed" mice can then be bred with mice that express Cre recombinase, driven by a reporter of interest **(Fig 2-1B)** [202,203]. The simultaneous expression the floxed gene with Cre recombinase will induce specific excision of the DNA located between the two loxP sites.
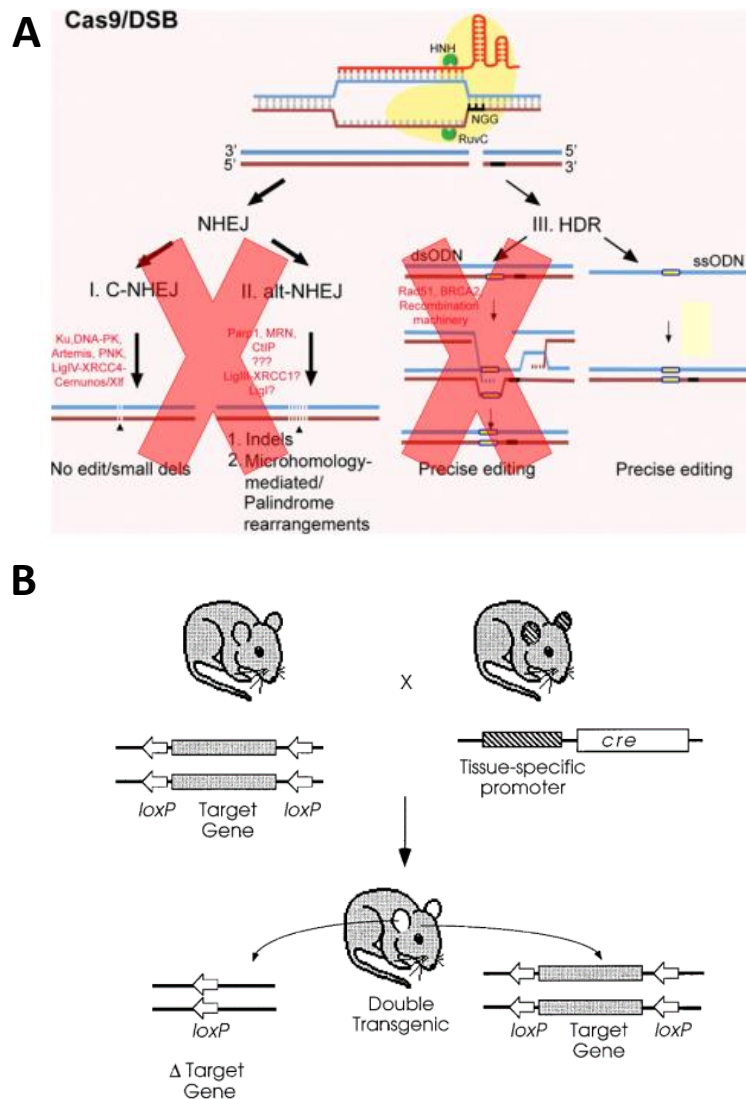
Figure 2-1: **The generation of tissue specific knockout mice using the CRISPR/Cas and Cre/lox approach.** *A*, gRNA allows for the specific targeting of a DNA sequence of interest. The Cas9 protein recognizes the DNA, and is able to induce a double strand DNA break. In the presence of single strand DNA donors, new DNA can be incorporated into the target sequence via homology driven DNA repair mechanisms, allowing for precise editing to occur. Figure from Singh et al [204]. Adapted by permission from Genetics © 2015. *B*, Mating of the floxed mice with mice that are Cre mutants will generate double-transgenic mice, resulting in the tissue-specific ablation of the floxed gene in tissues that express the Cre recombinase transgene. Figure from Sauer [202]. Adapted by permission from Elsevier: Methods © 1998.

Experimental Procedures

Generation of Intestine-specific LFABP null Mice

Conditional knockout mice were generated at The Rutgers Genome Editing Core Facility. The type II bacterial CRISPR/Cas system was used as gene-targeting technology [197,198,201] to generate mice with loxP sites flanking critical exons of the *fabp1* gene **(Fig 2-2A)**. Initially, two separate guide RNAs (gRNAs) were developed, each formed to contain a targeting sequence (crRNA), and a Cas9 nuclease-recruiting sequence (tracrRNA). The crRNA was a 20-nucleotide sequence that was homologous to sequences either upstream or downstream of exons 2 and 3 of the *fabp1* gene and located near a protospacer adjacent motif (PAM) sequence, allowing for the Cas9 nuclease activity to be directed to the *fabp1* alleles. Cas9 nuclease was used to induce double-strand breaks (DSBs) at the sites of recognition. In addition to the gRNAs and Cas9, single stranded (ss) DNA donors were used to introduce both loxP sites via homology driven repair (HDR) **(Fig 2-2B)**. Like the WT *fabp1* gene, the ssDNA sequence also contains the crRNA targeting sequence. However, when the addition of the loxP site is successful, this causes the crRNA sequence to be separated from the PAM sequence that is required Cas9 recognition, preventing further DSBs from occurring. The ssDNA donor for the upstream loxP site also contained a PsiI restriction site, while the ssDNA donor for the upstream loxP site contained an EcoRI restriction site.

C57BL6/N mouse oocytes were microinjected with Cas9 protein, the ssDNA donors containing loxP, and the gRNA targeting downstream of the *fabp1* gene. Once fertilized with sperm from C57BL6/J mice, the resultant mice contained alleles having only one loxP site. The microinjection process was repeated for the oocytes from these mice, but the gRNA targeting the upstream site of the *fabp1* gene was substituted to ensure that critical exons of the *fabp1* gene would be flanked by loxP sites (LFABP^fl/fl).
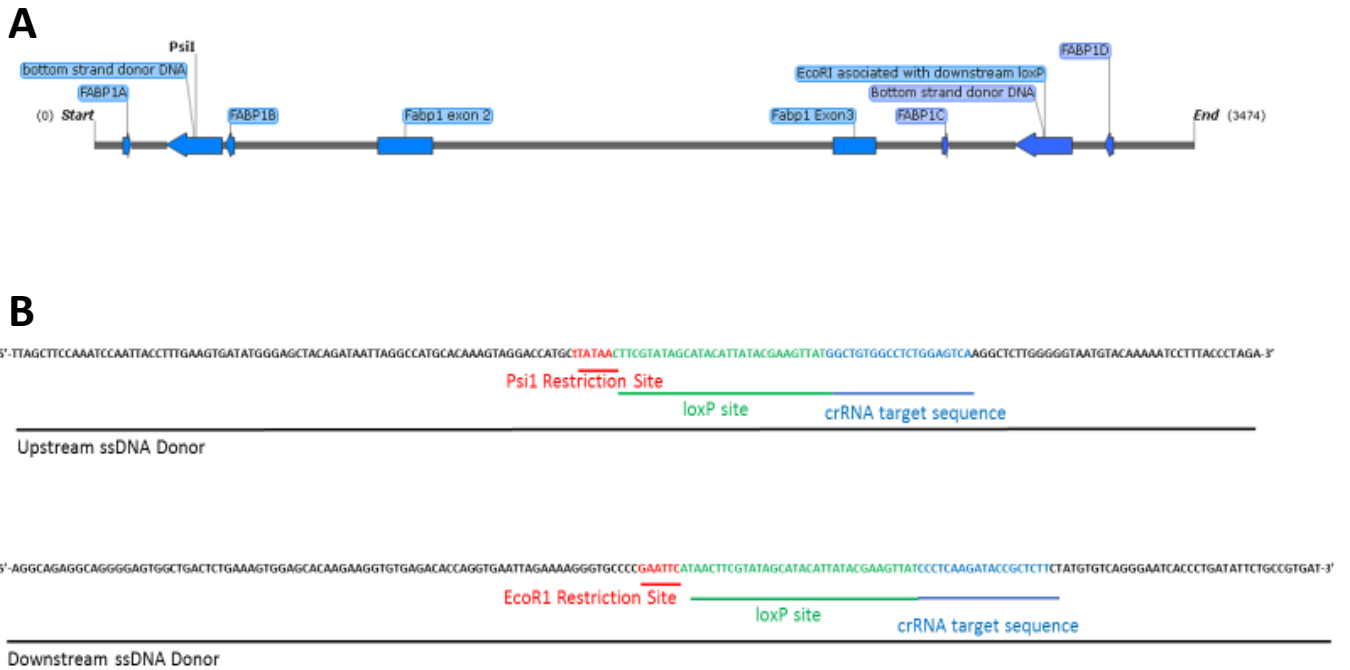
Figure 2-2: **Strategy used to generate LFABP-cKO mice.** *A*, The sequence map for the altered Fabp1 gene. Distinct gRNAs were used to target locations upstream and downstream of critical exons 1 and 3 for the *fabp*1 gene. Double strand DNA breaks were induced via recognition by and recruitment of Cas9 nuclease. In the presence of ssDNA donors, homology driven DNA repair results in the incorporation of new DNA into the *fabp1* gene. *B*, Sequences for the upstream and downstream ssDNA donors. Each donor contains loxP sequences and distinct crRNA targeting sequences. Upon the successful incorporation of the loxP site, the Cas9 nuclease is no longer able to targert the crRNA, preventing further DSBs from occurring. The upstream ssDNA donor contains a PsiI restriction site, while the downstream ssDNA donor contains an EcoRI restriction site, enabling for the resultant mice to be assessed for the presence of both the upstream and downstream loxP sites.

Animals

LFABP^fl/fl mice on the mixed C57BL6/J and C57BL6/N background were backcrossed with WT C57BL6/J mice 4 additional times, yielding congenic LFABP^fl/fl mice on the C57BL6/J background. The resultant LFABP^fl/fl mice were then be bred with mice that are hemizygous for Cre driven by the villin promoter (Vcre/+) to generate double-mutants (LFABP^fl/+;Vcre/+), which were then be crossed to generate intestine-specific LFABP knockout (LFABP^fl/fl;Vcre/+ or LFABP^int-/-) mice. This breeding scheme also allows for the continued propagation of LFABP^fl/fl, which are used as littermate WT controls for their LFABP^int-/- counterparts. Mice were maintained on a 12-hour light/dark cycle, and allowed *ad libitum* access to standard rodent chow (Purina Laboratory Rodent Diet 5015) until the start of the study at 2 months of age.

DNA Extraction for Genotyping

DNA extraction was performed as described previously [15]. In brief, a 0.5cm tail biopsy was incubated overnight at 37°C in lysis buffer (0.3M sodium acetate, 10mM Tris-HCL pH7.9, 1mM EDTA, 1% SDS, 0.2mg/mL proteinase K). The following morning, the lysate was cooled on ice, and the precipitate was pelleted. The supernatant was then placed into a new cool microcentrifuge tube, with subsequent ethanol precipitation being used to isolate the DNA.

For the genotyping of the LFABP^fl/fl mice, forward and reverse primers were developed that allow for the assessment of the upstream lox P site, while a sperate set of forward and reverse primers assessed the downstream loxP site in two separate PCR reactions. The primer sequences for the LFABP^fl/fl protocols are as follows:

Primers used for the upstream loxP

FABP1A- AGACAAGTCAAAGATCATGAATGTGAG

FABP1B- TGGCTCTTAGAGTGGGAACACTTC

Primers used for the downstream loxP

FABP1C- CGGAGTTGATAGATATCAGATC

FABP1D- GAAACAGGGCAAGGCCAGCTATG

After performing the reactions, the PCR products for the upstream loxP reaction were digested with PsiI, while the PCR products for the downstream loxP site were digested with EcoRI. Subsequently, gel electrophoresis on a 2% agarose gel was performed. WT mice that do not have the inserted loxP sites will only have one band for both the upstream (350BP) and downstream (540BP) reactions. However, LFABP$^{fl/fl}$ mice will have two smaller bands for both the upstream (231BP and 119BP) and downstream (325BP and 215BP) reactions.

The genotyping protocol for the Vcre/+ mice used 3 primers for two separate PCR reactions. One primer, Vcre common, was used for both reactions. The Vcre-WT primer was used to detect a band that can be found in WT mice (~186BP), while the Vcre-mutant primer was used to detect a band that should only be observed in Vcre/+ mice (~150BP). Since the Vcre/+ mice must be maintained as hemizygotes [205], they should have bands for both the Vcre-WT reaction and the Vcre-mutant reaction. The primer sequences for the Vcre genotyping protocols are as follows:

Vcre-WT reaction

Vcre-Common- GCCTTCTCCTCTAGGCTCGT

Vcre-WT- TATAGGGCAGAGCTGGAGGA

Vcre-Mutant reaction

Vcre-Common- GCCTTCTCCTCTAGGCTCGT

Vcre-Mutant- AGGCAAATTTTGGTGTACGG

High Fat Feeding, Body Weight, and Body Composition

At 8 weeks of age, male and female mice were fed a 45% Kcal fat semipurified HF diet (D10080402, Research Diets, New Brunswick, NJ). The mice were maintained on this diet for 12 weeks, with BW measurements recorded weekly. Fat mass measurements were taken by MRI (Echo Medical Systems, LLC., Houston, TX) 2-3 days prior to starting the feeding protocol, and 2-3 days prior to sacrifice. The instrument was calibrated each time according to the manufacturer's instructions. At each time point, two measurements were recorded for each mouse and averaged.

Indirect Calorimetry, Activity, and Food Intake

Energy expenditure was assessed using the Oxymax system (Columbus Instruments, Columbus, OH) during week 11 of HF feeding. Mice were placed in an indirect calorimetry chamber (1 mouse per chamber) with food for 96 hours. The first 48 hours were used as an acclimation period, while the second 48-hour period was used to record activity, food intake, and energy metabolism measurements. VO2 and VCO2 (VCO2/VCO2) were used to determine the Respiratory Exchange Ratio (RER). Energy expenditure was measured by the using the gas exchange measurements as follows: $(3.815 + 1.232 \times RER) \times VO2$ [206].

Oral Glucose Tolerance Tests

During week 11 of the HF feeding protocol, mice were be fasted for 6 hours prior to OGTT experiments. Blood was obtained via the tail vein, and glucose was measured using an Accu-

Check monitor (Roche). An oral gavage of 2g glucose/Kg body weight was administered, and blood was sampled at time points of 30, 60, 90, and 120 minutes post gavage.

Treadmill Exercise Protocol

Exercise testing used a treadmill incline at 25°. Mice were acclimated one day prior to the test by walking at 5 m/min. The test speed began at 6 m/min; after the first 5 minutes, the speed was increased by 3 m/min every 2 minutes. The treadmill makes use of a shock grid at the base (only contacted when the mice fail to keep up with the treadmill belt), which was kept at a low intensity. Fatigue was indicated when mice remained on the shock grid for 5 seconds, at which time the mice were removed from the apparatus, and the time to fatigue and total distance traveled were recorded [207,208].

Blood and Tissue Preparation

At the end of the experiment mice were fasted for 16 hours prior to sacrifice. At sacrifice whole blood was drawn; plasma was isolated after room temperature centrifugation for 6 minutes at 4000 rpm, and stored at -80°C. The livers were removed, weighed, immediately placed on dry ice, and stored at -80°C for further analysis. The small intestine from the pyloric sphincter to the ileocecal valve was removed, measured lengthwise, rinsed with 60mL of ice-cold 0.1M NaCl, and opened longitudinally. Intestinal mucosa was scraped with a glass microscope slide into tared tubes on dry ice.

Blood Analysis

ELISA kits were used to measure plasma insulin (EZRMI-13K, MilliporeSigma) and plasma leptin (EZML-82K, MilliporSigma). Samples were prepared and the analysis occurred following the manufacturer's instructions. For plasma leptin, a leptin index was calculated that normalized values to fat mass for each animal. This was determined by taking the plasma leptin values for each mouse, and dividing it by their respective fat mass values.

Western Blotting

Small intestinal mucosa was harvested as described above, and homogenized in 10x volume of PBS pH 7.4 with 0.5% (vol/vol) protease inhibitors (Sigma8340) on ice with a Potter Elvejhem homogenizer for 20 strokes. Total cytosolic fractions were obtained by ultracentrifugation (100,000g, 1 hour at 4°C) and protein concentrations were determined by Bradford assay [209]. Thirty micrograms of protein were loaded onto 15% polyacrylamide gels and separated by SDS-PAGE. The proteins were then transferred onto 0.45μm nitrocellulose membranes using a wet transfer system (Bio-Rad) for 1 hour at 100 V. After transfer, total protein was visualized using Ponceau staining. Membranes were then blocked by incubating in 5% nonfat dry milk overnight at 4°C, and were subsequently incubated with an α-LFABP primary antibody (1:2000 for 1 hour at room temperature). After thorough washing, blots were then incubated in α-rabbit IgG-horseradish peroxidase conjugate (1:10,000) for 1 hour, and developed by chemiluminescence (WesternBright Quantum, Advansta, Menlo Park, CA). Protein expression was quantified by densitometric analysis with LI-COR Image Studio (Lite version 5.2). Target protein content was normalized to total protein content within a sample.

Statistical Analysis

All group data are shown as average ± SEM. Statistical comparisons were determined between genotypes on the same diet using a two-sided Student's *t* -test. Differences are considered significant for P<0.05.

Results

The ablation of LFABP was specific to the small intestine

LFABP$^{fl/fl}$ mice were crossed with Vcre hemizygotes to generate mice that are double mutants, with one allele that has the floxed LFABP gene, and one allele that contains villin-Cre (LFABP$^{fl/+;Vcre/+}$). Subsequently, double mutant mice were crossed with LFABP$^{fl/fl}$ mice to obtain

the intestine-specific LFABP$^{-/-}$ mice (LFABP$^{fl/fl;Vcre/+}$ to be called LFABP$^{int-/-}$), and littermate LFABP$^{fl/fl}$ mice that were used as controls **(Fig 2-3AB)**. Ablation of LFABP in the intestine, but not the liver, of LFABP$^{int-/-}$ mice was confirmed by Western blotting **(Fig 2-3C)**. Control LFABP$^{fl/fl}$ mice, which should be phenotypically similar to WT mice, express LFABP in both their liver and intestine **(Fig 2-3C)**.
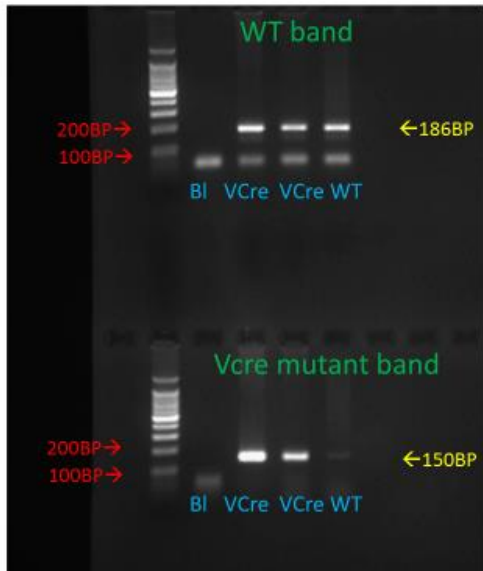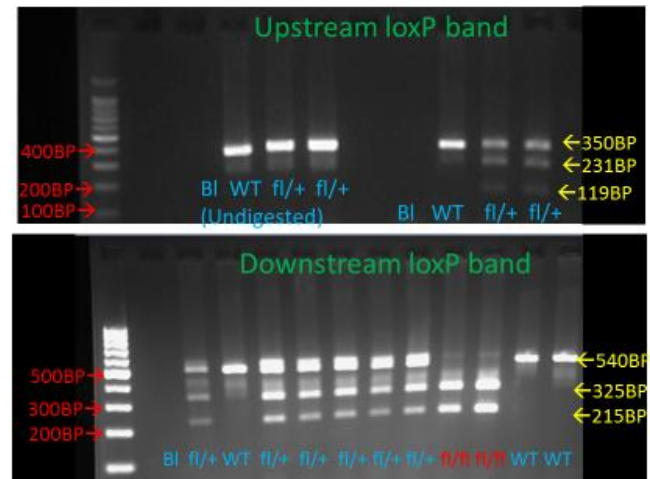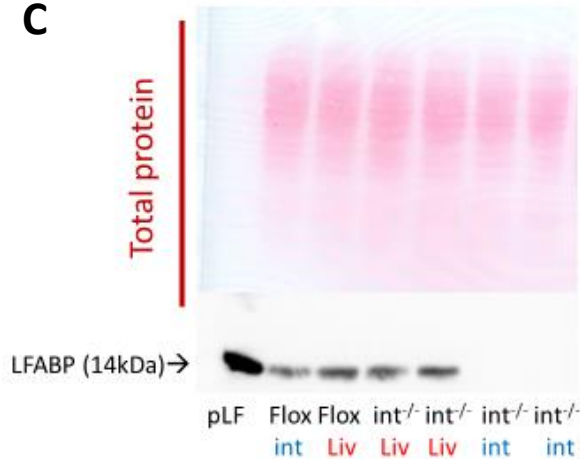
Figure 2-3: **Confirmation of generation of LFABP^fl/fl and LFABP^int-/- mice.** *A*, DNA gel showing PCR reactions for Vcre genotyping; *B*, DNA gel showing PCR reactions for lox P sites flanking the *fabp1* gene. For the upstream loxP site the band at 350BP is indicative of an uncut WT band, while the 231BP and 119BP fragments are indicative an allele that contain the loxP site. For the downstream loxP site, 540BP indicated a WT allele, while 325BP and 215BP indicate an allele with the loxP site; *C*, Western blotting confirming the intestine-specific ablation of LFABP in LFABP^int-/- mice. Purified LFABP protein (pLF) was used as a positive control.

Male LFABP$^{int-/-}$ mice do not have altered body weight or body composition; female LFABP$^{int-/-}$ mice have higher body weight and increased fat mass

At 8 weeks of age, male and female LFABP$^{fl/fl}$ and LFABP$^{int-/-}$ mice were challenged with a 45% Kcal fat HF diet. After 12 weeks on the diet, no differences were observed between male LFABP$^{fl/fl}$ and LFABP$^{int-/-}$ mice in weekly BW **(Fig 2-4A)** or BW gain **(Fig 2-4B)**. Additionally, the intestine-specific ablation of LFABP did not result in any alterations in body composition, with no changes in fat mass observed **(Fig 2-4C)**. For females however, it was observed that the BW of LFABP$^{int-/-}$ mice was significantly greater than that of their LFABP$^{fl/fl}$ counterparts starting at week 6 of their HF challenge **(Fig 2-4D)**. Overall, female LFABP$^{int-/-}$ mice also had higher BW gain **(Fig 2-4E)** and greater fat mass than female LFABP$^{fl/fl}$ mice **(Fig 2-4F)**.
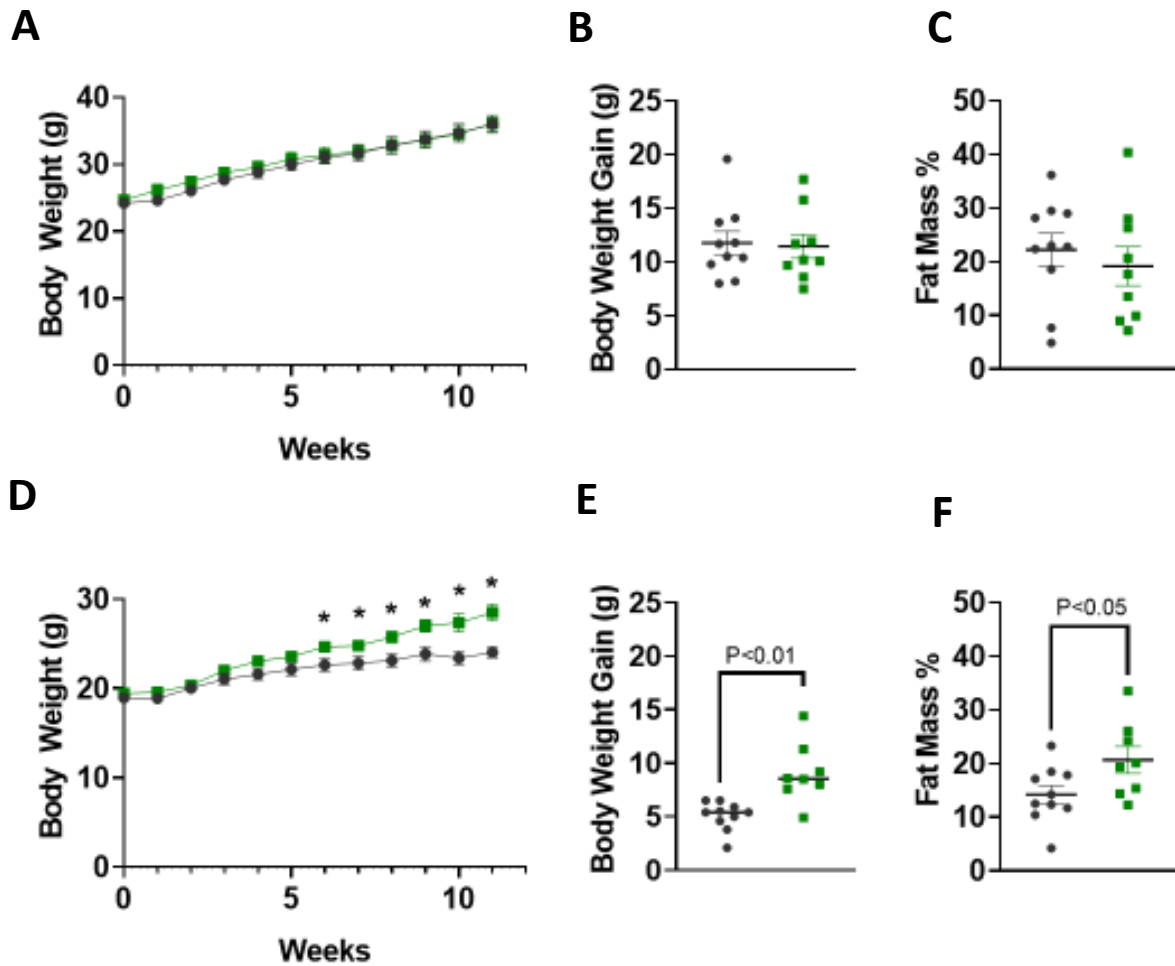
Figure 2-4: **Body weight, body weight gain, and fat mass for LFABP$^{fl/fl}$ (●) and LFABP$^{int-/-}$ (■)**

mice after 12 weeks of 45% Kcal HF feeding. *A*, Male mice body weights (n=10); *B*, Male mice

body weight gain (n=10); *C*, Male mice fat mass percentage (n=10); *D*, Female mice body weights

(n=8-10); *E*, Female mice body weight gain (n=8-10); *F*, Female mice fat mass percentage (n=10).

The intestine-specific ablation of LFABP does not result in altered energy homeostasis

Mice were placed into the Oxymax system to assess food intake, respiratory exchange ratio (RER), and energy expenditure. For male LFABP$^{fl/fl}$ and LFABP$^{int-/-}$ mice there was no difference observed in the amount of food that was consumed **(Fig 2-5 A and B)**. The intestine-specific ablation of LFABP in male mice did not result in differences in the average 24-hour RER as well **(Fig 2-5C)**. Additionally, no differences in energy expenditure were observed **(Fig 2-5D)**. Despite the observed differences in BW and body composition for the female LFABP$^{fl/fl}$ and LFABP$^{int-/-}$ mice, other energy homeostasis-related phenotypes were not altered, with no differences being observed in food intake **(Fig 2-5E and F)**, 24-hour RER **(Fig 2-5G)**, or energy expenditure **(Fig 2-5H)**.
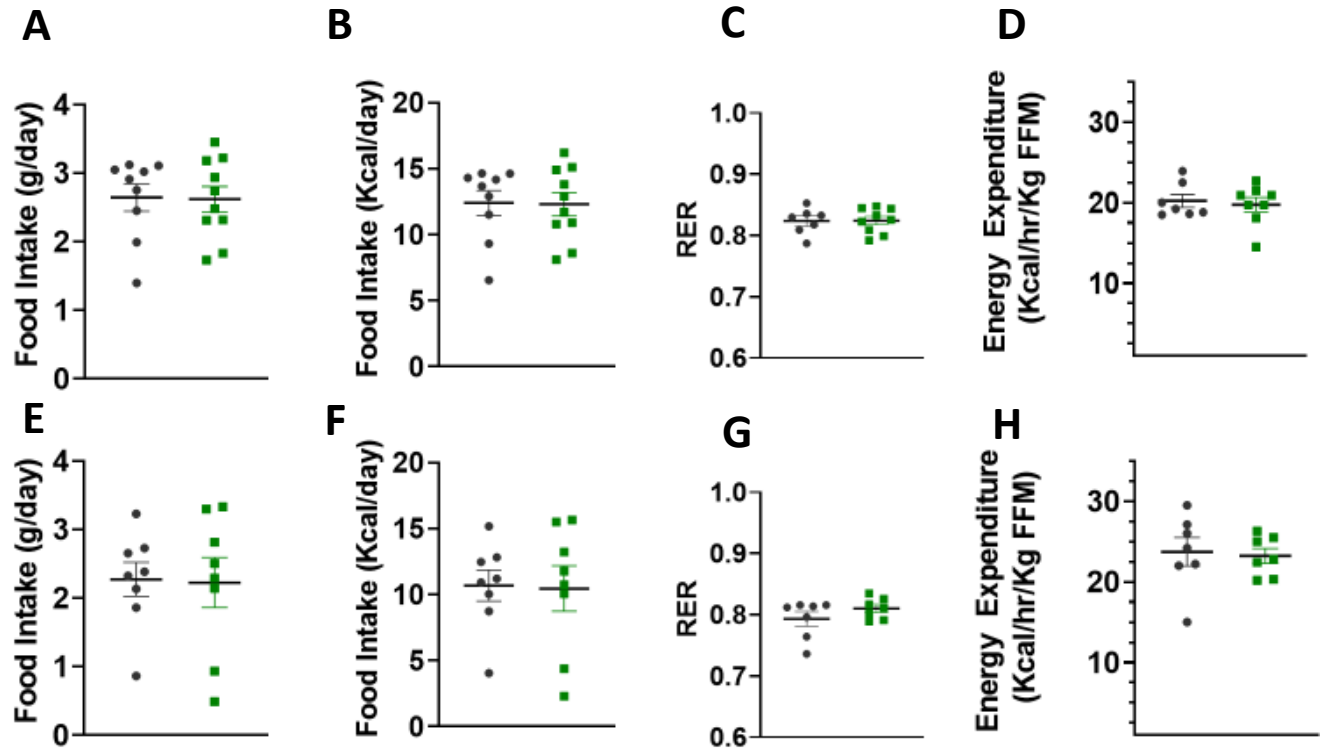
Figure 2-5: **Body weight, body weight gain, and fat mass for LFABP$^{fl/fl}$ (●) and LFABP$^{int-/-}$ (■)**

mice after 12 weeks of 45% Kcal HF feeding. *A,B*, Male mice 24-hour food intake (n=9-10); *C*,

Male mice 24-hour respiratory exchange ratio (n=7-9); *D*, Male mice energy expenditure (n=7-9);

E,F, Female mice 24-hour food intake (n=8-9); *G*, Female mice 24-hour respiratory exchange

ratio (n=7); *H*, Female mice energy expenditure (n=7).

LFABP^{int-/-} mice do not have alterations in plasma markers of energy balance

Oral glucose tolerance tests were performed on 6 hour fasted HF fed LFABP^{fl/fl} and LFABP^{int-/-} mice after 12 weeks of HF feeding. There were no differences in blood glucose concentrations for the male mice at any time point **(Fig 2-6A and B)**. Fasting plasma insulin **(Fig 2-6C)** and leptin levels **(Fig 2-6D and E)** also did not differ between the two groups. For female mice, like the male mice, no changes were observed in glucose tolerance **(Fig 2-6F and G)** or fasting plasma insulin **(Fig 2-6H)**. Fasting plasma leptin was found to be higher in female LFABP^{int-/-} mice relative to female LFABP^{fl/fl} mice **(Fig 2-6I)**, but a calculation of leptin index factoring in fat mass revealed no significant difference between these two groups **(Fig 2-6J)**.
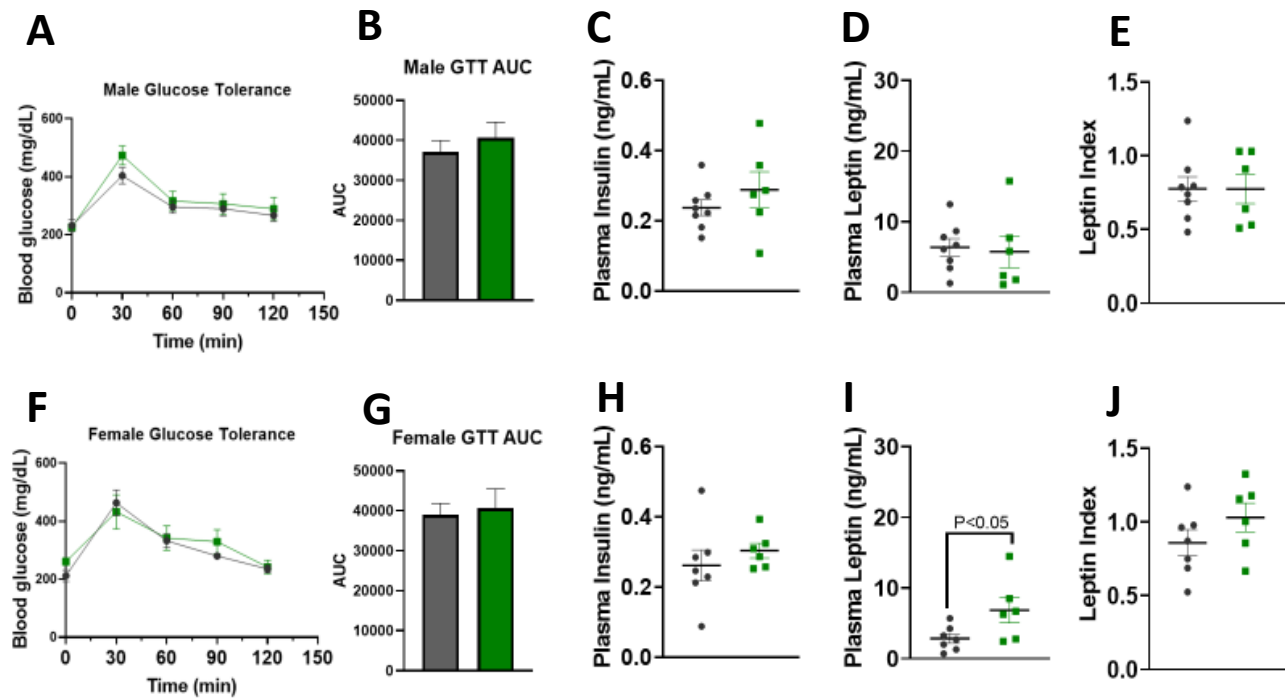
Figure 2-6: **Blood analyses for LFABP^fl/fl (●) and LFABP^int-/- (■) mice after 12 weeks of 45%**

Kcal HF feeding. *A,* Male mice glucose tolerance test (n=8); *B*, Male mice glucose tolerance area

under the curve (n=8); *C*, Male mice fasting plasma insulin (n=6-8); *D*, Male mice fasting plasma

leptin (n=6-8); *E*, Female mice leptin index (n=6-8); *F,* Female mice glucose tolerance test (n=6-

7); *G*, Female mice glucose tolerance area under the curve (n=6-7); *H*, Female mice fasting

plasma insulin (n=6-7); *I*, Female mice fasting plasma leptin (n=6-7); *J*, Female mice leptin index

(n=6-7).

LFABP^{int-/-} mice retain their exercise capacity following chronic HF feeding

Both spontaneous and induced physical activity parameters were assessed in the male and female LFABP-cKO mice. An assessment of 24-hour spontaneous activity revealed no differences between male LFABP^{fl/fl} and LFABP^{int-/-} mice **(Fig 2-7A)**. However, LFABP^{int-/-} mice were found to have higher exercise endurance relative to the LFABP^{fl/fl} mice, being able to run on the treadmill for a longer time **(Fig 2-7B)** and a farther distance **(Fig 2-7C)**. Like their male counterparts, the female LFABP-cKO mice did not have alterations in spontaneous activity **(Fig 2-7D)**, but female LFABP^{int-/-} mice did also display higher exercise endurance relative to their LFABP^{fl/fl} controls **(Fig 2-7E and F)**.
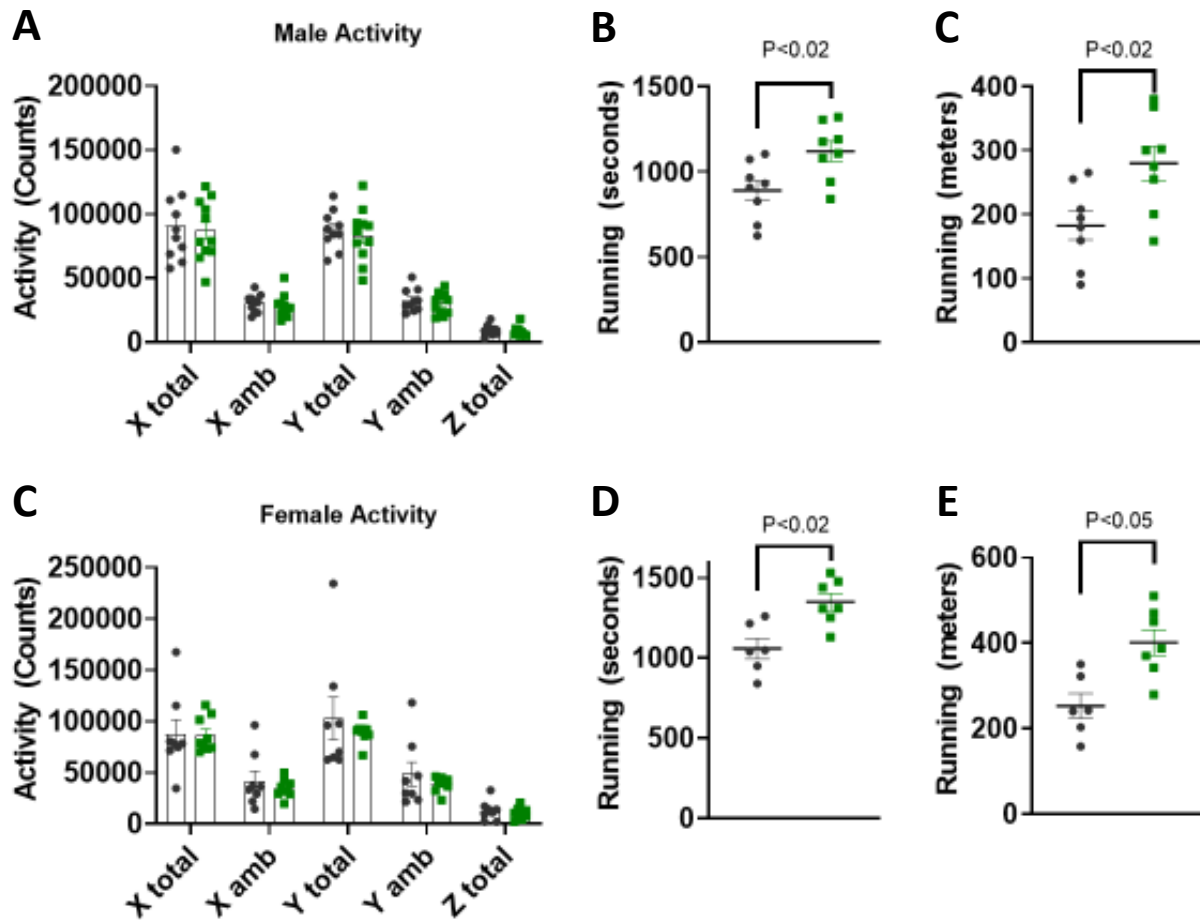
Figure 2-7: **Analyses of spontaneous of activity and endurance capacity for LFABP^{fl/fl} (●) and LFABP[int-/-] (■) mice after 12 weeks of 45% Kcal HF feeding.** *A,* Male mice 24-hour spontaneous activity (n=10-11); *B*, Male mice exercise endurance running time (n=8); *C*, Male mice exercise endurance running distance (n=8); *D*, Female mice 24-hour spontaneous activity (n=8-9); *E*, Female mice exercise endurance running time (n=6-7); *F*, Female mice exercise endurance running distance (n= 6-7).

Discussion

In previous studies, feeding whole-body LFABP^{-/-} male mice a HF diet resulted in increased body weight, fat mass, and food intake relative to WT mice [16]. While LFABP^{-/-} mice become obese they appear to be metabolically healthy, being normoglycemic, normoinsulinemic, and also displaying reduced hepatic steatosis, and intestinal TG secretion rates similar to those of lean mice despite their obesity [16,113,187,192]. Additionally, HF fed LFABP^{-/-} mice are more active and have greater exercise endurance that WT mice [16]. While whole-body LFABP^{-/-} mice appear to be a model of the MHO phenotype, it is unknown if the phenotypes observed are due to liver-LFABP, intestinal-LFABP, or if the ablation of both is necessary. In order to assess the role of intestinal-LFABP in the observed whole-body phenotypic response to HF feeding, LFABP conditional knockout (cKO) were generated. In this study, the intestine-specific LFABP null mouse was examined in order to determine the role of intestinal LFABP in the phenotype of the whole body LFABP-/-.

Unlike the whole-body male LFABP^{-/-} mice, male LFABP[int-/-] mice do not appear to become more obese in response to HF feeding. Their BW, BW gain, and body composition were similar to that of their WT-LFABP^{fl/fl} controls, and the WT controls of the previous HF feeding study [16]. While the obese phenotype of the LFABP^{-/-} mice can be partly explained by increased food intake, the LFABP[int-/-] mice did not have any observable differences in amount of food consumed. It is likely that the lack of differences observed in BW and body composition are partly due to the fact that food intake was not altered as well. The lack of changes observed here suggests that the ablation of LFABP in the liver is needed as well to induce increased food intake, BW, and fat mass.

Indirect calorimetric assessments using the Oxymax system previously demonstrated that HF fed LFABP^{-/-} mice have lower average RERs and increased spontaneous activity when compared to their WT counterparts, implying LFABP^{-/-} mice relied more so on lipid for metabolic fuel [16]. Additionally, an assessment of exercise endurance revealed that LFABP^{-/-} mice, despite being more obese, were able to run on a treadmill for a longer period than WT mice [16]. Unlike the LFABP[-]

[-] mice, male LFABP[int-/-] mice were found to have RER values comparable to their WT-LFABP^{fl/fl} controls, suggesting that the ablation of liver-LFABP is necessary to induce greater lipid usage at the whole-body level. Additionally, no changes were observed in spontaneous activity of the male LFABP-cKO mice.

While no alterations in spontaneous activity were observed, male LFABP[int-/-] mice retained their exercise capacity after chronic HF feed in response to an induced exercise bout, being able to run for a greater distance and period of time when compared to the LFABP^{fl/fl} mice. It had been hypothesized previously that LFABP^{-/-} mice might have better exercise endurance than WT mice because of their increased spontaneous activity. It was thought that this increase in activity might act as a self-induced form of chronic training, allowing the LFABP^{-/-} mice to be better adapted to potential exercise challenges. However, the increased exercise capacity of the LFABP[int-/-] mice does not support this notion, suggesting that the ablation of LFABP specifically in the intestine is able to influence exercise capacity. We have recently found that at rest the skeletal muscle of whole-body LFABP^{-/-} mice have increased glycogen stores and intramuscular TG (IMTG) levels [210], suggesting that LFABP^{-/-} mice have increased availability of carbohydrate and lipid substrates. Additionally, LFABP^{-/-} mouse skeletal muscle was observed to have increased FA oxidation and mitochondrial enzyme activity [210], which implies that there is increased substrate utilization occurring in LFABP^{-/-} skeletal muscle as well. Since LFABP is not expressed in the skeletal muscle, this suggests that there is interorgan cross talk occurring between tissues that express LFABP and skeletal muscle. Interestingly, moreover, there is evidence of cross talking occurring between the gut, skeletal muscle, and cardiac muscle that influences physiological responses to exercise or overnutrition [211–214]. It is thought that this communication is bidirectional, being mediated by the microbiome and mitochondria [213]. For example, some commensal bacteria are able to produce short chain fatty acids (SCFAs), which are able to modulate mitochondrial function, impacting energy production and mitochondrial biogenesis [213]. Mitochondria, in turn, are

able to modify the activity of the microbiome by altering innate immune responses [213]. Thus, it is feasible that the intestine specific ablation of LFABP, a protein that is normally highly abundant in the small intestine, can yield a phenotype in skeletal and/or cardiac muscle.

Aspects of whole-body metabolic signaling were previously assessed in HF fed male LFABP^{-/-} mice. Despite being more obese, it was observed that LFABP^{-/-} mice had fasting insulin levels similar to that of their leaner WT counterparts. It was also shown that HF fed LFABP^{-/-} mice had elevated plasma leptin and leptin index values; low fat (LF) fed LFABP^{-/-} mice, which were as lean as LF fed WT mice, also had elevated plasma leptin and leptin index values, indicating that the elevation of plasma leptin was intrinsic to the whole-body ablation of LFABP and not alterations in fat mass [16]. Male LFABP[int-/-] mice did not have elevated leptin levels or leptin index values, suggesting that the ablation of liver-LFABP is necessary for the elevated leptin phenotype to be present.

In contrast to these observations, and unlike what was observed for male LFABP[int-/-] mice, female LFABP[int-/-] mice gained more weight and had greater fat mass when compared to female LFABP^{fl/fl} mice. Despite these alterations in BW and body composition, no differences were observed in food intake, RER, or energy expenditure. It is possible that, instead, these changes are induced by altered intestinal transit of nutrients. We have recently found that whole-body HF fed LFABP^{-/-} have decreased total fecal output and slower intestinal transit times (unpublished data), which may partly explain their obese phenotype as well. A longer intestinal transit time would provide more time for digestive enzymes to interact with chyme in the small intestine, which may lead to more efficient or complete nutrient absorption [215,216]. It remains to be determined whether or not the transit phenotype is also present in the female LFABP[int-/-] mice.

Aside from differences in BW and body composition, the phenotypic observations made in the female LFABP-cKO mice were similar to that of the male LFABP-cKO mice. While no differences were observed for glucose tolerance or fasting plasma insulin, female LFABP[int-/-] mice were found

to have higher fasting leptin levels. However, once fat mass was factored in there were no longer significant differences between the female WT and KO mice. Additionally, while spontaneous activity did not differ between female LFABP[int-/-] and LFABP[int-/-] mice, it was observed that the LFABP[int-/-] mice also retained their exercise capacity in response to chronic HF feed, having greater running endurance when compared to LFABP^{fl/fl} mice. This suggests that, unlike the body composition phenotype, the exercise endurance phenotype is not gender dependent, and only requires the ablation of intestinal-LFABP.

Others have assessed obesity-related phenotypes in female LFABP^{-/-} mice. In the hands of one group in St. Louis, female LFABP^{-/-} mice fed a 41% Kcal butter fat HF diet were found to be resistant to induced obesity and the development of hepatic steatosis [187,217]. However, a group in Texas demonstrated that female LFABP^{-/-} gained more weight when challenged with a HF diet [190]. Additionally, female LFABP^{-/-} mice maintained on standard chow were more prone to obesity in response to aging [188]. However, the St. Louis group found that under similar conditions, female LFABP^{-/-} mice were resistant to age induced obesity [113]. As mentioned above, the St. Louis LFABP^{-/-} mice tend to gain less weight than WT in response to different challenges, while the Texas mice and our mice become obese [11,16,113,186,188]. Differences may be attributable to differences in gene knockout strategies, background strain, or the gut microbiome. Despite the differences in weight gain responses, however, the St. Louis LFABP^{-/-} and Texas LFABP^{-/-} lines share many similarities, including defective hepatic FA uptake, oxidation, and VLDL secretion [161,185,187,190]. We have not previously assessed female whole-body LFABP^{-/-} mice. Given differences observed in the female LFABP[int-/-] mice, it is of interest to pursue similar studies in HF fed female LFABP^{-/-} mice.

Many of the phenotypes observed in the HF fed male LFABP^{-/-} mice were not present in HF fed male LFABP[int-/-] mice. It is possible that phenotypic changes, such as the obesity, elevated leptin, and alterations in RER require either the ablation of liver-LFABP alone or the simultaneous

ablation of bother liver- and intestine-LFABP. Studies of liver-specific LFABP^{-/-} mice (LFABP[Liv-/-]) are underway to help determine the tissue specific origins of the MHO phenotype observed in the male LFABP^{-/-} mice. Additionally, since differences were observed in the response of male and female LFABP[int-/-] mice to HF feeding, it will be important to determine the sex specific interactions that may influence, or be influenced by, the presence or absence of LFABP.

Chapter 3

Mechanisms Underlying Reduced Weight Gain in Intestinal Fatty Acid-Binding Protein (IFABP) Null Mice

Abstract

Intestinal-fatty acid binding protein (IFABP; FABP2) is a 15 kDa intracellular protein abundantly present in the cytosol of the small intestinal enterocyte. High fat (HF) feeding of IFABP$^{-/-}$ mice resulted in reduced weight gain and fat mass relative to wild-type (WT) mice. Here, we examined intestinal properties that may underlie the observed lean phenotype of high fat-fed IFABP$^{-/-}$ mice. No alterations in fecal lipid content were found, suggesting that the IFABP$^{-/-}$ mice are not malabsorbing dietary fat. However, the total excreted fecal mass for the IFABP$^{-/-}$ mice was increased relative to WT mice. Moreover, we found reduced intestinal transit time in the IFABP$^{-/-}$ mice. IFABP$^{-/-}$ mice were observed to have a shortened average villus length, a thinner muscularis layer, reduced goblet cell density, and reduced Paneth cell abundance. The number of proliferating cells in the crypts of IFABP$^{-/-}$ mice did not differ from that of WT mice, suggesting that the blunt villi phenotype is not due to alterations in proliferation. IFABP$^{-/-}$ mice were observed to have altered expression of genes related to intestinal structure, while immunohistochemical analyses revealed increased staining for markers of inflammation. Taken together, the ablation of IFABP leads to changes in gut motility and morphology which likely contribute to the relatively leaner phenotype occurring at the whole-body level. Thus, these results suggest that IFABP is likely involved in dietary lipid sensing and signaling, influencing intestinal motility, intestinal structure, and nutrient absorption, thereby impacting systemic energy metabolism.

Introduction

The small intestine is the primary site of dietary lipid absorption, where the absorptive enterocytes are responsible for processing the hydrolysis products of dietary lipids. Though dietary triacylglycerol (TG) content is particularly high in Western diets, absorption from the lumen of its hydrolysis products , fatty acid (FA) and monoacylglycerol (MG), is highly efficient, with greater than 95% of dietary lipid taken up [11,33]. Intracellular carrier proteins are thought to be required for efficient trafficking of these hydrophobic lipid species within the hydrophilic cytoplasmic milieu, although this has not been definitively shown. The intestinal-fatty acid binding protein (IFABP; FABP2) is a member of the FABP family, a group of 14-15 kDa intracellular proteins that are present in high abundance (1-5%) in the cytosol of most tissues [11,12,126]. Like other members of the FABP family, IFABP has a high affinity for long-chain fatty acids (LCFAs) [144] and *in vitro* studies have shown that IFABP transfers FAs to membranes via a collisional mechanism that is typical of most members of the FABP family [147]. Several *in vitro* and *ex vivo* studies have suggested that IFABP is involved in enterocyte uptake of FA from both the intestinal lumen and the bloodstream [148,184]. However, a number of studies in animal models lacking IFABP have found that FA uptake is not impaired [15,16,191].

We previously showed that on a 45% Kcal fat high fat diet (HFD) IFABP^{-/-} mice remained lean when compared to WT mice, displaying reduced body weight (BW), BW gain, and lower fat mass percentage [16]. Food intake was significantly lower in the IFABP^{-/-} mice, but food efficiency calculations indicated that the observed decrease in BW of the IFABP^{-/-} mice could not be fully explained by the decrease in food intake [16]. Since, as noted above, the enterocyte FABPs have long been thought to be involved in dietary lipid uptake and assimilation [11], it is tempting to speculate that mice lacking IFABP might malabsorb lipid, thus explaining their observed lean phenotype. Fecal lipid content did not vary between groups, however, suggesting that the IFABP^{-/-} mice were not malabsorbing lipid [16]. As it is possible that the lipid content of the 45% Kcal HFD

is not sufficient to stress the absorptive capacity of the small intestinal enterocytes, in the present studies we examined fecal fat in mice fed a supraphysiological 60% Kcal fat diet. In addition, we determined not only fecal lipid content, but also the small intestinal localization of FA absorption along the proximal to distal axis, total fecal excretion, and the intestinal transit time of mice fed the 45% Kcal HFD.

During organ collection, it was observed that the intestinal tissue of the HF fed IFABP^{-/-} mice seemed to be more fragile than that of WT mice. We, therefore, hypothesized that the ablation of IFABP may lead to alterations in intestinal structure and, perhaps, inflammation. Thus, gene expression, histological, and immunohistochemical analyses were performed to assess small intestinal integrity and inflammatory status. Additionally, we assessed small intestine goblet cell density, since mucus production by the goblet cells is important for intestinal integrity [41]. We also examined Paneth cell density, as Paneth cells secrete antimicrobial peptides and other molecules that regulate cell proliferation and differentiation [44].

The results showed no differences, relative to WT mice, in the fecal lipid content of IFABP^{-/-} mice, even when challenged with the 60% Kcal HFD. Interestingly, however, HF fed IFABP^{-/-} mice were found to have increased total fecal excretion and reduced energy absorption, which was explained, at least in part, by a more rapid intestinal transit rate. Additionally, IFABP^{-/-} mice were found to have altered expression of genes encoding intestinal structural markers and markers of ER stress, shorter proximal small intestinal villi, a thinner muscularis layer, a reduction in Paneth cell abundance, and a reduced goblet cell density. Collectively, these changes in the IFABP^{-/-} intestinal mucosa indicate a heretofore unappreciated role for IFABP in intestinal motility and integrity, and suggests that reduced weight gain is secondary to increased fecal excretion of lipids, and likely, other nutrients.

Experimental Procedures

Animals and Diets

As previously reported, the IFABP^{-/-} mice used in this study are a substrain bred by intercrossing of an original strain of IFABP^{-/-} mice and are congenic on a C57BL/6J background [15,128,191]. C57BL/6J mice from The Jackson Laboratory (Bar Harbor, ME) were bred as wild-type (WT) controls. Mice were housed 2-3 per cage unless specified otherwise, maintained on a 12-hour light/dark cycle, and allowed *ad libitum* access to standard rodent chow (Purina Laboratory Rodent Diet 5015). At 2 months of age, male WT and IFABP^{-/-} mice were fed either a 45% Kcal fat high fat diet (HFD) (D10080402; Research Diets, Inc., New Brunswick, NJ), a 60% Kcal HFD (D04051705; Research Diets), or a 10% Kcal fat low fat diet (LFD) (D10080401; Research Diets) as indicated. Body weights (BW) were measured weekly for a period of 12 weeks. Fat mass measurements were taken by MRI (Echo Medical Systems, LLC., Houston, TX) 2-3 days prior to starting the feeding protocol, and 2-3 days prior to sacrifice. The instrument was calibrated each time according to the manufacturer's instructions. At each time point, two measurements were taken for each mouse and averaged.

Preparation of Tissue and Plasma

Mice were fasted for 16 hours prior to sacrifice unless otherwise stated. At sacrifice blood was drawn; plasma was isolated after centrifugation for 6 minutes at 4000 rpm, and stored at -80°C. Epididymal fat pads and livers were removed, immediately placed on dry ice, and stored at -80°C for further analysis. The small intestine from the pyloric sphincter to the ileocecal valve was removed, measured lengthwise, rinsed with 60mL of ice-cold 0.1M NaCl, and opened longitudinally. Intestinal mucosa was scraped with a glass microscope slide into tared tubes on dry ice and stored for future use.

RNA Extraction and Real-Time PCR

Total mRNA was extracted from small intestinal mucosa and analyzed as previously described [15,16]. Primer sequences were obtained from Primer Bank (Harvard Medical School QPCR Primer Database) and are shown in Table 1. The efficiency of PCR amplifications was analyzed for all primers to confirm similar amplification efficiency. Real time PCRs were performed in triplicate using an Applied Biosystems 7300 instrument. Each reaction contained 80ng of cDNA, 250nM of each primer, and 12.5µL of SYBR Green Master Mix (Applied Biosystems, Foster City, CA) in a total volume of 25µL. Relative quantification of mRNA expression was calculated using the comparative Ct method, normalized to TATA-binding protein (TBP). Primer sequences for the genes that were analyzed are shown in Table 1.

Western Blot Analysis

Small intestinal mucosa was harvested as described above, and homogenized in 10x volume of PBS pH 7.4 with 0.5% (vol/vol) protease inhibitors (Sigma 8340) on ice with a Potter Elvejhem homogenizer. Total cytosolic fractions were obtained by ultracentrifugation (100,000g, 1 hour at 4°C) and protein concentration determined by Bradford assay [209]. Thirty micrograms of cytosolic protein was mixed with an Instant-Bands pre-stained protein sample loading buffer in a 2:1 (v/v) ratio (EZBiolab, Carmel, IN) to allow for visualization of total sample protein. Samples were loaded onto 15% polyacrylamide gels and separated by SDS-PAGE. The proteins were transferred onto 0.45µm nitrocellulose membranes using a semidry transfer system (Bio-Rad) for 1 hour and 45 minutes at 23 V. Membranes were blocked by incubating in 5% nonfat dry milk overnight at 4°C, and were incubated with a primary antibody of either α-LFABP (1:2000 for 1 hour at room temperature[15]) or α-IFABP (1:10,000 for 1 hour at room temperature; generous gift from B. Corsico, U. La Plata). For assessing phosphorylated and total eIF2α, membranes were blocked in 5% milk for 1 hour at room temperature, and then incubated with either α-phospho(S51)-eIF2α (1:5000, Cell Signaling Technology, CST 3597) or α-eIF2α (1:5000, Santa Cruz, sc-11386)

overnight at 4°C [218]. After thorough washing, blots were incubated in α-rabbit IgG-horseradish peroxidase conjugate (1: 20,000) for 1 hour, and developed by chemiluminescence (WesternBright Quantum, Advansta, Menlo Park, CA). Protein expression was quantified by densitometric analysis with LI-COR Image Studio (Lite version 5.2). Target protein content was normalized to total protein content within a sample.

Fecal Lipid Content

During the 12-week high fat feeding periods, feces were collected between weeks 10 and 12 of the feeding protocol, and subsequently dried at 60°C for 3 days. 0.5g (dry weight) of feces was dissolved in water overnight, and lipids extracted using the Folch method [219]. The extracted lipids in 2:1 chloroform/methanol (v/v) were placed in pre-weighed glass tubes, dried down completely under a nitrogen stream, and recovered lipid mass determined by weight difference. The weight of the extract was divided by the original dry weight of the feces to determine the percent fecal lipid.

Fat Absorption Localization Experiment

The protocol described by Nelson et al. was modified to perform fat absorption localization experiments [220]. In short, following a 4.5 hour fast, mice were gavaged with 8 µCi of ^{3}H-labeled TG in 200µL olive oil. The mice were then anesthetized 1.5 hour after the gavage and the small intestine was excised, rinsed with 0.85% NaCl, and then cut into 2 cm sections. The intestinal sections were digested overnight in 500µL of 1 M NaOH at 60°C. The next day 300µL of 1 N HCl was added to quench, and the radioactivity of each section was measured in a scintillation counter.

Intestinal Transit Time

Individually housed mice were allowed *ad libitum* access to food and water. After two hours of acclimation, mice were given 200µL of 6% carmine red and 0.5% methylcellulose (Sigma-Aldrich,

St. Louis, MO) in PBS by oral gavage. The cages were inspected every 10 minutes post gavage, and the time of appearance of the first red fecal pellet was recorded [221,222].

Total Fecal Excretion

Mice were housed 2-3 per cage. Feces from each cage were collected every 3-4 days, and subsequently dried overnight and weighed. The weight of the feces was divided by the number of mice in the cage, and by the number of days of collection. To control for differences in food intake, the results for each genotype were normalized to their respective 24-hour food intakes, to generate values of g feces excreted/g consumed/mouse/day.

Bomb Calorimetry

Fecal energy content was assessed using a microbomb calorimeter (Parr) with a benzoic acid standard. Briefly, 6 fecal pellets were homogenized in 2mL water to form a uniform slurry. Fecal samples were then frozen at -80°C. Thawed samples were lyophilized and each sample was used to form 2 uniform pellets with a pellet press. Each pellet was separately loaded into the microbomb calorimeter for caloric density assessment. Each pellet represented one measure per sample, allowing for samples to be measured in duplicate. Energy absorbed was determined by calculating the energy ingested from the semi-purified HF diet/24h minus the energy excreted in the feces/24h.

Plasma Endotoxin Analysis

Plasma endotoxin levels were assessed using a Pierce™ LAL Chromogenic Endotoxin Quantitation Kit (Cat no. 88282, ThermoFisher Scientific), according to manufacturer's instructions. Samples were run in triplicate and averaged to provide a plasma endotoxin value for each mouse.

FITC-Dextran Intestinal Permeability Assay

Intestinal permeability was assessed by a modified version of the protocol described by Wotin and Blaut [216]. Briefly, after a 6 hour fast, mice were orally gavaged with 150 µL of fluorescein isothiocyanate (FITC)–dextran (100 mg/mL) (Cat no. 60842-46-8, Millipore Sigma). Four hours post-gavage, mice were sacrificed and whole blood was collected. Serum was isolated by centrifugation and kept in the dark at room temperature for 30 minutes prior to analysis. A standard curve was developed on a 96-well plate using FITC-dextran concentrations in a range between 100 µg/mL to 1 µg/mL. Fluorescence intensities of the standards and samples were then measured using an excitation of 485nm and emission of 528nm. Following blank subtraction, sample FITC concentrations were determined based on the standard curve, in ug/ml.

Histochemical and Immunohistochemical (IHC) Analyses

Small intestines were removed as described above. The first 6th of the SI, representing the proximal SI, was isolated, rinsed with a cold 0.85% sodium chloride solution, opened longitudinally, Swiss rolled, and fixed overnight at 4°C in 3% paraformaldehyde (PFA) and 2% sucrose in phosphate buffered saline. Tissues were then embedded in paraffin. For initial histological analysis, 5µm intestinal tissue sections were stained with hematoxylin and eosin (H&E) (Rutgers Pathology Services, Piscataway, NJ). Average villus length was assessed by dividing H&E stained Swiss roll sections into 5 quadrants and measuring 20 villi per quadrant, for a total of 100 villi measured per animal. To assess average muscularis thickness, 80 separate measurements were recorded for each animal. These were averaged to provide a value specific to that mouse. Goblet cells were enumerated using periodic acid-Schiff (PAS)/Alcian blue, which stained acidic and neutral mucins, respectively. Goblet cell count was normalized to villus length, allowing for goblet cell density to be determined. For the visualization of Paneth cells, phloxine-tartrazine staining was performed (Lendrum's stain kit; Cat no. ES9540, ThermoFisher Scientific). For IHC studies, 5µm intestinal sections were deparaffinized, rehydrated, and blocked with 100%

normal goat serum at room temperature for 2 hr. The tissue sections were then incubated overnight at 4°C with a primary rabbit polyclonal COX-2 antibody (1:500, Abcam, Cambridge, MA), mucin 2 antibody (1:100, Abcam), iNOS antibody (1:100, Abcam), Claudin 2 antibody (1:200, Abcam), Claudin 5 antibody (1:200, Abcam), or mouse polyclonal MCP1 antibody (1:200, Abcam). Tissue sections were then incubated for 30 min with a either a biotinylated goat anti-rabbit secondary antibody (1:10000, Vector Labs, Burlingame, CA) or biotinylated horse anti-mouse secondary antibody (1:10000, Vector Labs). Antibody binding was visualized using a DAB Peroxidase Substrate Kit (Vector Labs). Tissue sections were scanned using the VS120-L100 Olympus virtual slide microscope (Waltham, MA).

Bromodeoxyuridine Assays

Proliferation was assessed by measuring the incorporation of bromodeoxyuridine (BrdU). Mice were injected with 200μL of BrdU (BD Biosciences) intraperitonially 2 hours or 48 hours prior to sacrifice. Small intestines were removed, Swiss rolled and fixed overnight at 4°C in a 3% PFA solution. IHC staining for BrdU was then performed using an anti-BrdU antibody (1:400; BD Biosciences). Tissue sections were then incubated for 30 min with a biotinylated horse anti-mouse secondary antibody (1:10000, Vector Labs, Burlingame, CA). Antibody binding was visualized using a DAB Peroxidase Substrate Kit (Vector Labs).

Statistical Analysis

All group data are shown as average ± SEM. Statistical comparisons were determined between genotypes on the same diet using a two-sided Student's *t* -test. Differences were considered significant for $P<0.05$.

Table 1: Primer sequences used for qPCR analyses.

TBP-F	5'-CAAACCCAGAATTGTTCTCCTT-3'
TBP-R	5'-ATGTGGTCTTCCTGAATCCCT-3'
Claudin1-F	5'-GCCTTGATGGTAATTGGCATCC-3'
Claduin1-R	5'-GGCCACTAATGTCGCCAGAC-3'
Claduin2-F	5'-AGTACCCTTTTAGGACTTCCTGC-3'
Claudin2-R	5'-CCCACCACAGAGATAATACAAGC-3'
Claduin3-F	5'-ACCAACTGCGTACAAGACGAG-3'
Claudin3-R	5'-CGGGCACCAACGGGTTATAG-3'
Claduin4-F	5'-ATGGCGTCTATGGGACTACAG-3'
Claduin4-R	5'-GAGCGCACAACTCAGGATG-3'
Claudin5-F	5'-GCAAGGTGTATGAATCTGTGCT-3'
Claduin5-R	5'-GTCAAGGTAACAAAGAGTGCCA-3'
CDH1-F	5'-CAGGTCTCCTCATGGCTTTGC-3'
CDH1-R	5'-CTTCCGAAAAGAAGGCTGTCC-3'
Occludin-F	5'-ACCCGAAGAAAGATGGATCG-3'
Occludin-R	5'-CATAGTCAGATGGGGGTGGA-3'
ZO1-F	5'-TGGGAACAGCACACAGTGAC-3'
ZO1-R	5'-GCTGGCCCTCCTTTTAACAC-3'
JAMA-F	5'-CTGATCTTTGACCCCGTGAC-3'
JAMA-R	5'-ACCAGACGCCAAAAATCAAG-3'
Beta Actin-F	5'-GGCTGTATTCCCCTCCATCG-3'
Beta Actin-R	5'-CCAGTTGGTAACAATGCCATGT-3'
LFABP-F	5'-GGGGGTGTCAGAAATCGTG -3'
LFABP-R	5'-CAGCTTGACGACTGCCTTG-3'
IFABP-F	5'-GTGGAAAGTAGACCGGAACGA-3'
IFABP-R	5'-CCATCCTGTGTGATTGTCAGTT-3'
HFABP-F	5'-ACCTGGAAGCTAGTGGACAG-3'
HFABP-R	5'-TGATGGTAGTAGGCTTGGTCAT-3'
AFABP-F	5'-AAGGTGAAGAGCATCATAACCCT-3'
AFABP-R	5'-TCACGCCTTTCATAACACATTCC-3'
KFABP-F	5'-TGAAAGAGCTAGGAGTAGGACTG-3'
KFABP-R	5'-CTCTCGGTTTTGACCGTGATG-3'
ILBP-F	5'-CTTCCAGGAGACGTGATTGAAA-3'
ILBP-R	5'-CCTCCGAAGTCTGGTGATAGTTG-3'

Results

IFABP^{-/-} mice remain lean on supraphysiologic high fat diets

At 8 weeks of age, prior to the start of HF feeding, IFABP^{-/-} and WT mice had similar BW, fat mass, and fat free mass (data not shown). As previously demonstrated [16], after 12 weeks of 45% Kcal HF feeding, IFABP^{-/-} mice gain less weight and remain lean when compared to WT mice **(Fig 3-1)**. When challenged with a supraphysiologic 60% Kcal HFD for 12 weeks the same pattern is observed, with IFABP^{-/-} mice still gaining less weight and remaining leaner than WT mice **(Fig 3-1)**.

Ablation of IFABP does not cause compensatory upregulation of LFABP in HF diet-fed mice

The expression of LFABP in response to ablation of IFABP was assessed after 12 weeks of 45% Kcal fat high fat feeding. As was observed previously for mice fed a low-fat chow diet, IFABP^{-/-} mice do not have increased LFABP mRNA or protein levels relative to WT mice **(Fig 3-2A and B)**. Additionally, we found no compensatory upregulation of the distal small intestinal FABP, ileal FABP (ILBP, FABP6); other FABPs that are not typically expressed within the SI were also not observed in either WT or IFABP^{-/-} intestine from the HF-fed mice **(Fig 3-2A)**.
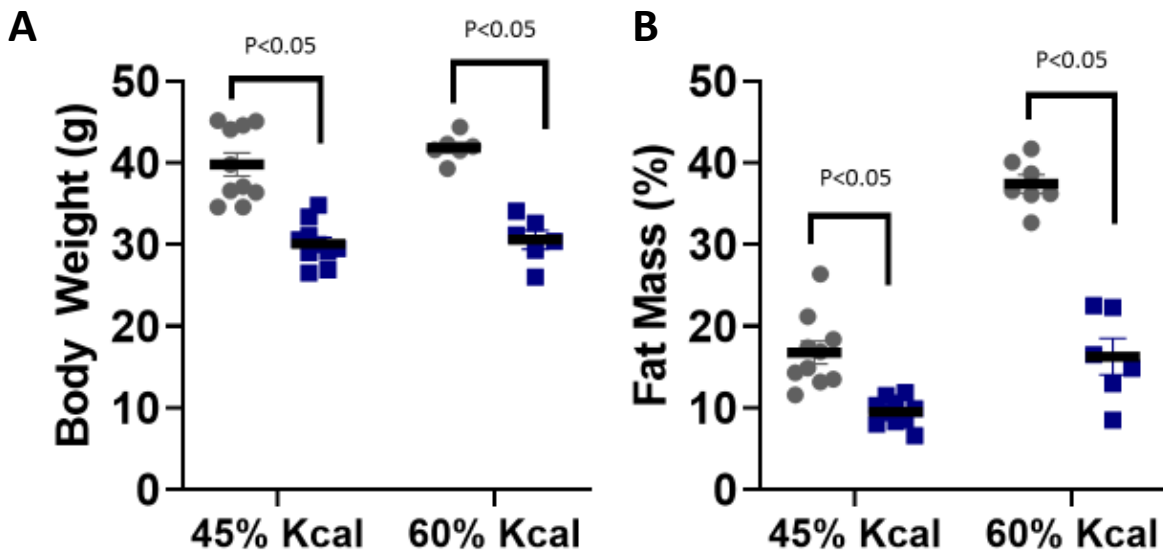
Figure 3-1: **Body weight and fat mass for WT (●) and IFABP$^{-/-}$ (■) mice after 12 weeks of 45%**

Kcal or 60% Kcal fat feeding. *A*, body weights on 45% Kcal fat (n=10) or 60% Kcal fat HFD

(n=6-7); *B*, body fat percentage on 45% Kcal fat (n=10) or 60% Kcal fat HFD (n=6-7).
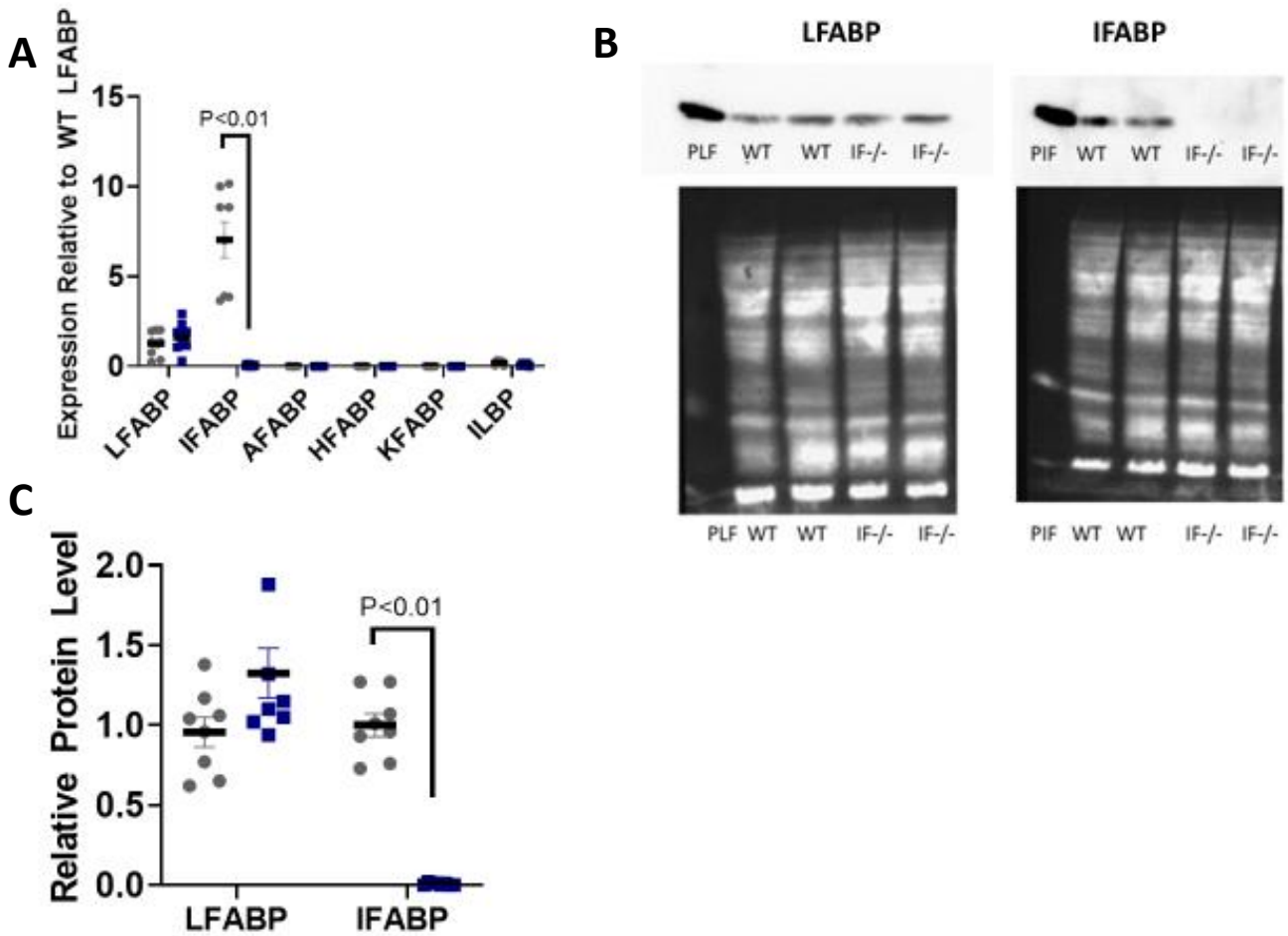
Figure 3-2: **mRNA expression and protein levels of proximal small intestine FABPs in WT (●) and IFABP$^{-/-}$ (■) mice after 12 weeks of 45% Kcal HFD.** *A*, relative gene expression of FABP family members (n=5-12); *B*, the top panels are Western blot membranes blotting for either LFABP (left) or IFABP (right). The bottom panels show the total protein content of the Western membranes. PLF, purified LFABP, PIF, purified IFABP; *C*, relative protein levels of IFABP or LFABP (n=8). Purified LFABP (pLF) and Purified IFABP (pIF) were loaded as positive controls for the Western blots.

Mice lacking IFABP have increased fecal mass, reduced energy absorption, and rapid intestinal transit

Consistent with previous observations, IFABP^{-/-} mice do not appear to malabsorb lipid on a 45% Kcal HF diet, based on fecal fat content **(Fig 3-3A)**. Similarly, in mice challenged with the very high 60% Kcal fat diet, no differences in fecal fat content were noted between IFABP^{-/-} and WT mice **(Fig 3-3A)**. Additionally, no shift in [^{3}H]-FA uptake along the proximal to distal axis of the small intestine was observed in mice challenged with the 45% Kcal HFD **(Fig 3-3B)**. Interestingly, however, analysis of total fecal mass showed that 45% Kcal HF fed IFABP^{-/-} mice have a significant increase in total fecal excretion, controlling for total food intake **(Fig 3-3C)**. Further, the IFABP^{-/-} mice had significantly shorter intestinal transit times, indicating that nutrients moved from mouth to anus more rapidly **(Fig 3-3D)**. Together these data imply that the IFABP^{-/-} mice are, indeed, absorbing less lipid than WT mice. Moreover, they may be absorbing less of other nutrients as well; as evidenced by the increase in fecal mass without a change in fecal fat content. This was confirmed by bomb calorimetric assessment of fecal caloric density, which revealed that there were no differences between WT and IFABP^{-/-} mice **(Fig 3-3E)**. Indeed, since IFABP^{-/-} mice ingest less calories per day and secrete the same amount of calories per day in their feces, they have a net reduction in energy that is absorbed from the diet when compared to their WT counterparts. The rapid transit time, increased fecal excretion, and reduced energy absorption suggest that IFABP may play a role in the regulation of intestinal motility and, hence, in lipid and nutrient absorption.
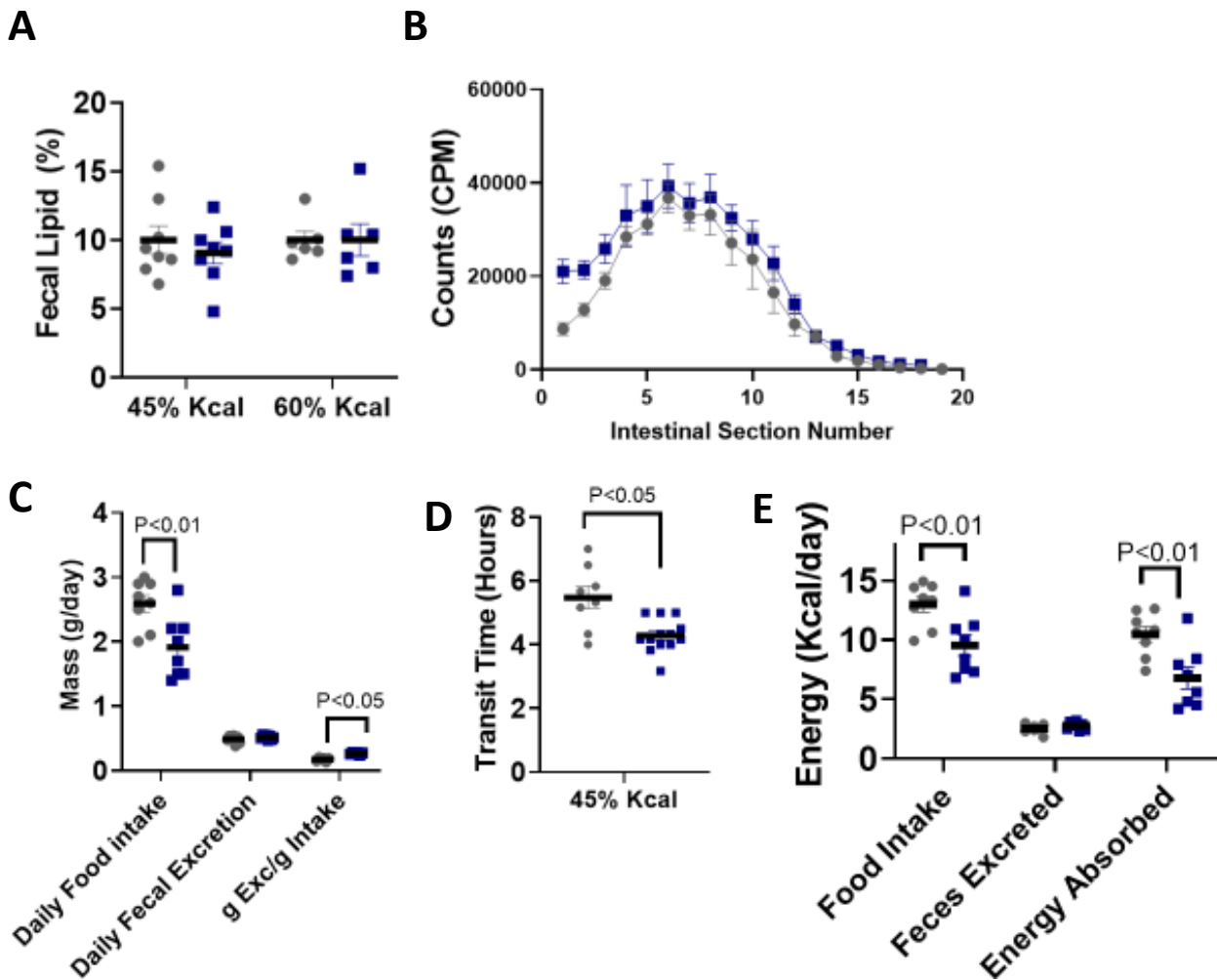
Figure 3-3: **Fecal lipid content, fat absorption localization, total fecal output, and intestinal transit times in WT (●) and IFABP$^{-/-}$ (■) mice after 12 weeks of HF feeding.** *A,* fecal lipid percentage from 45% Kcal HF fed WT and IFABP$^{-/-}$ mice (n=8) and fecal lipid percentage from 60% Kcal HF fed WT and IFABP$^{-/-}$ mice (n=6). B, localization of intestinal lipid absorption 1.5 hours after oral gavage of [^{3}H]TG in olive oil in mice fed the 45% Kcal HFD (n=6-8). *C,* daily food intake and fecal excretion in WT and IFABP$^{-/-}$ mice fed the 45% Kcal HFD, and fecal excretion normalized for intake (n=6). *D,* intestinal transit time in WT and IFABP$^{-/-}$ mice fed the 45% Kcal HFD (n=8-13). *E,* daily energy intake and energy absorption (accounting for energy excretion) in WT and IFABP$^{-/-}$ mice fed the 45% Kcal HFD (n=8).

Alterations in small intestine morphology and structure

IFABP$^{-/-}$ mice were found to have a 7% shorter small intestine length when compared to WT mice **(Fig 3-4A)** (p< 0.05), however when normalized to average BW, IFABP$^{-/-}$ mice have an 8% longer SI for their size, relative to WT mice **(Fig 3-4B)** (p<0.05). Analysis of H&E stained sections revealed that the proximal small intestinal villi of HF-fed IFABP$^{-/-}$ mice are 39% shorter than the villi of WT mice **(Fig 3-5)** (p< 0.01). In addition to having shortened villi, IFABP$^{-/-}$ mice were also found to have a thinner muscularis layer **(Fig 3-5)**. Alcian blue/PAS staining revealed that IFABP$^{-/-}$ mice have significantly fewer small intestinal goblet cells than WT mice, and when normalized to average villus length, a reduced goblet cell density **(Fig 3-5)** (p< 0.01). In addition to having a reduced goblet cell density, Lendrum's staining revealed that the other major secretory cells of the small intestine, Paneth cells, were also in low abundance in IFABP$^{-/-}$ mice **(Fig 3-5)**.
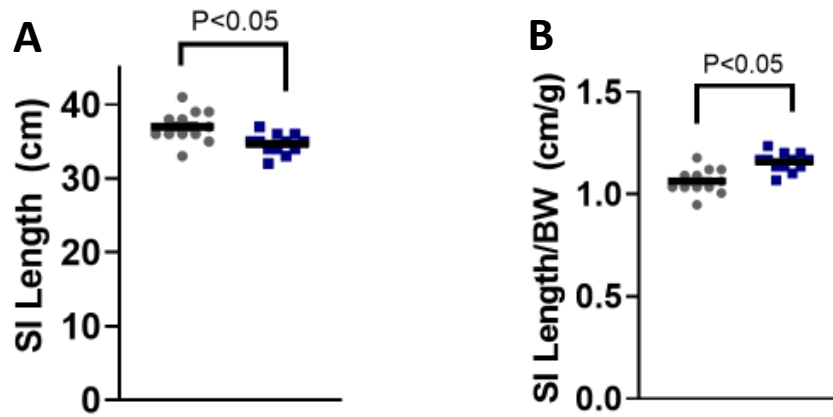
<u>Figure 3-4:</u> **Average length of small intestine in WT (●) and IFABP$^{-/-}$ (■) mice that have been fed a 45% Kcal HFD for 12 weeks.** *A,* average small intestine length in HF fed WT and IFABP$^{-/-}$ mice. *B*, average small intestine length normalized to the average body mass in HF fed WT and IFABP$^{-/-}$ mice (n=12).
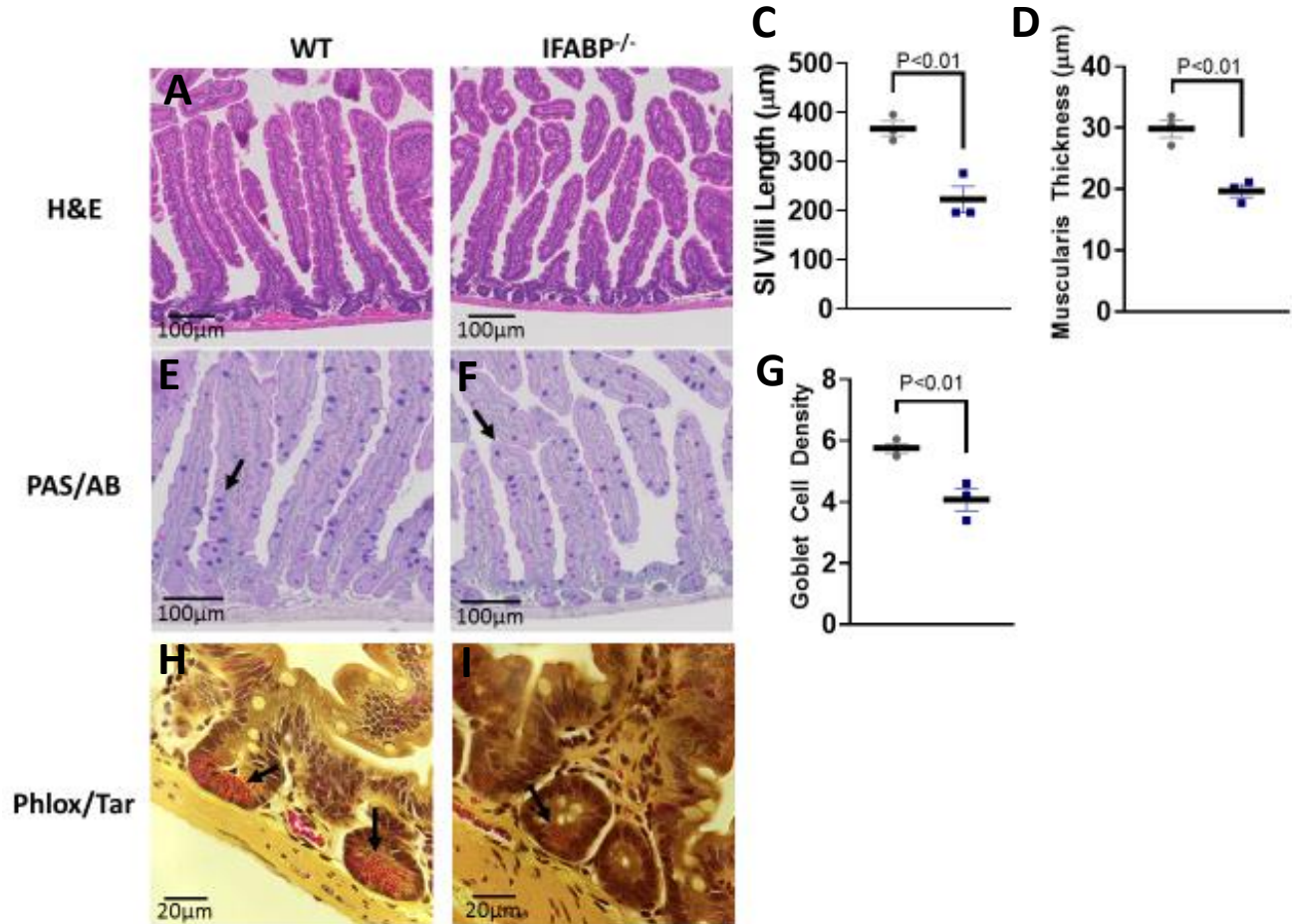
Figure 3-5: **Small intestinal structure in 45% Kcal HF fed WT (●) and IFABP$^{-/-}$ (■) mice.** *AB,* Hematoxylin and eosin (H&E) stained small intestinal tissue sections (6.6X). *CD,* Periodic acid-Schiff (PAS)/Alcian blue used to visualize goblet cells (8X). The arrows point to positive staining for mucins. *EF*, Lendrum's stain used to visualize secretory Paneth Cells (40X) The arrows point to positive staining for the acidophilic granules of the Paneth cells. *G*, average villus length of proximal small intestinal villi. *H*, average muscularis thickness in proximal small intestine. *I*, average goblet cell density in proximal small intestine. (n=3).

Mice null for IFABP have increased incidence of cell death in proximal small intestine

While both goblet cell staining and Paneth cell staining revealed a reduced amount of those specific cell types, a BrdU proliferation assay where mice were gavged with BrdU 2 hours prior to excision indicated that the amount of proliferating cells in the crypts was not significantly different between IFABP$^{-/-}$ mice and WT mice **(Fig 3-6)**. However, 48 hours after gavage with BrdU IFABP$^{-/-}$ mice were found to have less BrdU positive cells in their villi when compared to WT mice. While the whole villus of the IFABP$^{-/-}$ stained positively for BrdU, WT mice displayed unstained cells towards the tips of their villi, with the middle and lower portions of their villi staining positively for BrdU **(Fig 3-6)**. The positive staining in tissue collected from mice 2 hours post BrdU is considered representative of actively proliferating cells, while the positive staining associated with tissue collected from mice 48 hours post gavage is considered to be more representative of cell migration up the villus tips.
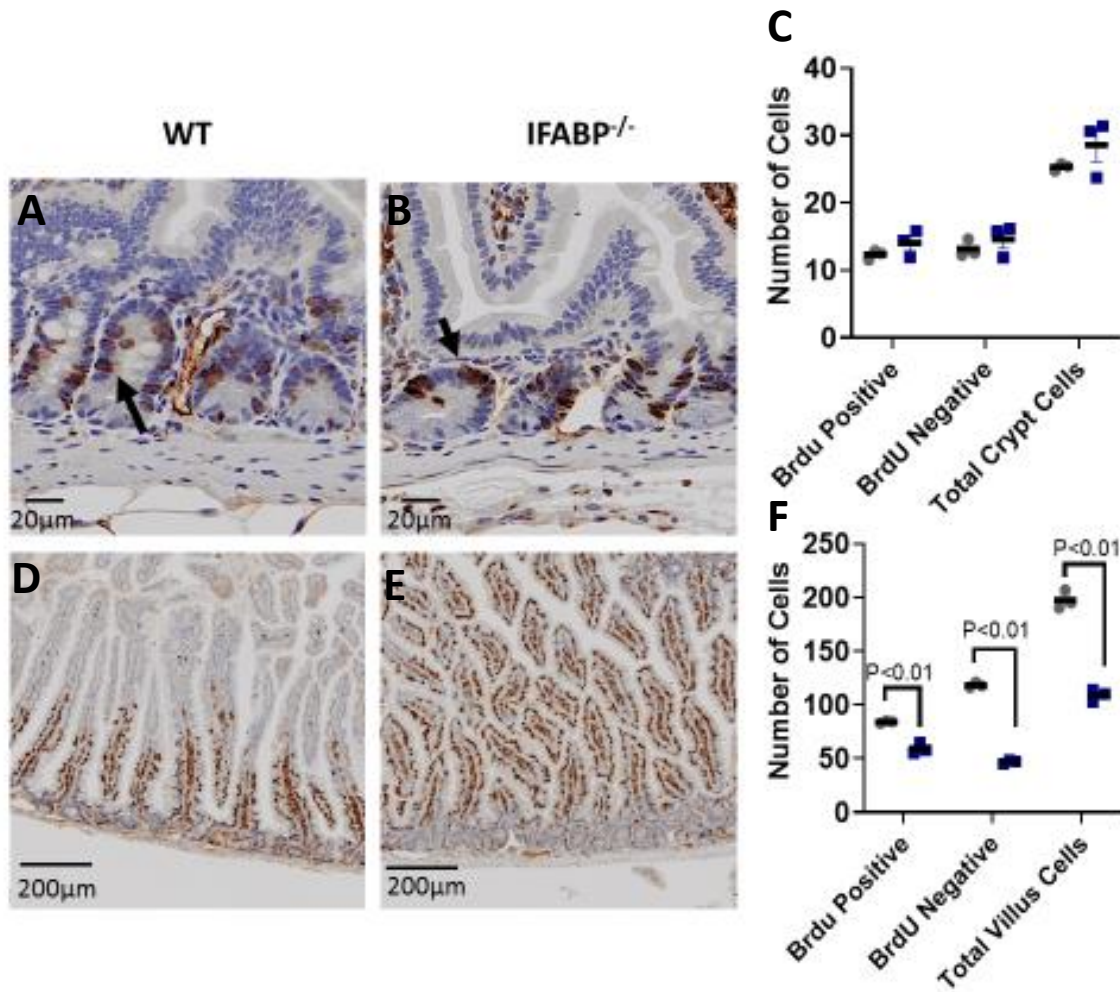
Figure 3-6: **BrdU staining for 2h or 48h in the small intestinal crypts and villi of WT (●) and IFABP$^{-/-}$ (■) mice fed a 45% Kcal HFD for 12 weeks.** *AB,*Small intestinal sections from mice 2 hours post-BrdU injection stained with anti-BrdU (20X). Arrows point to positive staining. *C,* quantification of BrdU positive cells and total cells in the crypt. 50 crypts were assessed per animal (n=3). *DE,* Small intestinal sections from mice 48 hours post-BrdU injection stained with anti-BrdU (4X). *F,* quantification of BrdU positive and total cells in the villus. 15 villi were assessed per animal (n=3).

Mice null for IFABP have increased intestinal permeability

Intestinal permeability was assessed in two ways. Plasma endotoxin (lipopolysaccharide or LPS) levels were analyzed as an indirect measure of intestinal permeability, and it was found that HF fed IFABP$^{-/-}$ mice have similar plasma endotoxin levels as their obese WT counterparts **(Fig 3-7A)**. A direct assessment of permeability using a fluorescein isothiocyanate (FITC)–dextran assay demonstrated that IFABP$^{-/-}$ mice have increased intestinal permeability relative to WT mice **(Fig 3-7B)**.

A Plasma Endotoxin (EU/mL)

B Serum FITC-D (μg/mL), P<0.01
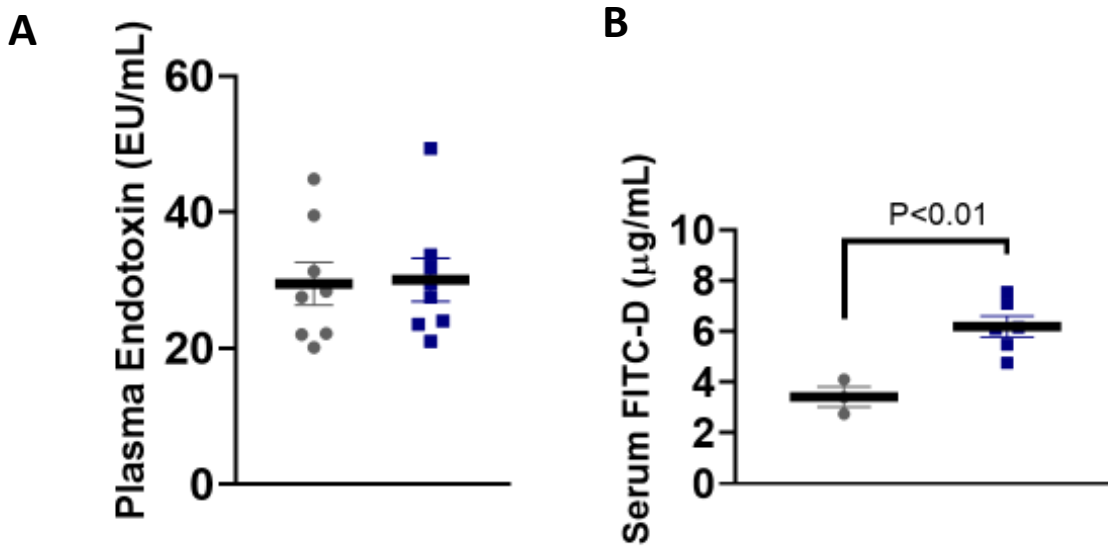
Figure 3-7: **Assessments of intestinal permeability in WT (●) and IFABP$^{-/-}$ (■) mice fed a 45% Kcal HFD for 12 weeks.** *A,* Plasma endotoxin is expressed in endotoxin units (EU) per milliliter (n=8). *B,* Serum FITC-dextran levels in mice 4 hours after gavage (n=3-6).

Alterations in expression of tight junction genes, markers of inflammation, and markers of ER stress

qPCR analysis was used to assess small intestinal structure, inflammation, and ER stress, revealing that IFABP^{-/-} mice have a 56% increased expression of claudin 2, a gene associated with a pore forming tight junction (TJ) protein, and 57% decreased expression of claudin 5, a gene associated with a tightening TJ protein **(Fig 3-8A)** ($p < 0.05$). Both increased claudin 2 expression and decreased claudin 5 expression are associated with increased intestinal permeability. At the level of gene expression, it was found that IFABP^{-/-} mice have increased expression of caspase 3 ($p < 0.01$) and activating transcription factor 6 (ATF6) ($p < 0.05$), both of which are markers of ER stress and apoptosis **(Fig 3-8B)**. Interestingly, while the abundance of mucin producing goblet cells was significantly lower in the small intestine of IFABP^{-/-} mice, gene expression for mucin 2, the most abundant mucin produced by small intestinal goblet cells, was similar to that of WT mice **(Fig 3-8B)**. However, IHC analysis of mucin 2 showed reduced staining in IFABP^{-/-} mice, indicating a reduced abundance of mucin 2 protein **(Fig 3-9).** Additionally, in agreement with the directional changes observed at the level of gene expression, claudin 2 staining was increased and claudin 5 staining was decreased in the HF fed IFABP^{-/-} mice **(Fig 3-9)**. Staining for monocyte chemoattractant protein 1 (MCP1), a marker of inflammation, endoplasmic reticulum (ER) stress, and immune cell infiltration, was increased in IFABP^{-/-} mice **(Fig 3-10)**. Further, IHC staining for inducible nitric oxide synthase (iNOS) and cyclooxygenase 2 (COX2), which are also markers of inflammation and ER stress, showed increased expression in IFABP^{-/-} mice when compared to WT mice **(Fig 3-10)**. However, when the phosphorylation of eukaryotic initiation factor 2 alpha (eIF2α), another marker of ER stress, was assessed, no difference was found between groups **(Fig 3-10)**.

A

B
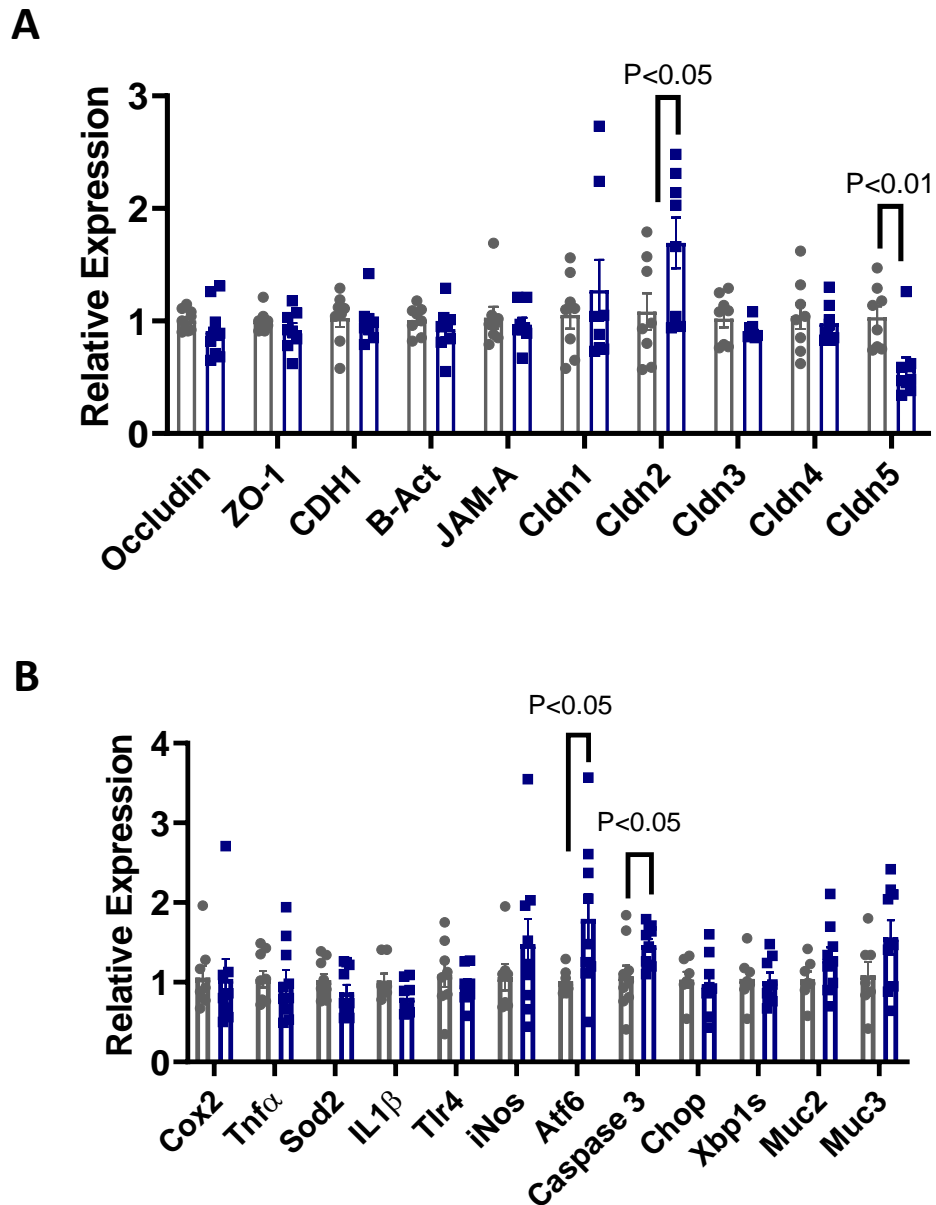
<u>Figure 3-8:</u> **Relative quantitation of mRNA expression of genes related to small intestinal structure and inflammation in 45% Kcal fat HF fed WT (●) and IFABP$^{-/-}$ (■) mice.** *A*, structure-related genes. *B*, inflammation-related genes (n=8-12).
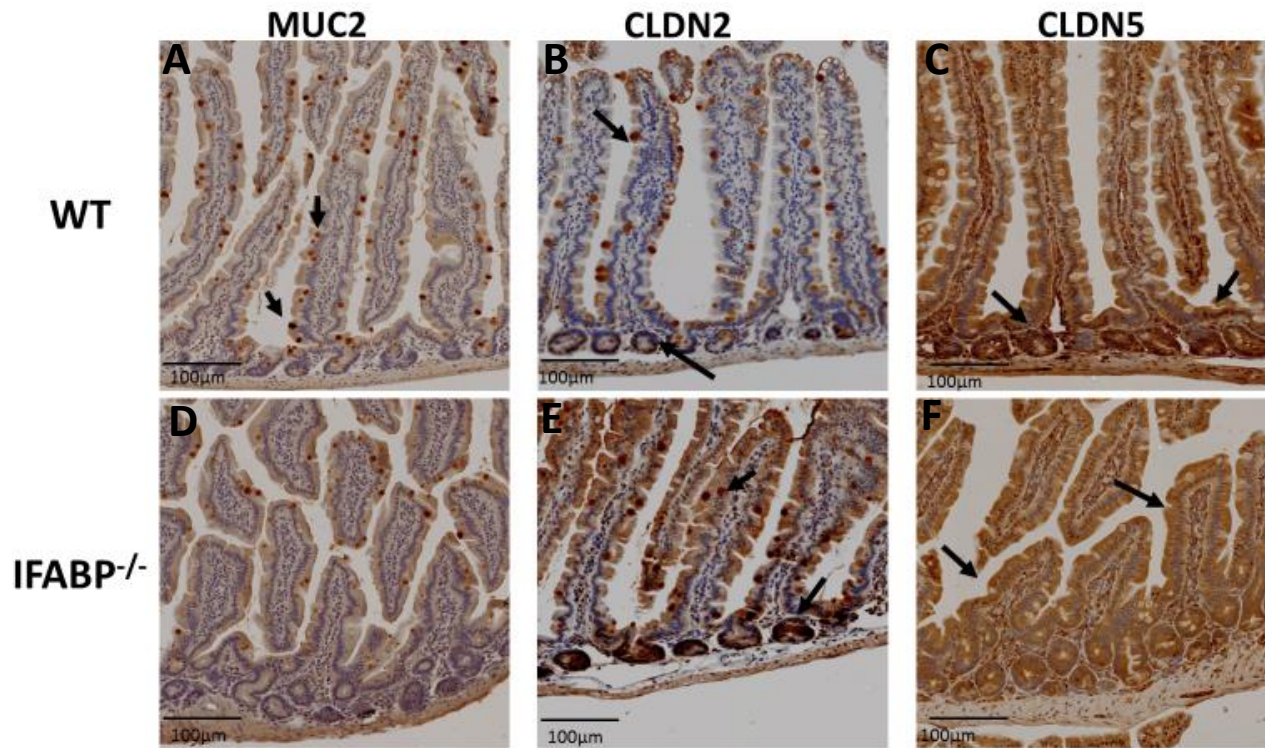
Figure 3-9: **Assessment of small intestinal structure in 45% Kcal fat HF fed WT (●) and IFABP-/- (■) mice.** *A-F*, Proximal small intestine sections stained with either anti-MUC2, anti-Claudin 2, or anti-Claudin 5 antibodies. Arrows point to positive staining (n=3).
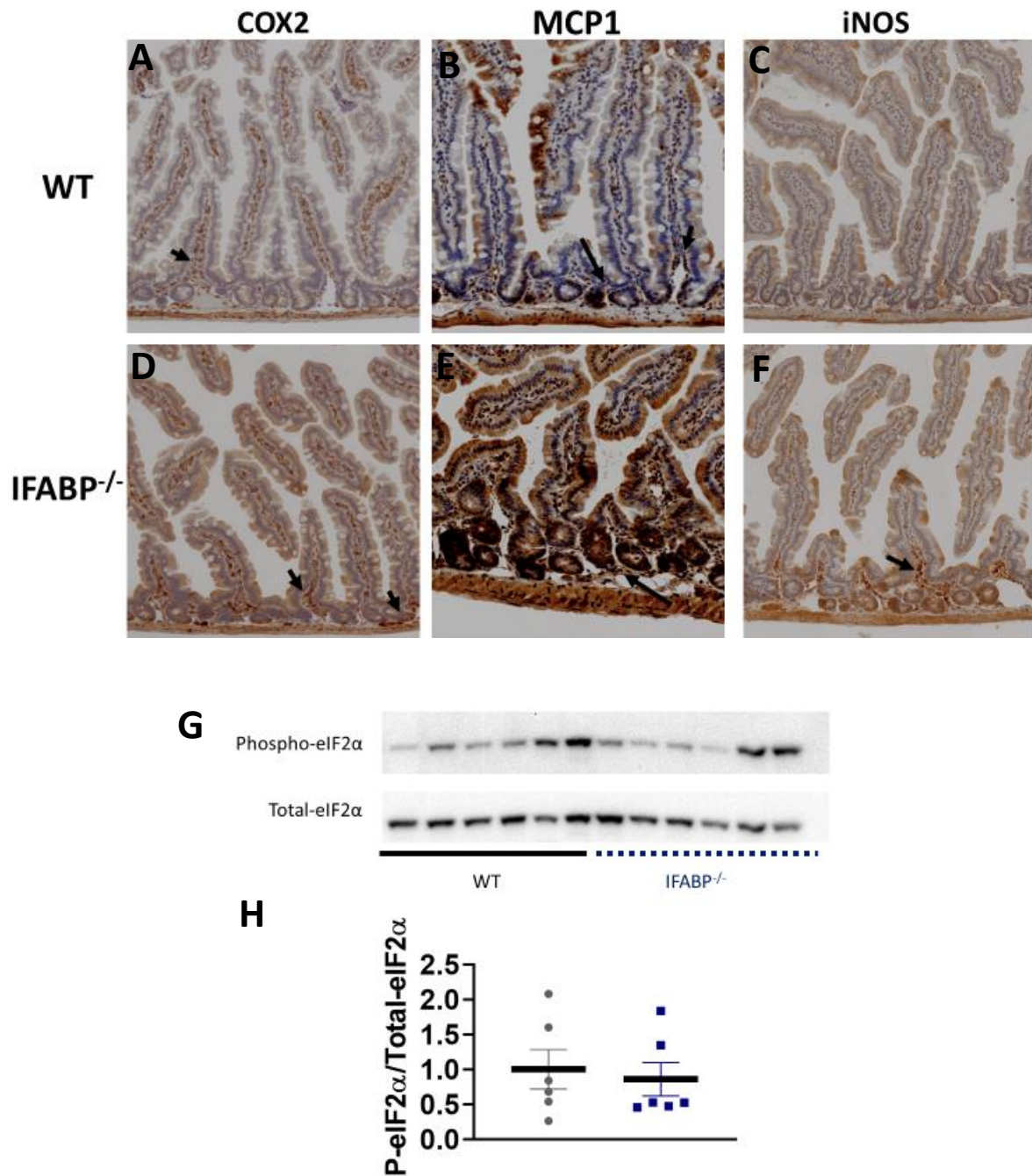
Figure 3-10: **Assessment of small intestinal inflammation and ER stress in 45% Kcal fat HF fed WT (●) and IFABP⁻/⁻ (■) mice.** *A-F*, Proximal small intestine sections stained with either anti-COX2, anti-iNOS, or anti-MCP1 antibodies. Arrows point to positive staining (n=3). *G,* Western blot showing phosphorylated eIF2α and total eIF2α (n=6). *H*, Relative quantification of phosphorylated eIF2α normalized to total eIF2α (n=6).

Some phenotypes observed in HF fed IFABP^{-/-} mice are influenced by dietary fat content

Since the above-described phenotypes found in the IFABP^{-/-} mice were found in HF diet-fed animals, we wondered whether the effects were due solely to the ablation of IFABP, or whether the chronic exposure to a HF challenge was needed to develop the blunt villus and other phenotypic changes observed in the IFABP^{-/-} mouse. Thus, a cohort of IFABP^{-/-} and WT mice were fed a 10% Kcal fat LF diet for 12 weeks beginning at 8 weeks of age. LF fed IFABP^{-/-} mice were found to have an average villus length that was 17% shorter than their WT counterparts (P<0.01) **(Fig 3-11A),** about half the decrease found under HF feeding (Fig 3-5). Unlike the HF fed mice, no reduction in muscularis thickness was observed in the IFABP^{-/-} compared to the WT group **(Fig 3-11B)**. As expected for mice that have shorter villi, IFABP^{-/-} mice had less total goblet cells (P<0.05) **(Fig 3-11C)**. However, when the amount of goblet cells was normalized to the average villus length, no difference in goblet cell density between groups was found **(Fig 3-11D)**. In addition to histological assessments, total fecal output and intestinal transit time were determined for the LF fed IFABP^{-/-} and WT mice. Unlike their HF fed counterparts, no differences were observed in total fecal output or intestinal transit time **(Fig 3-11EF)**.
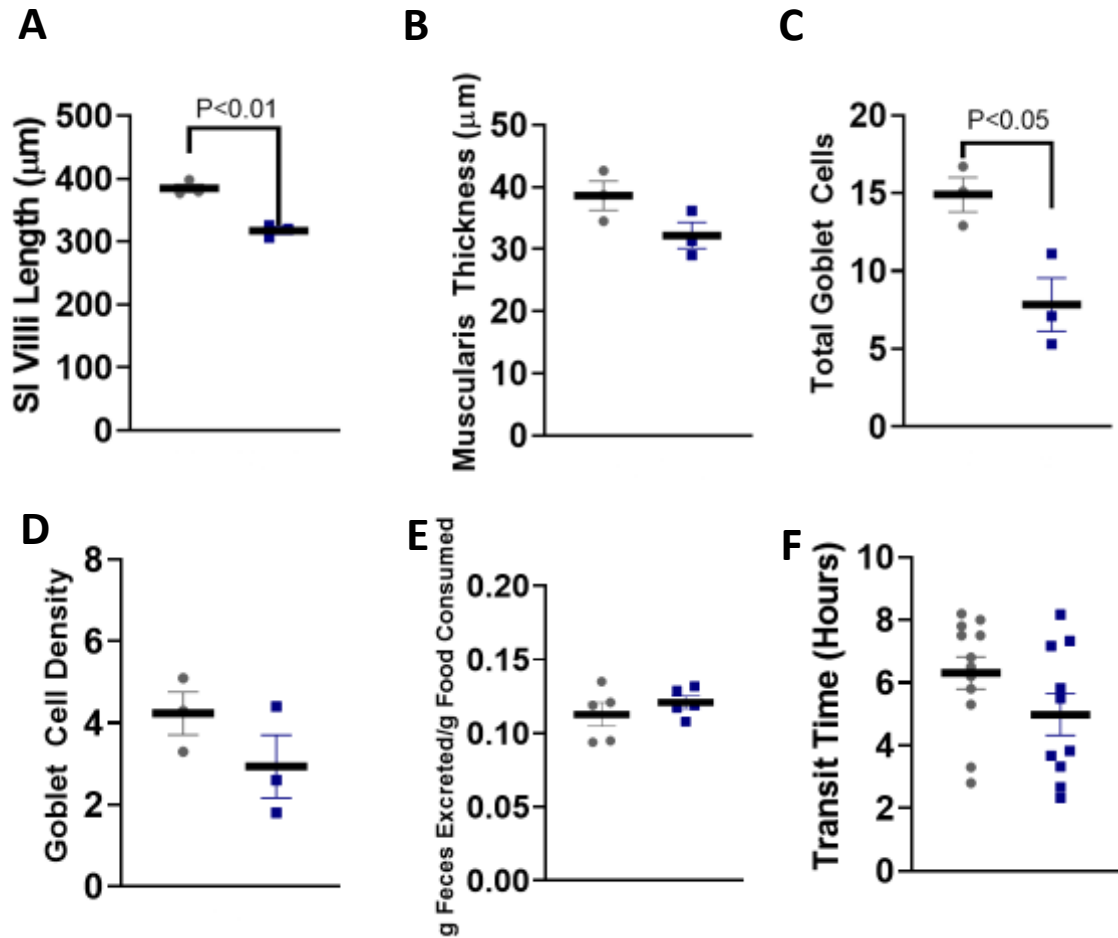
Figure 3-11: **Initial small intestinal phenotype assessments in 10% Kcal fat HF fed WT (●)**

and IFABP$^{-/-}$ (■) mice. *A*, Average villus length (n=3). *B*, Average muscularis thickness (n=3). *C*,

Total villus goblet cells (n=3). *D*, Average goblet cell density (n=3). *E,* Assessment of total fecal

excretion normalized to average food intake (n=5). *F*, Assessment of intestinal transit time (n=10-

12).

Discussion

Proximal intestinal enterocytes express the FABPs, IFABP and LFABP. In humans, IFABP is less abundant than LFABP [135,136], however mice express similar levels of LFABP and IFABP within the small intestinal mucosa [135–137]. While no compensatory upregulation of LFABP was observed in chow-fed IFABP null mouse intestine [15], we wondered whether a high fat diet might lead to increased LFABP expression. We found, however, that as with the chow fed mice, HF fed IFABP^{-/-} mice did not have a compensatory increase in LFABP gene expression or protein abundance, and no change in the gene expression of the distal small intestinal FABP, ileal-FABP (ILBP; FABP6) was observed. Thus, the phenotypic changes observed in the IFABP^{-/-} mice appear to be independent of the abundance of other FABPs, further supporting the independent and distinct roles of the proximal small intestine FABPs, IFABP and LFABP, in intestinal and whole-body homeostasis.

Notably, total fecal mass per gram of food intake of HF fed IFABP^{-/-} mice was markedly greater than that of the WT mice. This increase in fecal output in the absence of changes in lipid concentration was unanticipated and suggested that intestinal transit time might be impacted by IFABP^{-/-} deletion. Indeed, we found that the HF fed IFABP^{-/-} mice had significantly more rapid intestinal transit, relative to WT mice. Thus, the enhanced intestinal transit and increased fecal excretion suggests that IFABP^{-/-} mice are in fact malabsorbing nutrients in general, including lipid. Indeed, bomb calorimetric assessments revealed reduced energy absorption in HF fed IFABP^{-/-} mice. It is therefore likely that the reduced absorption energy absorption coupled with decreased food intake, explains why the IFABP^{-/-} mice remain lean on both HF and very HF diets. The alterations in total fecal output and intestinal transit time appear to be absent in LF fed IFABP^{-/-} mice, suggesting that the ablation of IFABP in addition to a HF challenge are necessary for these physiological alterations to be observed. Ironically, these studies support the prevailing hypothesis that IFABP is involved in efficient dietary lipid assimilation, although the present results

indicate that the effects of IFABP ablation are not related to specific alterations in intestinal lipid processing.

It is interesting to note that the shorter villi may also contribute to the observed more rapid intestinal transit rates. Villus length decreases from the duodenum to the ileum, allowing for peristaltic contractions to more rapidly move intestinal contents as they descend [223], while still allowing for the efficient absorption of dietary nutrients [11]. Shorter proximal intestinal villi in IFABP^{-/-} mice small intestine would provide less resistance for passing luminal contents, allowing them to more rapidly traverse the GI tract. Additionally, the shorter villi may explain, in part, the leanness of HF fed IFABP^{-/-} mice, with more rapid intestinal motility leaving less time and less surface area for efficient nutrient absorption.

It was found that the muscularis layer of the proximal small intestine is thinner in HF fed IFABP^{-/-} mice, which may explain, in part, the above noted fragility of the SI. Additionally, the shorter average villus length of IFABP^{-/-} mice suggests that there is less surface area for tight junction (TJ) and adherens junction (AJ) interactions. We initially hypothesized that the shorter villi might be a result of reduced crypt cell proliferation. However, mice injected with BrdU 2 hours prior to tissue collection revealed that both groups have comparable levels of BrdU positive cells in their crypts. Instead, it is likely that the blunt villus phenotype is due to enhanced cell death, since samples acquired from mice 48 hours after BrdU injection demonstrated that IFABP^{-/-} mice had significantly less BrdU positive cells present in their villi, when compared to WT mice. It is possible that the IFABP^{-/-} small intestinal cells are susceptible to ER stress induced apoptosis [224]. Some markers of ER stress, such as ATF6 and caspase 3 gene expression, were elevated in the mucosa of HF fed IFABP^{-/-} mice. Additionally goblet cells and Paneth cells, hypersecretory cells present within the small intestine, are more sensitive to more deleterious effects of ER stress, and tend to have reduced abundance in response to chronic inflammation and ER stress [224,225]. Since IFABP^{-/-} mice have reduced goblet cell density and Paneth cell abundance, it is possible

that these cells, along with other cell types in the small intestine, are dying via apoptosis, and inducing the blunt villus phenotype that is observed.

The vagus nerve (VN) plays a major role in the regulation of GI motility. Visceral afferent endings of the VN in the intestine express a diverse array of mechanosensitive and chemical receptors [107]. These receptors bind gut peptide hormones that are released from enteroendocrine cells of the GI tract, responding to nutrients, distension of the stomach, and neuronal signals [107]. Vagal afferent neurons also express cannabinoid receptor 1 (CB1R), which is part of the complex endocannabinoid system (ECS), a signaling system that is known to play a large role in the regulation of food intake [115,226,227]. Interestingly, chemical inhibition of CB1R in rodents results in increased intestinal motility [119]. Additionally, whole-body and VN-specific inhibition of CB1R both result in increased intestinal propulsion in mice [118,228]. Taken together, CB1R-related signaling within the VN appears to play an important role in modulated GI motility. Several FABPs have been shown to bind ECs, and appear to be involved in the regulation of intracellular EC levels [128,129,131]. Mice Interestingly, we showed that the IFABP$^{-/-}$ mice had somewhat lower mucosal levels of 2-arachidinoylglycerol (2-AG) [16], an EC that acts as a full agonist of CB1R [115,229]. Activation of CB1R by receptor agonists has been shown to decrease intestinal motility in rodent models, while antagonism leads to more rapid intestinal transit [120,228,230,231]. Thus, in HF fed IFABP$^{-/-}$ mice the observed increase in intestinal motility may be secondary to altered vagal tone caused by reduced CB1R activation, as a result of lower mucosal EC levels.

Overall, the shorter length of the IFABP$^{-/-}$ mucosal villi would appear to have important implications for intestinal transit, nutrient absorption, and intestinal integrity. Others have reported that the villus length of IFABP$^{-/-}$ mice maintained on a low fat chow diet did not differ from that of their WT counterparts [232], while we found a small but significant decrease, relative to WT, on a semi-purified 10% kcal LF diet, and a large decrease in villus length on the 45% kcal HF diet. It is likely that dietary fat amount and type play an important role in these differences. Over the past few years,

it has become evident that diets rich in lipids, especially saturated fats, lead to alterations in intestinal structure and physiology [233]. Thus, the IFABP^{-/-} mice may be more sensitive to the effects of lipid-rich diets, leading to more drastic alterations in villus morphology in response to HFDs. The differences in the observed villus length phenotypes in response to different diets could also be due to alterations in the composition of the gut microbiota, which play a role in shaping, and are shaped by, the environment within the intestinal lumen. It has been demonstrated that HF feeding can induce intestinal dysbiosis, leading to pathophysiological changes that include chronic low-grade inflammation, impaired mucus production, and altered expression of tight junction proteins [233]. In relation to potential alterations in the microbiome, differences in the villus length phenotypes of the chow fed IFABP^{-/-} mice compared to our LF fed and HF fed IFABP^{-/-} mice may also be due to the fact that semi-purified diets used differs from standard chow diets in fiber quality as well [16,232,234]. Many LF and HF semi-purified diets use cellulose, and insoluble fiber, as the sole source of dietary fiber [234]. However, standard chow also contains soluble fiber, which is able to be processed by the microbiome to provide energy for the microbes that are present [234]. The lack of soluble fiber in the semi-purified diets subsequently "starves" the microbes that are present within the GI tract, which can drastically alter the structure and composition of the microbiome. The lack of soluble fiber appears to influence the morphology and structure of the GI tract as well, with chronic intake of diets that lack soluble fiber leading to reduced colon length, colon weight, and cecum weight [234]. Interestingly, the addition of inulin, a soluble fiber, to a semi-purified HF diet rescues the mice from the physiological alterations that are observed with diets that lack soluble fiber, with HF fed inulin supplemented mice having colon length, colon weight, and cecum weights similar to that of chow fed mice [234]. Thus, it is possible that the previously reported absence of changes observed in the intestinal morphology of chow fed IFABP^{-/-} mice, relative to the present changes observed in the intestinal morphology of IFABP^{-/-} mice fed semi-purified LF and HF diets, may also be due to difference in soluble fiber content.

It has been reported that HF fed obese mice have elevated levels of plasma endotoxin, a bacterial component that passes from the intestinal lumen into the circulation when there is increased intestinal permeability [52,53,235]. Interestingly, we found that although the 45% Kcal HF fed IFABP^{-/-} are leaner than their WT counterparts, they have similar levels of plasma endotoxin. In fact, both the IFABP^{-/-} mice and WT mice have plasma endotoxin levels that are similar to those that have been observed in mouse models of diet induced obesity [53], suggesting that the IFABP^{-/-} mice, though lean, may experience increased intestinal permeability in response to chronic HF feeding.. As a more direct assessment of intestinal permeability, FITC-dextran assays were performed, revealing that IFABP^{-/-} mice have increased intestinal permeability. Together with the alterations found in TJ-related gene expression levels, increased permeability likely explains the initially observed intestinal fragility phenotype of the IFABP^{-/-} mouse.

Among the TJ proteins of the GI tract, claudins constitute the major transmembrane component [46,48]. Claudins act as "gatekeepers", and can be classified as either barrier-forming or channel-forming [48]. Different claudins polymerize to form mesh-like structures in which the integrity is influenced by the balance of barrier-forming and channel-forming claudins. An imbalance of either group can lead to dysfunctional tissue that is more prone to structural damage and inflammation [46,48–50]. In the IFABP^{-/-} mucosa, we found increased expression of the channel-forming claudin 2 and decreased expression of the barrier-forming claudin, claudin 5. These same directional changes were observed with IHC staining, with IFABP^{-/-} mice having increased claudin 2 staining and decreased claudin 5 staining. These changes are associated with a "leaky gut" phenotype [49,50,236,237], which may partly explain why the IFABP^{-/-} mice have increased intestinal permeability. Interestingly, this pattern of gene expression has been observed in samples obtained from patients with Crohn's disease, an inflammatory bowel disease in which the integrity of the small intestine is compromised [48,49]. Indeed, there is evidence that FABPs present in the small intestine change their expression pattern in celiac disease, another GI-related disease that involves chronic

inflammation [238] and in which damaged villi cause a variety of symptoms, some of which are related to nutrient malabsorption [239]. In intestinal mucosa from celiac disease patients, both IFABP and LFABP appear to be expressed not only in cells of the remnant epithelium but also within the hyperproliferative crypts, where FABPs are typically not expressed. It is possible that abnormal FABP expression, such as a lack of IFABP expression or induced expression of FABPs in the crypts, may be a common phenotype of GI-related disorders that include altered intestinal morphology, structure, and the overall "leaky gut" phenomenon.

It should be noted that dysbiosis-induced inflammation may not easily occur in mice that have more rapid intestinal transit. Early studies in which intestinal motor activity was assessed in the context of small intestinal bacterial clearance demonstrated that the action of peristalsis is the primary line of defense against abnormal bacterial colonization of the small intestine [240]. Thus, it is possible that the rapid intestinal transit time of the IFABP$^{-/-}$ mice may be a compensatory response to the alterations occurring in their SI structure and morphology that would normally make them more susceptible to the induction of inflammation.

In addition to the array of junctional and junction-related proteins that directly or indirectly alter the permeability of the intestinal epithelium, secretory goblet cells along the GI tract secrete mucus that acts as an initial defensive barrier, providing protection from physical and chemical challenges [37–41]. The mucus layer can be divided into two functional components: the top layer, or loosely adherent layer, which is able to trap bacteria and prevent them from interacting with the epithelium, and the bottom layer, or firmly adherent layer, which provides structural support and provides a critical barrier for preventing bacterial adhesion to the epithelium [38,42,43]. Interestingly, deficiency of the primary component of the GI mucus layer, the glycoprotein mucin 2 (MUC2), leads to the elimination of the mucus layer, increased intestinal permeability, and increased bacterial adhesion to the epithelial surface [241,242]. It is worth noting that goblet cells are also able to secret trefoil factors (TFFs), which play important roles in the maturation and

maintenance of many small intestinal components [37,38]. Additionally, it has been demonstrated that chronic inflammation of the GI tract can result in depletion of goblet cells, leading to alterations of the not only the mucus layer, but intestinal morphology and structure as well [37,38,41]. The reduced goblet cell density of the HF fed IFABP^{-/-} mucosa implies that there is a reduced or altered mucus layer, which in turn may contribute to the fragility of IFABP^{-/-} mice small intestine. Interestingly, while HF fed IFABP^{-/-} mice had both a reduction in total goblet cells and villus length-independent goblet cell density, LF fed IFABP^{-/-} mice only displayed a villus length-dependent reduction in total goblet cell, suggesting that the HF challenge in addition to the ablation of IFABP is necessary to induce villus-length independent alterations in goblet cell density.

It should be noted that while reductions of both goblet cell number and mucin 2 protein levels were observed in the small intestine of HF fed IFABP^{-/-} mice, mucosal mucin 2 and mucin 3 gene expression did not differ between IFABP^{-/-} mice and WT mice. It is known that highly secretory cells, such as goblet cells, are very sensitive to the deleterious effects of chronic ER stress [224,225]. Additionally, iNOS, COX2, and MCP1 are known to be markers of ER stress, with increased expression and abundance being observed in chronic ER stress responses [243–251] . Thus, the maintenance of mucin 2 and mucin 3 gene expression in conjunction with decreased goblet cell density, reduced mucin 2 staining, and increased iNOS, COX2, and MCP1 staining in the small intestine of IFABP^{-/-} mice suggests that ER stress may play a role in the development of the HF fed IFABP^{-/-} intestinal phenotypes. The upregulated expression of ATF6 and Caspase 3, both of which are markers of ER stress and apoptosis [224,225] supports this suggestion. Additionally, reduced Paneth cells were also found in the small intestine of HF fed IFABP^{-/-} mice; these hypersecretory cells, which secrete an array of antimicrobial peptides are known to be particularly sensitive to ER stress [44,224]. Despite these observed alterations it is important to note that the expression of CCAAT-enhancer-binding protein homologous protein (Chop) and spliced X-box-binding protein1 (Xbp1s), which are also markers of ER stress, were not elevated in the IFABP^{-/-}

mucosa. Additionally, enhanced phosphorylated eIF2α, which is a well-accepted marker of ER stress induction [224,225] , was also not observed suggesting that if ER stress is playing a role in the phenotypes observed in the IFABP^{-/-} mice, it is likely not a major role. However, it is important to mention that the mice assessed in these studies were all fasted for 16 hours prior to tissue collection, unless stated otherwise. ER stress is known to be influenced by circadian cycling [252–254], so it is possible that more robust ER stress-related phenotypes in IFABP^{-/-} mice may be observed at different ages or in response to different fasting challenges.

It is possible that the ablation of IFABP may make the intestinal epithelial cells more susceptible to FA-induced lipotoxicity, which could subsequently promote ER stress. Interestingly, some of the phenotypes that are observed in HF IFABP^{-/-} mice have also been observed in mice with an intestine-specific ablation of X-box-binding protein1 (XBP1). XBP1 is a transcription factor that is essential to the unfolded protein response (UPR) that is a hallmark of the physiological attempt to resolve ER stress [255]. Intestine-specific XBP1^{-/-} mice were found to have almost no Paneth cells, and a reduction in goblet cell abundance [255]. As mentioned above, since IFABP^{-/-} mice do not appear to have reduced crypt cell proliferation, it is tempting to speculate that the blunt villus phenotype and alterations in goblet cell and Paneth cell populations might be due, instead, to enhanced apoptosis that may occur via the ER stress response. Indeed, IFABP^{-/-} mice that were exposed to BrdU 48 hours prior to tissue collection appear to have enhanced cell death; this apparent enhancement of cell death may be due to ER stress-related apoptosis, ER stress-independent apoptosis, or anoikis (cell shedding) [256,257].

The present results indicate that IFABP is not specifically essential for dietary lipid assimilation. Rather, it appears to be functioning, perhaps via EC or FA binding, to regulate intracellular signaling and/or transcriptional programing. Indeed, some members of the FABP family have been shown to interact with nuclear hormone receptors (NHRs) such as peroxisome-proliferator activated receptors (PPARs) and hepatocyte nuclear factors (HNFs) [113,155,158,258]. Taken together

the changes observed in IFABP$^{-/-}$ mouse proximal small intestinal morphology, structural genes, markers of ER stress, Paneth cell abundance, and goblet cell density are likely indicative of reduced structural integrity. Thus, these studies suggest that IFABP likely plays a role in dietary lipid sensing and signaling, modulating intestinal structure and capacity for nutrient absorption, thereby subsequently altering whole-body energy metabolism.

Chapter 4

General Conclusions and Future Directions

The Ablation of Intestinal LFABP Does Not Fully Recapitulate the MHO Phenotype of the whole body LFABP null mouse

Obesity is a multifaceted disease that is characterized by excessive fat storage that is often accompanied by metabolic dysfunction [4]. A subset of the obese population appears metabolically healthy despite their obesity (MHO), not displaying various comorbidities that are common [195,196]. Although male HF fed LFABP$^{-/-}$ mice become more obese they remain relatively healthy, being normoglycemic, normoinsulinemic, and retain exercise endurance similar to that of leaner mice [16,113,187,192]. Here, we have shown that the intestine-specific ablation of LFABP does not result in male mice that are more obese. However, in response to a chronic HF challenge LFABP$^{int-/-}$ mice still had an exercise capacity that was similar to that of a healthy LF fed animal. Female LFABP$^{int-/-}$ did appear more akin to an MHO model, displaying both obesity and a retained exercise capacity, normal fasting insulin, and normal glucose tolerance when compared to their leaner LFABP$^{fl/fl}$ controls. However, other health parameters, such as hepatic TG content and serum lipids in, should be assessed in both male and female LFABP-cKO mice to continue a determination of relative health. Additionally, HF fed female whole-body LFABP$^{-/-}$ mice should also be assessed to determine if they display a MHO set of phenotypes as well. Others have assessed HF fed female LFABP$^{-/-}$ mice, with one group finding that they were resistant to diet-induced obesity [187,217], while another group demonstrated that female LFABP$^{-/-}$ gained more weight when challenged with a HF diet [190]. It should be noted that the male mice assessed by these groups also followed a similar pattern, with one group observing resistance to diet induced obesity in their male LFABP$^{-/-}$ mice [187,217], while the other group (and our group) saw increased adiposity [189,190]. The underlying reasons for different phenotypes may include strain background, gene ablation strategies, and different diet compositions used, as previously discussed [11,16]. It is also possible that differences and similarities observed between our LFABP$^{-/-}$ mice and the Texas mice, compared to the LFABP$^{-/-}$ mice used by the St. Louis group is due to differences in microbiomes

between the groups. Ongoing studies are occurring to assess the microbiomes of the enterocyte FABP null mice, to determine what bacteria or bacterial products may influence the whole-body phenotypic changes that have been observed in both LFABP^{-/-} and IFABP^{-/-} mice.

While we have not yet assessed how the whole-body female LFABP^{-/-} mice respond to the HF feeding protocol in our hands, it is likely that they would be prone to increased adiposity. Indeed, similar to the observed increased BW gain and fat mass in female LFABP[int-/-] mice, female LFABP[Liv-/-] mice also appear to become more obese in response to chronic HF feeding (unpublished observations). It is likely that female LFABP^{-/-} mice will retain, or have an exacerbated, obese phenotype.

These current studies using the IFABP^{-/-} mice have demonstrated that alterations in intestinal morphology and structure can have dramatic influences on whole-body physiological responses. Future studies assessing aspects of the MHO phenotype in LFABP-cKO mice should also include assessments of intestinal physiology. Recently, we have found that male HF fed LFABP^{-/-} mice display a reduction in fecal output that can be partly explained by having a longer intestinal transit time **(unpublished data)**, a phenotype that is opposite of what is found in the leaner HF fed IFABP^{-/-} mice. The reduction in fecal output, in addition to increased food intake [16], may, at least in part, explain the obese phenotype that is observed in the HF fed LFABP^{-/-} mice. In addition to alterations in intestinal transit, histological examination of HF fed LFABP^{-/-} mice small intestine revealed no differences in average villus length, but a significant reduction in goblet cell density **(unpublished data)**. Whether these transit and morphology phenotypes are present in female LFABP^{-/-} or male and female LFABP[int-/-] mice remains to be determined. Overall, it is apparent that the ablation of LFABP specifically in the intestine is able to influence aspects of whole-body physiology. Additionally, sex-related differences observed between the male and female LFABP[int-/-] responses to chronic HF feeding, suggests an important role for gender as well.

Alterations Specific to the Intestine Can Induce Dramatic Whole-Body Responses

It is interesting that LFABP^{-/-} and LFABP[int-/-] mice are able to retain their exercise capacity in response to chronic HF feeding, being able to run for a longer time during an induced exercise challenge, whereas HF-fed WT mice show a significant decline in exercise capacity. Since LFABP[int-/-] mice and LFABP^{fl/fl} mice had similar values for spontaneous activity, the retained exercise capacity in the LFABP[int-/-] mice seems to be independent of changes in spontaneous activity, and suggest that there may be crosstalk occurring between the intestine, skeletal muscle, and perhaps cardiac muscle. Indeed, other studies have demonstrated that exercise induces signals that allow for intestine/muscle communication, and it appears that these signals are mediated by the microbiome and mitochondria [213,214]. Recent studies have demonstrated that short chain fatty acids and secondary bile acids produced by commensal gut microbiota might influence mitochondrial functions related to mitochondrial biogenesis, energy production, redox balance, and inflammation [213,259–261]. For example, commensal gut bacteria are able to reduce reactive oxygen species (ROS) production via SCFA induced signaling, which can protect mitochondria from the presence of excessive ROS that occur in response to endurance exercise training [213,262]. Future studies should focus on elucidating the mechanism by which intestinal ablation of LFABP is able to influence responses to endurance training bouts. These studies should include a detailed analysis of the microbiome, and the metabolites that might be generated that can influence intestinal, skeletal muscle, and cardiac muscle responses to endurance exercise. It also may be of interest to observe if LFABP^{-/-} or LFABP[int-/-] mice respond better to chronic endurance training when compared to WT controls.

The ablation of IFABP, a protein that is only expressed in the intestine, also appears to have great influence over whole-body phenotypic responses. Most notable, of course, is the lean phenotype that is observed in response to chronic HF feeding. It is apparent that this phenotype is, at least partly, influenced by intestinal physiology, having an etiology that appears to be linked to

alterations in morphology and peristaltic contractile movement. The blunt villus phenotype has implications relating to nutrient absorption, intestinal transit, and structural stability. Additionally, the reductions observed in specific cell populations, such as Paneth cells and goblet cells, in addition to the observed increase in villus cell death, suggest an integral role for IFABP in the maintenance of a normal, functional small intestinal epithelium. It is especially important to note that these changes appear to be, at least partially, independent of dietary fat content, since the morphological phenotypes are present, albeit to a lesser extent, in the LF fed as well as the HF fed IFABP^{-/-} mice.

An important question that remains to be answered is, how does the ablation of IFABP result in more rapid intestinal transit in HF fed animals? The more rapid transit might be influenced by the blunt villus phenotype, since there would be less surface area to provide resistance for passing intestinal contents. However, LF fed IFABP^{-/-} mice also displayed a blunt villus phenotype without having significant alterations in intestinal transit time. Instead, it is possible that the ablation of IFABP in conjunction with chronic HF feeding results in altered gut/brain communication. There is substantial evidence that the gut/brain axis plays a role in regulating movement of foodstuffs throughout the GI tract [97,216,263,264]. We have observed that HF fed IFABP^{-/-} mice appear to have altered mucosal levels of endocannabinoids (EC) and EC-like molecules, which are thought to play a role in how the gut and brain communicate [114,265]. It is also possible that the ablation of IFABP may influence cell populations in addition to Paneth cells and goblet cells. Enteroendocrine cells, such as K cells or L cells, secrete hormones that are able to modulate appetite and intestinal motility[103,104]. For example, gastric inhibitory polypeptide (GIP) has traditionally been thought to be involved in reducing GI motility, though more recent studies have revealed that the primary role of GIP is to induce insulin secretion from pancreatic beta cells [99,104]. Another peptide hormone, motilin, has been shown to induce GI movement, and its secretion is reduced in response to elevated insulin signaling [97,101]. Historically, the dogma involving enteroendocrine

cells and the hormones that they secrete is that each cell type secretes a specialized hormone **(see Chapter 1, Fig 1-3B)**. However, more recent studies have revealed that each type of enteroendocrine cell is able to secrete an array of hormone peptides, and that the types of peptides that are secreted is likely influenced more so by the location of the cells in the GI tract [99,104]. It is thought that the relative balance of secreted hormones, termed the "secretome", determines the messages that the GI tract sends to other organs [104]. Since the intestine of IFABP^{-/-} mice has alterations in other cell populations, and they appear to have enhanced cell death, it is possible that the relative abundance of various enteroendocrine cell types might also be affected, which would in turn, altered the intestinal secretome. Alterations in the intestinal secretome would have important implications relating to gut/brain communication. For example afferent endings of the vagus nerve (VN) in the intestine express an array of mechanosensitive and chemical receptors [107]. The chemical receptors are able to bind gut peptide hormones that are released from enteroendocrine cells of the GI tract[107]. In addition to having receptors for gut peptide hormones, VN afferents also express the EC receptor, cannabinoid 1 receptor (CB1R) [123,266]. Chemical inhibition and genetic silencing of CB1R in rodent models results in increased GI motility [119,228]. Moreover, VN-specific ablation of CB1R also results in increased GI motility, suggesting that ECS signaling in the VN plays an important role in regulating motility [118]. It is possible that the trend toward lower EC and EC-like molecules observed in the mucosa of IFABP^{-/-} mice may lead to reduced EC stimulation of VN CB1R, which in turn, could result in more rapid GI motility. Future studies should assess the potential crosstalk occurring between the small intestine and various regions of the brain and central nervous system. A detailed analysis of the EC system in both tissues may help elucidate the mechanisms that may regulated alterations in intestinal transit in the HF fed IFABP^{-/-} mice. The analysis of intestine/brain crosstalk should also include plasma and tissue levels of enteroendocrine cell peptide hormones, such as GIP and motlilin. Additionally, it will be important to analyze mice that have not been fasted, in addition to

the fasted mice, since the regulation of EC and enteroendocrine peptide levels are influenced by fasting/feeding challenges [115,121].

The Ablation of IFABP Induces an Intestinal Fragility Phenotype

It was observed during tissue collection that HF fed IFABP^{-/-} mice have small intestines that appear to be more fragile relative to their WT counterparts. Here, we have demonstrated that HF fed IFABP^{-/-} mice have a blunt villus phenotype, a thinner muscularis layer, reduced goblet cell and Paneth cell densities, and increased intestinal permeability. Some, but not all, of these phenotypes appear to be present in the LF fed IFABP^{-/-} mice. For example, while the LF fed IFABP^{-/-} mice do display the blunt villus phenotype, they do not have a thinner muscularis layer. Future studies will focus on the mechanism of how the ablation of IFABP induces intestinal fragility. As mentioned above, members of the FABP family have been proposed to act as lipid chaperones, being able to influence lipid related signaling through the transport of, or sequestration of, lipid ligands [130,267,268]. We have recently shown that IFABP^{-/-} mice have altered gene expression for several transcription factors, including HNF4α, RXRα, RARβ, and SREBP1 **(see Appendix)**. Some of these transcription factors, such as HNF4α, are known to influence cell growth, development, and death [158,159,269]. Thus, it is possible that the ablation of IFABP alters the intestinal transcriptome in a way that either reduces cell differentiation, which would explain the reduced populations of goblet and Paneth cells, and/or in a way that increases the rate of cell death, which would explain both the blunt villus and altered cell population phenotypes. Future studies should assess transcriptional targets of the transcription factors in which altered expression was observed. Additionally, those transcription factors should also have their relative protein abundance determined, to determine if changes in gene expression correlate with similar changes in protein abundance.

The Gastrointestinal Tract Plays a Large Role in Whole-body Responses to Nutrient Challenges

While the integral role the GI tract plays in efficient nutrient absorption and assimilation has been appreciated for many years, it is evident that alterations induced in or related to this organ system can have drastic impacts on whole-body physiological responses. This work has demonstrated a role for enterocyte lipid binding proteins in efficient uptake and trafficking of not only dietary lipid, but nutrients in general. These studies have also revealed a heretofore unappreciated role for the enterocyte FABPs in modulating intestinal physiology, intestinal morphology, and whole-body ramifications of such modulations. These studies also reaffirm the importance of assessing the potential for tissue-tissue crosstalk to be occurring in response to various stimuli. While studies that assess gut-brain communication are relatively common, there is a notable gap in the literature relating to studies that assess cross talk between gut and muscle. For future studies, in order to assess how the intestine is able to influence whole-body phenotypic responses, it will be important to specifically focus on the bi-directional communication that can occur between various organs and organ systems.

Appendix

Ablation of IFABP Reduces CRBP2 Expression without altering CRBP2 Abundance, Modulates Mucosal Expression of Vitamin A Related Genes, and Alters Whole-Body Retinoid Status

Abstract

Intestinal-fatty acid binding protein (IFABP; FABP2) is a 15 kDa intracellular protein abundantly present in the cytosol of the small intestinal enterocyte. High fat (HF) feeding of IFABP$^{-/-}$ mice resulted in reduced weight gain and fat mass relative to wild-type (WT) mice. IFABP$^{-/-}$ mice were also found to have alterations in intestinal morphology and structure. We have previously demonstrated that the ablation of IFABP does not result in compensatory upregulation of liver-FABP (LFABP; FABP1), another highly expressed intestinal FABP. Another member of the FABP gene family, Cellular retinol binding protein 2 (CRBP2), is also expressed in small intestine. In this study we assessed the level of CRBP2 gene expression and protein abundance in IFABP$^{-/-}$ mice. We found a drastic reduction in mucosal CRBP2 message in IFABP$^{-/-}$ mice. Nevertheless, CRBP2 protein levels were comparable to that of WT mice, suggesting that CRBP2 mRNA stability and/or protein stability was altered in response to the ablation of IFABP. Additionally, both low fat (LF) and HF fed IFABP$^{-/-}$ mice were found to have altered mucosal expression of vitamin A-related genes, and altered retinoid levels in liver and plasma.

Introduction

The fatty acid binding protein (FABP) family is a class of small (14-15 KDa) cytosolic proteins that are able to bind an array of hydrophobic molecules with high affinity. The family consists of 9 FABPs, with additional cellular retinol binding proteins (CRBPs) also comprising part of the family. It is thought that these proteins are necessary for the efficient intracellular transport of various hydrophobic ligands, and that they may play a role in preventing fatty acid (FA) induced cytotoxicity. Given that the small intestine is responsible for the uptake and assimilation of the large amount of dietary FA, it has been hypothesized that the enterocyte FABPs are necessary for efficient trafficking of dietary lipids [11,12].

Indeed, the small intestine expresses at least 4 different members of the FABP family, with three of these members being very highly expressed throughout the length of the tissue. Liver-FABP (LFABP or FABP1) is highly expressed in both the intestine and liver [11]. LFABP is an atypical member of the FABP family, having 2 ligand binding domains and transferring ligands with a diffusional transfer mechanism [146,147]. Intestinal-FABP (IFABP or FABP2) is only found in the small intestine [11] and is more representative of the typical ligand interactions that are observed with the FABP family, having only one binding domain and transferring ligands with a collisional transfer mechanism [146,147]. In addition to LFABP and IFABP, the small intestine also has high expression of CRBP2 [127,138]. Unlike LFABP and IFABP, which have high affinities for FAs, CRBP2 has a high affinity for retinol, and has been hypothesized to be necessary for the efficient uptake of dietary retinol. More recently, we have shown that CRBP2 is also able to bind 2-monoacylglycerols (2-MGs), such as the endocannabinoid (EC) 2-arachidonoyl glycerol (2-AG) (*Lee et al., 2019 Submitted*). The last small intestinal FABP that is expressed in the small intestine is the ileal bile acid binding protein (ILBP or FABP6) [11]. While LFABP, IFABP, and CRBP2 are found throughout the small intestine, with the highest expression of each being observed in the more proximal

region when compared to the more distal region, ILBP is expressed mainly in ileum, where it is thought to play a role in bile acid metabolism [11,138,270,271].

Previous *in vitro* and *ex vivo* studies suggested that LFABP and IFABP may be necessary for the efficient absorption of dietary FAs [148,184]. Since LFABP and IFABP are similar in structure and they bind similar ligands, it was hypothesized that the ablation of one FABP may lead to increased expression of the other FABP, compensating for the loss of a highly expressed protein. Previously, we have shown that the ablation of LFABP in chow mice did not cause compensatory upregulation of IFABP mRNA or protein; the ablation of IFABP did not result in upregulation of LFABP as well [15]. More recently we have demonstrated that mice challenged with a 45% Kcal fat high fat (HF) diet also do not appear to have compensatory upregulation of other FABPs **(see Chapter 3)**. In that set of experiments, in addition to LFABP and IFABP, the gene expression of ILBP and other FABPs that are not typically expressed in the small intestine were assessed. However, the expression of CRBP2, the other major intestinal FABP, has not previously been analyzed. Therefore, in the present studies, we assessed intestinal mucosal expression of CRBP2 and other vitamin A related genes in low fat (LF) and HF fed wild-type and IFABP^{-/-} mice. Additionally, intestinal mucosal, liver, and plasma retinoid levels were measured to obtain a general assessment of vitamin A status.

Experimental Procedures

Animals and Diets

As previously reported, the IFABP^{-/-} mice used in this study are a substrain bred by intercrossing of an original strain of IFABP^{-/-} mice and are congenic on a C57BL/6J background [15,128,191]. C57BL/6J mice from The Jackson Laboratory (Bar Harbor, ME) were bred as wild-type (WT) controls. Mice were housed 2-3 per cage unless specified otherwise, maintained on a 12-hour light/dark cycle, and allowed *ad libitum* access to standard rodent chow (Purina Laboratory

Rodent Diet 5015). At 2 months of age, male WT and IFABP^{-/-} mice were fed either a 45% Kcal fat high fat diet (HFD) (D10080402; Research Diets, Inc., New Brunswick, NJ), or a matched 10% Kcal LFD (D04051701; Research Diets) as indicated. The vitamin A content for both diets was 4IU/g. Body weights (BW) were measured weekly for a period of 12 weeks.

Preparation of Tissue and Plasma

Mice were fasted for 16 hours prior to sacrifice unless otherwise stated. At sacrifice blood was drawn; plasma was isolated after centrifugation for 6 minutes at 4000 rpm, and stored at -80°C. Livers were removed, immediately placed on dry ice, and stored at -80°C for further analysis. The small intestine from the pyloric sphincter to the ileocecal valve was removed, measured lengthwise, rinsed with 60mL of ice-cold 0.1M NaCl, and opened longitudinally. Intestinal mucosa was scraped with a glass microscope slide into tared tubes on dry ice and stored for future use.

RNA Extraction and Real-Time PCR

Total mRNA was extracted from small intestinal mucosa and analyzed as previously described [15,16]. Primer sequences were obtained from Primer Bank (Harvard Medical School QPCR Primer Database) and are shown in Table 1. The efficiency of PCR amplifications was analyzed for all primers to confirm similar amplification efficiency. Real time PCRs were performed in triplicate using an Applied Biosystems 7300 instrument. Each reaction contained 80ng of cDNA, 250nM of each primer, and 12.5µL of SYBR Green Master Mix (Applied Biosystems, Foster City, CA) in a total volume of 25µL. Relative quantification of mRNA expression was calculated using the comparative Ct method, normalized to TATA-binding protein (TBP).

Western blotting

Small intestinal mucosa was harvested as described above, and homogenized in 10x volume of PBS pH 7.4 with 0.5% (vol/vol) protease inhibitors (Sigma 8340) on ice with a Potter Elvejhem homogenizer. Total cytosolic fractions were obtained by ultracentrifugation (100,000g, 1 hour at

4°C) and protein concentration determined by Bradford assay [209]. Thirty micrograms of cytosolic protein for each sample were loaded onto 15% polyacrylamide gels and separated by SDS-PAGE. The proteins were transferred onto 0.45μm nitrocellulose membranes using a semidry transfer system (Bio-Rad) for 1 hour and 45 minutes at 23 V. Prior to blocking, total protein was visualized with Ponceau staining. Membranes were blocked by incubating in 5% nonfat dry milk overnight at 4°C, and were incubated with the primary antibody, α-CRBP2 (1:10000, for 1 hour at room temperature; Abcam ab180494). After thorough washing, blots were incubated in α-rabbit IgG-horseradish peroxidase conjugate (1: 20,000) for 1 hour, and developed by chemiluminescence (WesternBright Quantum, Advansta, Menlo Park, CA). Protein expression was quantified by densitometric analysis with LI-COR Image Studio (Lite version 5.2). Target protein content was normalized to total protein content within a sample.

HPLC Analysis of Tissue and Plasma Retinoids

Reverse-phase HPLC analysis of retinol and retinyl ester was performed as described by Kim et al [272]. In short, tissues were homogenized in 10 volumes of phosphate-buffered saline using a PRO200 homogenizer (Oxford, CT). Retinoids present in the homogenates were extracted into hexane and separated on a 4.6 × 250 mm Ultrasphere C18 column (Beckman, Fullerton, CA) preceded by a C18 guard column (Supelco Inc., Bellefonte, PA), with 70% acetonitrile, 15% methanol, and 15% methylene chloride used as the running solvent flowing at 1.8 ml/min. Retinol and retinyl esters (retinyl palmitate, oleate, linoleate, and stearate) were separated and identified by comparing retention times and spectral data of experimental compounds with those of authentic standards. Concentrations of retinol and retinyl esters in the tissues were quantified by comparing peak integrated areas for unknowns against those of known amounts of purified standards. Loss during extraction was accounted for by adjusting for the recovery of retinyl acetate, the internal standard added immediately following homogenization of the tissues.

Statistical Analysis

All group data are shown as average ± SEM. Statistical comparisons were determined between genotypes on the same diet using a two-sided Student's *t* -test. Differences were considered significant for P<0.05.

Results

Mice lacking IFABP have drastically reduced expression of CRBP2 mRNA

The expression of CRBP2 mRNA in the intestinal mucosa was assessed in IFABP$^{-/-}$ mice after 12 weeks of HF feeding. It was found that IFABP$^{-/-}$ mice have dramatically reduced expression of CRBP2, with expression being 95% lower than that of WT mice **(Fig 1)**. Subsequent analysis of other vitamin A-related gene expression revealed that IFABP$^{-/-}$ mice have significantly increased expression of lecithin retinol acyl transferase (LRAT), retinoid X receptor alpha (RXRα), and sterol regulatory element binding protein 1 (SREBP1) **(Fig 1)**. Additionally, IFABP$^{-/-}$ mice have reduced expression of hepatocyte nuclear factor 4 alpha (HNF4α) and retinoic acid receptor beta (RARβ) **(Fig 1)**. Similar to the dramatic reduction in CRBP2 expression, the expression of RARβ was 74% lower than that of WT mice **(Fig 1)**.

Figure 1: **Relative quantitation of small intestine mucosal mRNA expression of CRBP2 and other vitamin A-related genes in 45% Kcal fat HF fed WT (●) and IFABP^{-/-} (■) mice.** (n=8).

IFABP^{-/-} mice have normal CRBP2 protein abundance

With there being such a dramatic reduction in CRBP2 mRNA observed in the IFABP$^{-/-}$ mice, it was anticipated that CRBP2 protein abundance would be lower as well. Western blotting was used to assess intestinal mucosal abundance of CRBP2 protein. Surprisingly, IFABP$^{-/-}$ mice have similar protein abundance of CRBP2, when compared to their WT counterparts **(Fig 2)**. Liver samples were used as a negative control, since CRBP2 is only expressed in the small intestine of adult animals. As expected, a band for CRBP2 was only present for small intestinal mucosal samples.
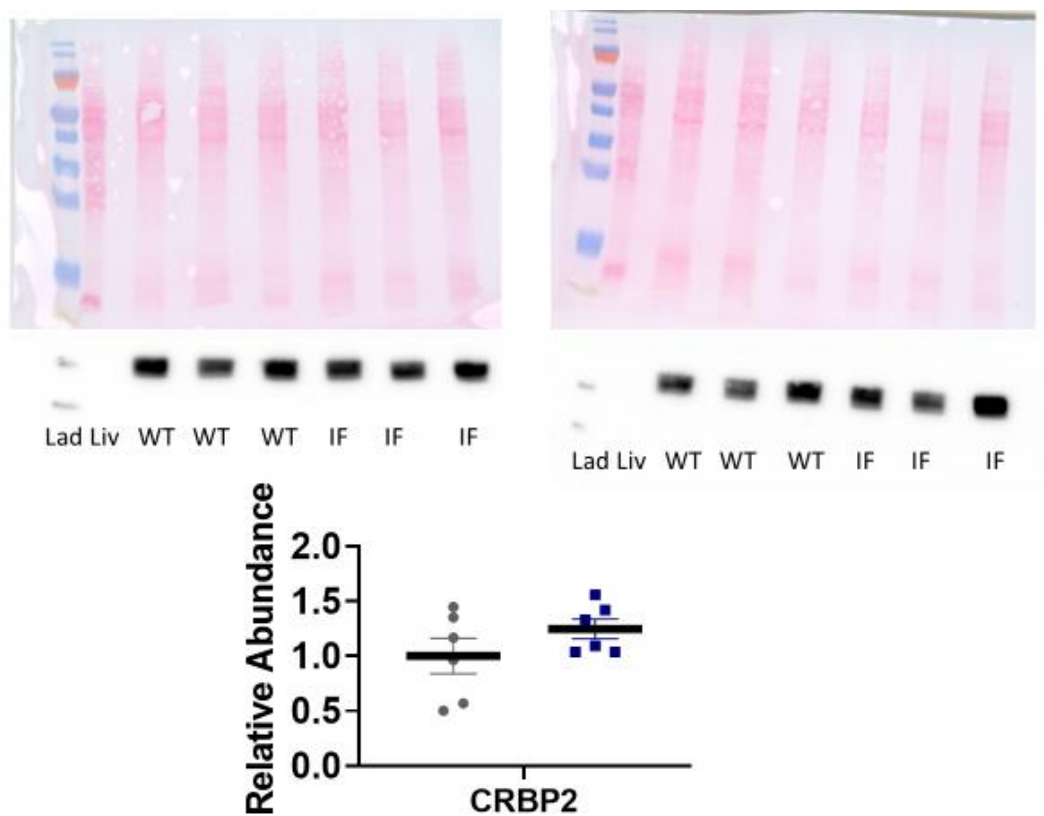
Figure 2: **Relative abundance of CRBP2 protein in 45% Kcal fat HF fed WT (●) and IFABP$^{-/-}$ (■) mice.** (n=6).

LF fed and HF fed IFABP^{-/-} mice have alteration in tissue retinoid levels

Plasma and tissue levels of retinol and retinyl ester was assessed in both LF and HF fed mice using HPLC. No changes were observed in small intestinal mucosal samples for both LF and HF fed mice **(Fig 3)**. In the liver, while no changes were observed with LF fed mice, HF fed IFABP^{-/-} mice were found to have lower retinol, and higher retinyl ester levels **(Fig 3)**. The only significant change observed in the LF fed mice was a reduction in plasma retinol in the IFABP^{-/-} mice **(Fig 3)**.
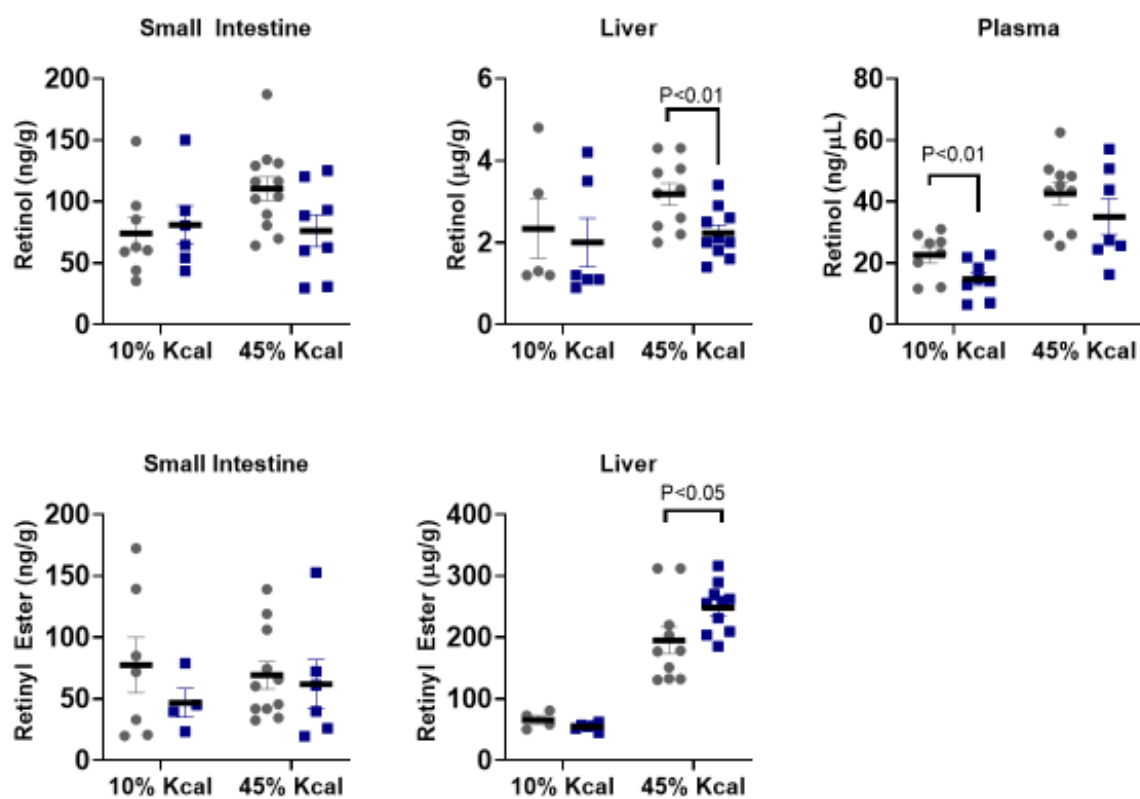
Figure 3: **Tissue and plasma retinol and retinyl ester levels in 10% Kcal LF fed and 45% Kcal fat HF fed WT (●) and IFABP$^{-/-}$ (■) mice.** (n=6-10).

LF fed IFABP$^{-/-}$ mice also have alterations in vitamin A-related gene expression

The expression of vitamin A-related genes were also assessed in LF fed IFABP$^{-/-}$ and WT mice. Like their HF fed counterparts, IFABP$^{-/-}$ mice also displayed a drastic reduction in CRBP2 gene expression relative to WT mice **(Fig 4)**. IFABP$^{-/-}$ mice also had reduced expression of SREBP1, peroxisome proliferator activated receptor alpha (PPARα), and LRAT, with a 52% reduction in LRAT being noted **(Fig 4)**. Aside from the change in CRBP2, none of the other changes observed in the LF fed animals were also seen in the HF fed animals, and none of the changes observed in HF fed animals occurred in LF fed animals **(Table 1)**.
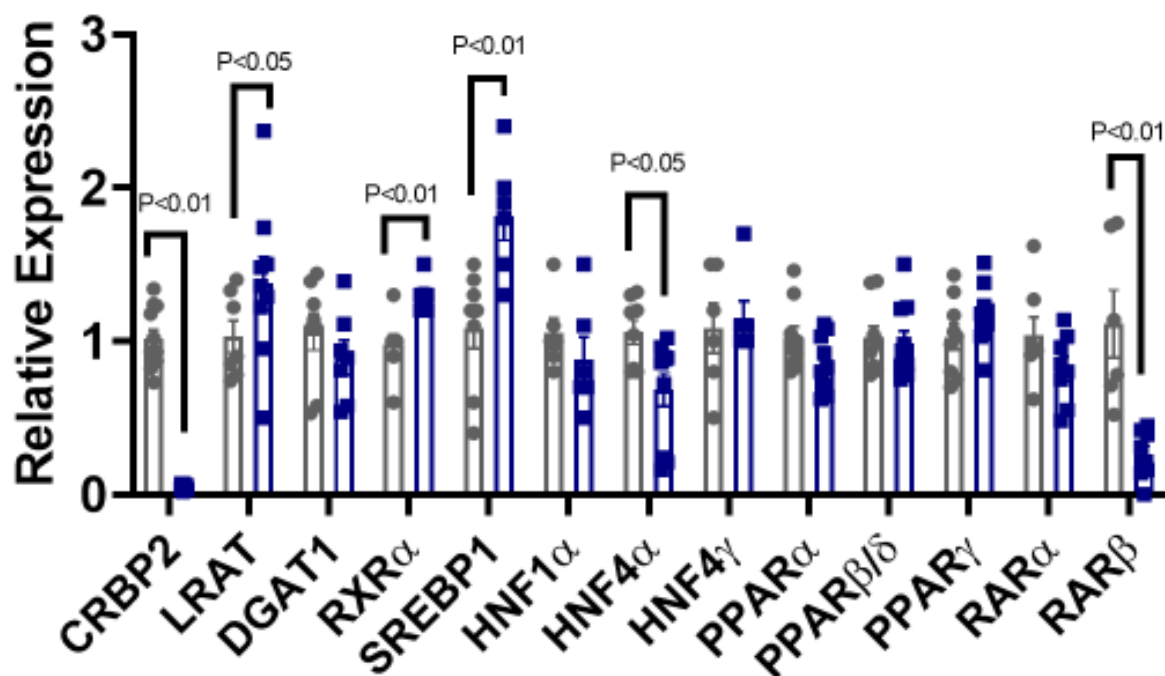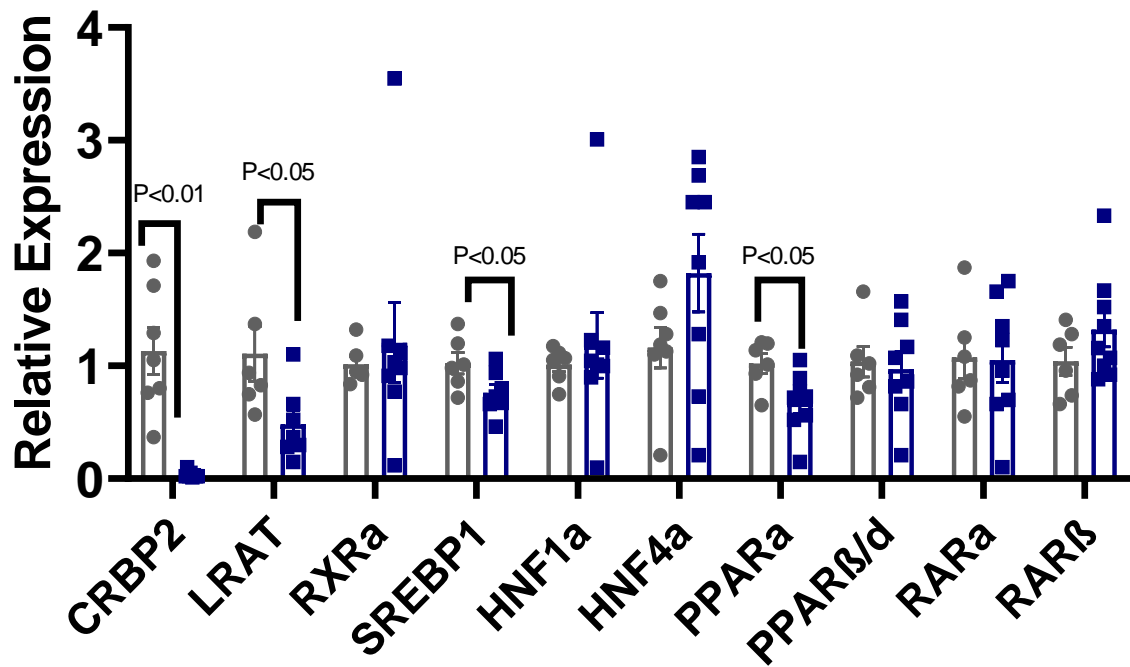
Figure 4: **Relative quantitation of small intestine mucosa mRNA expression of CRBP2 and other vitamin A-related genes in 10% Kcal fat LF fed WT (●) and IFABP$^{-/-}$ (■) mice.** (n=6-8).

Table 1: **Summary of gene expression analyses in LF and HF-fed small intestinal mucosa.**

No difference (≈). Not analyzed (NA).

45% Kcal HFD		10% Kcal LFD	
Gene	IFABP-/- (expression relative to WT	Gene	IFABP-/- (expression relative to WT
CRBP2	↓↓	CRBP2	↓↓
LRAT	↑	LRAT	↓
DGAT1	≈	DGAT1	NA
RXRα	↑	RXRα	≈
SREBP1	↑	SREBP1	↓
HNF1α	≈	HNF1α	≈
HNF4α	↓	HNF4α	≈
HNF4γ	≈	HNF4γ	NA
PPARα	≈	PPARα	↓
PPARβ/δ	≈	PPARβ/δ	≈
PPARγ	≈	PPARγ	NA
RARα	≈	RARα	≈
RARβ	↓↓	RARβ	≈

Discussion

Vitamin A, a fat soluble micronutrient, is essential to many tissues for normal cell growth and differentiation [138,273]. It is found in animal-based foods in the form of retinyl esters, and in plant based foods in the form of provitamin A carotenoids [138,274]. Prior to absorption, dietary retinol is cleaved by retinol ester hydrolase to release retinol, and after absorption, dietary carotenoids can be cleaved and eventually metabolized into retinol [138,275]. Subsequently, inside the enterocytes retinol is re-esterified into retinyl esters by the action of either LRAT or DGAT1, and packaged into chylomicrons for delivery to other tissues [275,276]. Similar to dietary FAs and MGs, it has been hypothesized the intracellular lipid binding proteins are necessary for the efficient uptake and trafficking of dietary retinol [11,127,138].

Proximal intestinal enterocytes express multiple FABPs, including IFABP, LFABP, and CRBP2. In humans, IFABP is less abundant than LFABP [135,136], however mice express similar levels of LFABP and IFABP within the small intestinal mucosa [135–137]. We have recently found that, as with the chow fed mice, HF fed IFABP^{-/-} mice do not have a compensatory increase in LFABP gene expression or protein abundance. Additionally, no change in the gene expression of the distal small intestinal FABP, ileal-FABP (ILBP; FABP6) was observed. However, the expression of CRBP2, the other major intestinal FABP, family member had not previously been assessed.

Since no changes were observed when assessing the expression of other FABP members in the intestinal mucosa, it was initially expected that the ablation of IFABP might induce a compensatory increase in CRBP2 gene expression, or no change in expression at all. Surprisingly, HF fed IFABP^{-/-} mice were found to have a 95% reduction in CRBP2 gene expression. With such a dramatic reduction in expression observed, it was hypothesized that the expression of other vitamin A-related genes might be perturbed as well in our HF fed IFABP^{-/-} mice. Indeed, numerous alterations were observed. Of note, the expression of LRAT was found to be ~40% higher in HF fed IFABP^{-/-} mice, while the expression of RARβ was ~74% lower. In the intestine, LRAT is

responsible converting dietary retinol back into retinyl ester, though it is important to note that this process requires retinol that is bound to CRBP2 [274]. Dietary retinol can also be converted into retinyl esters independent of CRBP2/LRAT through DGAT1, though this pathway does not seem to be the predominant one under normal physiological conditions [276,277]. RARβ is an important transcription factor that is able to influence an array of physiological processes, including cell growth and differentiation [278,279]. Additionally, RARβ is transcriptionally regulated by retinoic acid, with lower expression being associated with lower retinoic acid levels [280–282].

As mentioned above **(see Chapter 3)** IFABP^{-/-} mice have profound alterations in intestinal morphology and structure, displaying reduced average villus height, reduced goblet cell and Paneth cell densities, and altered expression of TJ-related genes. These changes were also accompanied by an altered barrier phenotype, with IFABP^{-/-} mice having increased intestinal permeability relative to WT mice. In the intestine, it has been demonstrated that retinoic acid is able to improve intestinal barrier function through activation of RARβ [283]. It has also been shown that vitamin A deficiency can impair the production of mucins, the main glycoprotein component that is produced by goblet cells that also acts to strengthen the intestinal barrier [37,273,284]. Since the HF fed IFABP mice appear to have reduced RARβ, it is likely that retinoic acid signaling in the small intestine is reduced, leading to alterations in small intestinal structure which may contribute to the observed increased intestinal permeability.

As mentioned above, the gene expression of CRBP2 was exceptionally low in HF IFABP^{-/-} mice. However, when CRBP2 protein abundance was assessed it was found that IFABP^{-/-} and WT mice had similar abundance. This observation was surprising, since historically members of the FABP family have been shown to be regulated transcriptionally, with changes in gene expression being highly correlated with similar directional changes in protein abundance [126,163,164,285–287]. Specifically, this transcriptional/translational pattern has been shown to occur not only for FA-binding members of the FABP family, but also with both CRBP1 and CRBP2 in various tissues

[287]. Such a large discrepancy between message and protein in the IFABP^{-/-} mice suggests some alteration in either mRNA and/or protein stability, and may imply that the regulation of FABPs at the level of gene expression and protein abundance may need to be reassessed under different physiological conditions.

How might the ablation of one intestinal FABP alter the gene expression of another intestinal FABP without inducing changes in the amount of protein present? It has been hypothesized that members of the FABP family are able to act as lipid chaperones, carrying various ligands to nuclear hormone receptors, or to membrane bound receptors, thereby inducing changes in gene transcription or signal transduction [91,157,268,288]. It is possible that IFABP is able to modulate the activity of a transcription factor that influences the expression of CRBP2. Without IFABP present, the proper ligand may not be able to interact with its transcription factor, leading to reduced CRBP2 expression. However, it is important to note that CRBP2 is necessary when challenged with low vitamin A diets, since CRBP2^{-/-} mice exposed to marginal vitamin A diets results in 100% mortality per litter within 24-hours after birth [289]. This suggest an integral role for CRBP2 in adapting to diets with varying amounts of vitamin A availability. Perhaps the retained protein abundance is compensatory, resulting in CRBP2 protein with a longer half-life. It is also possible that, if there is enhanced protein stability, that it is being induced by greater ligand availability and binding. Many members of the FABP family, including CRBP2, have been shown to have more rigid structures when bound to their ligands, while unbound FABPs have more flexible structures [14,128,271,290–293]. Additionally, there is evidence that greater rigidity may be correlated with increased structural stability [294–296], and increased protein half-life [297–299]. If there is greater ligand availability, and more CRBP2 bound to ligand, it is possible the CRBP2 present in the mucosa of IFABP^{-/-} mice is more stable than that of WT mice. LFABP and IFABP have an overlap in some of the ligands that they bind, with both being able to bind FAs [11]. Additionally, CRBP2 and LFABP also have an overlap of ligand binding, with both being able to bind 2-MGs [128] (*Lee et al., 2019*

Submitted). Perhaps the ablation of IFABP results in increased LFABP binding to FA. To compensate for the lack of available apo-LFABP, more 2-MGs may bind to CRBP2 instead. Future studies should assess CRBP2 protein half-life in WT and IFABP^{-/-} mice. If differences in half-life are observed, potential mechanisms of proteasomal degradation such as ubiquitination or ubiquitin-independent degradation [300–302], should also be assessed in the mucosa of WT and IFABP^{-/-} mice. For examples, it is possible that the CRBP2 present in the mucosa of IFABP^{-/-} mice is less prone to ubiquitination over time, resulting in a longer half-life. In addition to potential regulators of protein half-life, regulators of mRNA stability, such as micro RNAs (miRNA) should also be assessed [303,304]. miRNA are small non-coding RNAs that can be found in an array of cell types, being able to silence the expression of specific target genes [303,304]. The levels of specific miRNAs vary under different physiological conditions [303,304]. Perhaps the low level of CRBP2 gene expression is influenced by increased binding of miRNA to critical locations on the CRBP2 gene, silencing the gene without affecting the protein that has already been translated.

Since there were a number alterations in vitamin A-related gene expression in the HF fed IFABP^{-/-} mice, tissue and plasma retinoid status was assessed. Tissues and plasma from LF fed animals were also acquired; though the vitamin A content of the LF and HF diets are the same (4IU/g), it is important to note that the vitamin A from the HF diet is more likely to be efficiently absorbed. While no changes were found in the small intestine of either LF or HF fed mice, liver retinyl ester level was found to be higher and liver retinol was found to be lower in HF fed IFABP^{-/-} mice, suggesting greater storage of vitamin A. Plasma retinol levels are normally tightly regulated [127,305,306], yet it was found that LF fed IFABP^{-/-} mice have reduced plasma retinol levels. This may imply that the LF fed IFABP^{-/-} mice are more sensitive to LF challenges when compared to their WT counterparts, resulting in marginal vitamin A deficiency. To assess this idea further, gene expression studies were performed in LF fed mice as well.

Surprisingly, like their HF fed counterparts, LF fed IFABP^{-/-} also had ~95% reduction in CRBP2 gene expression. However, unlike HF fed IFABP^{-/-} mice, LF fed IFABP^{-/-} mice have a 52% reduction in LRAT gene expression. Such a drastic reduction of LRAT gene expression may suggest a reduced capacity to re-esterify dietary retinol for export in chylomicrons, which might partially explain the reduced plasma retinol levels that are observed. Aside from the reduced mRNA expression of CRBP2, the changes that were observed in HF fed IFABP^{-/-} mice were not observed in LF fed IFABP^{-/-} mice, and vice versa. Taken together, it is possible that the ablation of IFABP results in alterations in vitamin A-related metabolism in both HF and LF fed mice. However, it is important to note that all mice that were analyzed for this study were fasted for 16 hours. With this fasting time the circulating retinol would be indicative of use by liver stores, and not necessarily the responses induced by the intestinal processing [127,138]. In the future, it will be important to analyze tissue from mice that have either recently fed, or have been gavaged with retinol dissolved in oil, as this will give a better representation of intestinal handling of a vitamin A challenge. Additionally, CRBP2 protein abundance in LF fed IFABP^{-/-} mice needs to be assessed to see if a similar dissociation of message and transcript is observed.

It is also important to mention that while CRBP2 has historically be described as an FABP that is only able to bind retinol and retinal [127,307], we have recently demonstrated that it is able to bind MGs, such as the endocannabinoid 2-AG, as well (*Lee et al., 2019 Submitted*). As mentioned above **(see Chapter 3)** in addition to alteration in intestinal morphology and structure, IFABP^{-/-} mice were also found to have greater fecal output and more rapid intestinal transit. Endocannabinoid signaling is known to influence intestinal physiology and structure, playing a role in modulating motility, proliferation, differentiation, and inflammation [265,308,309]. For example, it has been shown that endocannabinoids are able to inhibit intestinal motility through activation of cannabinoid receptor 1 (CBR1) [227,266]. It been shown that some FABPs regulate endocannabinoid levels through enhancing hydrolysis [130,131]. Additionally, we have recently shown that CRBP2^{-/-}

mice have elevated mucosal levels of 2-AG, a potent CBR1 agonist (*Lee et al., 2019 Submitted*), suggesting that CRBP2 may play role in regulating 2-AG hydrolysis in the small intestine. We have also shown that IFABP^{-/-} mice trended towards having lower 2-AG levels [16], which may partly explain the more rapid intestinal transit time that is observed in these mice. It is possible that the low mucosal 2-AG levels might be due to binding by CRBP2, which may direct 2-AG towards MGL for hydrolysis, thus explaining part of the whole-body phenotyping alterations observed in the IFABP^{-/-} mice. Though hydrolysis of 2-AG through CRBP2 binding has not been definitively shown, if CRBP2 is influencing the whole-body phenotype of the IFABP^{-/-} mice, it is possible that the influence may be a result of altered MG metabolism rather than, or in addition to, altered vitamin A metabolism.

Overall, while the expression of LFABP and LFABP protein abundance were not found to be altered in IFABP^{-/-} mice, the gene expression of CRBP2 appears to be dramatically low despite having normal CRBP2 protein levels. IFABP^{-/-} mice were found to have alterations in vitamin A-related gene expression and tissue retinoid content, though whether these changes are due to the actions CRBP2 remains to be determined. Further studies are required to understand not only the influence that the intestinal FABPs may have on one another, but also the transcriptional and translation regulation of FABPs in different physiological states.

Literature Cited

1.   Phan CT, Tso P. Intestinal lipid absorption and transport. *Front Biosci*. 2001;6:D299-319.

2.   Fahy E, Subramaniam S, Murphy RC, et al. Update of the LIPID MAPS comprehensive classification system for lipids 1. 2009:9-14. doi:10.1194/jlr.R800095-JLR200

3.   Moe PW. Future directions for energy requirements and food energy values. *J Nutr*. 1994;124(9 Suppl):1738S-1742S. doi:10.1093/jn/124.suppl_9.1738S

4.   Haslam DW, James WPT. Obesity. *Lancet*. 2005;366(9492):1197-1209. doi:10.1016/S0140-6736(05)67483-1

5.   WHO. Global status report on noncommunicable diseases 2014. *World Health*. 2014:176. doi:ISBN 9789241564854

6.   Flegal KM, Carroll MD, Ogden CL, Curtin LR. Prevalence and trends in obesity among US adults, 1999-2008. *JAMA*. 2010;303(3):235-241. doi:10.1001/jama.2009.2014

7.   Barness LA, Opitz JM, Gilbert-Barness E. Obesity: Genetic, molecular, and environmental aspects. *Am J Med Genet Part A*. 2007;143A(24):3016-3034. doi:10.1002/ajmg.a.32035

8.   Wycherley TP, Moran LJ, Clifton PM, Noakes M, Brinkworth GD. Effects of energy-restricted high-protein, low-fat compared with standard-protein, low-fat diets: a meta-analysis of randomized controlled trials. *Am J Clin Nutr*. 2012;96(6):1281-1298. doi:10.3945/ajcn.112.044321

9.   Lottenberg AM, Afonso M da S, Lavrador MSF, Machado RM, Nakandakare ER. The role of dietary fatty acids in the pathology of metabolic syndrome. *J Nutr Biochem*. 2012;23(9):1027-1040. doi:10.1016/j.jnutbio.2012.03.004

10.   KM F, MD C, CL O, CL J. Prevalence and trends in obesity among us adults, 1999-2000. *JAMA*. 2002;288(14):1723-1727. doi:10.1001/jama.288.14.1723

11.   Gajda AM, Storch J. Enterocyte fatty acid-binding proteins (FABPs): Different functions of liver and intestinal FABPs in the intestine. *Prostaglandins Leukot Essent Fat Acids*. 2015;93:9-16. doi:10.1016/j.plefa.2014.10.001

12.   Storch J, Corsico B. The Emerging Functions and Mechanisms of Mammalian Fatty Acid – Binding Proteins. 2008. doi:10.1146/annurev.nutr.27.061406.093710

13.   Kursula P, Thorsell AG, Arrowsmith C, et al. Crystal structure of human FABP1. *TO BE Publ*. doi:10.2210/PDB2F73/PDB

14.   Zhang F, Lucke C, Baier LJ, Sacchettini JC, Hamilton JA. Solution structure of human intestinal fatty acid binding protein: implications for ligand entry and exit. *J Biomol NMR*. 1997;9(3):213-228.

15.   Lagakos WS, Gajda AM, Agellon L, et al. Different functions of intestinal and liver-type fatty acid-binding proteins in intestine and in whole body energy homeostasis Different functions of intestinal and liver-type fatty acid-binding proteins in intestine and in whole body energy homeostasis. 2011;(February):803-814. doi:10.1152/ajpgi.00229.2010

16.   Gajda AM, Zhou YX, Agellon LB, et al. Direct comparison of mice null for liver or intestinal fatty acid-binding proteins reveals highly divergent phenotypic responses to high fat feeding. *J Biol Chem*. 2013;288(42):30330-30344. doi:10.1074/jbc.M113.501676

17.   Ervin RB, Wright JD, Wang C-Y, Kennedy-Stephenson J. Dietary intake of fats and fatty acids for the United States population: 1999-2000. *Adv Data*. 2004;(348):1-6.

18.   Cordain L, Eaton SB, Sebastian A, et al. Origins and evolution of the Western diet: health implications for the 21st century. *Am J Clin Nutr*. 2005;81(2):341-354. doi:10.1093/ajcn.81.2.341

19.   Hussain MM. Intestinal Lipid Absorption and Lipoprotein Formation. *Curr Opin Lipid Biol*. 2014;25(3):200-206. doi:10.1016/j.jmb.2008.10.054.The

20.   Kennedy ET, Bowman SA, Powell R. Dietary-fat intake in the US population. *J Am Coll Nutr*. 1999;18(3):207-212.

21.   Prentice RL, Aragaki AK, Van Horn L, et al. Low-fat dietary pattern and cardiovascular disease: results from the Women's Health Initiative randomized controlled trial. *Am J Clin Nutr*. 2017;106(1):35-43. doi:10.3945/ajcn.117.153270

22.   Katan MB, Zock PL, Mensink RP. Dietary oils, serum lipoproteins, and coronary heart disease. *Am J Clin Nutr*. 1995;61(6 Suppl):1368S-1373S. doi:10.1093/ajcn/61.6.1368S

23.   Kushi LH, Lenart EB, Willett WC. Health implications of Mediterranean diets in light of contemporary knowledge. 1. Plant foods and dairy products. *Am J Clin Nutr*. 1995;61(6 Suppl):1407S-1415S. doi:10.1093/ajcn/61.6.1407S

24.   Lairon D. Macronutrient intake and modulation on chylomicron production and clearance. *Atheroscler Suppl*. 2008;9(2):45-48. doi:10.1016/j.atherosclerosissup.2008.05.006

25.   Goodman BE. Insights into digestion and absorption of major nutrients in humans. *Adv Physiol Educ*. 2010;34(2):44-53. doi:10.1152/advan.00094.2009

26.   Thomson ABR, Tso P. Overview of Digestion and Absorption. In: *Biochemical, Physiological, and Molecular Aspects of Human Nutrition*. 3rd ed. ; 2013:123-141.

27.   Brannon PM, Tso P, Jandacek RJ. Digestion and Absorption of Lipids. In: *Biochemical, Physiological, and Molecular Aspects of Human Nutrition*. 3rd ed. ; 2013:179-193.

28.   Ash R, Morton DA, Scott SA. Digestive System. In: *The Big Picture: Histology*. ; 2013.

29.   Boyer JL. Bile formation and secretion. *Compr Physiol*. 2013;3(3):1035-1078. doi:10.1002/cphy.c120027

30.   Chiang JYL. Bile acid metabolism and signaling. *Compr Physiol*. 2013;3(3):1191-1212. doi:10.1002/cphy.c120023

31.   Li T, Chiang JYL. Bile acids as metabolic regulators. *Curr Opin Gastroenterol*. 2015;31(2):159-165. doi:10.1097/MOG.0000000000000156

32.   Ruberte J, Carretero A, Navarro M. Digestive Tract. In: *Morphological Mouse Phenotyping*. ; 2017:89-146.

33.   Caspary WF. Physiology and Pathophysiology of Intestinal Absorption. *Am J Clin Nutr*. 1992;55:299-308.

34.   Crawley SW, Mooseker MS, Tyska MJ. Shaping the intestinal brush border. *J Cell Biol*. 2014;207(4):441-451. doi:10.1083/jcb.201407015

35. Shaker A, Rubin DC. Intestinal stem cells and epithelial-mesenchymal interactions in the crypt and stem cell niche. *Transl Res*. 2010;156(3):180-187. doi:10.1016/j.trsl.2010.06.003

36. Worthington JJ, Reimann F, Gribble FM. Enteroendocrine cells-sensory sentinels of the intestinal environment and orchestrators of mucosal immunity. *Mucosal Immunol*. 2018;11(1):3-20. doi:10.1038/mi.2017.73

37. Mccauley HA. Three cheers for the goblet cell : maintaining homeostasis in mucosal epithelia. 2015;21(8). doi:10.1016/j.molmed.2015.06.003

38. Kim YS, Ho SB. Intestinal Goblet Cells and Mucins in Health and Disease : Recent Insights and Progress. 2010:319-330. doi:10.1007/s11894-010-0131-2

39. Deplancke B, Gaskins HR. Microbial modulation of innate defense : goblet cells and the intestinal mucus layer. *Am J Clin Nutr*. 2001;73:1131S-41S.

40. Bennek E, Verdier J, Zhang K, et al. c-Jun N-terminal kinase 2 promotes enterocyte survival and goblet cell differentiation in the inflamed intestine. 2017;(November 2016):1-13. doi:10.1038/mi.2016.125

41. Kim JJ, Khan WI. Goblet Cells and Mucins: Role in Innate Defense Enteric Infections. 2013:55-70. doi:10.3390/pathogens2010055

42. Atuma C, Strugala V, Allen A, Holm L. The adherent gastrointestinal mucus gel layer : thickness and physical state in vivo. *Am J Gastrointest Liver Physiol*. 2001;280:922-929.

43. Johansson ME V, Thomsson KA, Hansson GC. Proteomic Analyses of the Two Mucus Layers of the Colon Barrier Reveal That Their Main Component , the Muc2 Mucin , Is Strongly Bound to the Fcgbp Protein research articles. *J Proteome Res*. 2009;8:3549-3557.

44. Clevers HC, Bevins CL. Paneth Cells: Maestros of the Small Intestinal Crypts. *Annu Rev Physiol*. 2013;75(1):289-311. doi:10.1146/annurev-physiol-030212-183744

45. CREAMER B, SHORTER RG, BAMFORTH J. The turnover and shedding of epithelial cells. I. The turnover in the gastro-intestinal tract. *Gut*. 1961;2:110-118. doi:10.1136/gut.2.2.110

46. Landy J, Ronde E, English N, et al. Tight junctions in inflammatory bowel diseases and inflammatory bowel disease associated colorectal cancer. *World J Gastroenterol*. 2016;22(11):3117-3126. doi:10.3748/wjg.v22.i11.3117

47. Khan N, Asif AR. Transcriptional Regulators of Claudins in Epithelial Tight Junctions. 2015;2015(1). doi:10.1155/2015/219843

48. Barmeyer C, Fromm M, Schulzke J-D. Active and passive involvement of claudins in the pathophysiology of intestinal inflammatory diseases. *Pflugers Arch Eur J Physiol*. 2017;469:15-26. doi:10.1007/s00424-016-1914-6

49. Zeissig S, Burgel N, Gu D, et al. Changes in expression and distribution of claudin 2, 5 and 8 lead to discontinuous tight junctions and barrier dysfunction in active Crohn's disease. *Gut*. 2007;56:61-72. doi:10.1136/gut.2006.094375

50. Luettig J, Rosenthal R, Barmeyer C, Schulzke JD. Claudin-2 as a mediator of leaky gut barrier during intestinal inflammation. *Tissue barriers*. 2015;3(1-2):e977176. doi:10.4161/21688370.2014.977176

51. Schulzke JD, Gitter AH, Mankertz J, et al. Epithelial transport and barrier function in occludin-deficient mice. *Biochim Biophys Acta - Biomembr*. 2005;1669(1):34-42. doi:10.1016/j.bbamem.2005.01.008

52. Cani PD, Bibiloni R, Knauf C, Neyrinck AM, Delzenne NM. Changes in gut microbiota control metabolic diet–induced obesity and diabetes in mice. *Diabetes*. 2008;57(6):1470-1481. doi:10.2337/db07-1403.Additional

53. Kim KA, Gu W, Lee IA, Joh EH, Kim DH. High Fat Diet-Induced Gut Microbiota Exacerbates Inflammation and Obesity in Mice via the TLR4 Signaling Pathway. *PLoS One*. 2012;7(10). doi:10.1371/journal.pone.0047713

54. Giammanco A, Cefalù AB, Noto D, Averna MR. The pathophysiology of intestinal lipoprotein production. 2015;6(March):1-10. doi:10.3389/fphys.2015.00061

55. Murota K, Storch J. Uptake of micellar long-chain fatty acid and sn-2-monoacylglycerol into human intestinal Caco-2 cells exhibits characteristics of protein-mediated transport. *J Nutr*. 2005;135(7):1626-1630. doi:10.1093/jn/135.7.1626

56. Ho SY, Storch J. Common mechanisms of monoacylglycerol and fatty acid uptake by human intestinal Caco-2 cells. *Am J Physiol Cell Physiol*. 2001;281(4):C1106-17. doi:10.1152/ajpcell.2001.281.4.C1106

57. Abumrad NA, Davidson NO. Role of the gut in lipid homeostasis. *Physiol Rev*. 2012;92(3):1061-1085. doi:10.1152/physrev.00019.2011

58. Cifarelli V, Abumrad NA. Intestinal CD36 and Other Key Proteins of Lipid Utilization: Role in Absorption and Gut Homeostasis. *Compr Physiol*. 2018;8(2):493-507. doi:10.1002/cphy.c170026

59. Storch J, Zhou YX, Lagakos WS. Metabolism of apical versus basolateral sn-2-monoacylglycerol and fatty acids in rodent small intestine. *J Lipid Res*. 2008;49(8):1762-1769. doi:10.1194/jlr.M800116-JLR200

60. Tranchant T, Besson P, Hoinard C, et al. Mechanisms and kinetics of alpha-linolenic acid uptake in Caco-2 clone TC7. *Biochim Biophys Acta*. 1997;1345(2):151-161.

61. Richieri G V, Kleinfeld AM. Unbound free fatty acid levels in human serum. *J Lipid Res*. 1995;36(2):229-240.

62. Shim J, Moulson CL, Newberry EP, et al. Fatty acid transport protein 4 is dispensable for intestinal lipid absorption in mice. *J Lipid Res*. 2009;50(3):491-500. doi:10.1194/jlr.M800400-JLR200

63. Stahl A, Hirsch DJ, Gimeno RE, et al. Identification of the major intestinal fatty acid transport protein. *Mol Cell*. 1999;4(3):299-308.

64. Nassir F, Wilson B, Han X, Gross RW, Abumrad NA. CD36 is important for fatty acid and cholesterol uptake by the proximal but not distal intestine. *J Biol Chem*. 2007;282(27):19493-19501. doi:10.1074/jbc.M703330200

65. Nauli AM, Nassir F, Zheng S, et al. CD36 is important for chylomicron formation and secretion and may mediate cholesterol uptake in the proximal intestine. *Gastroenterology*. 2006;131(4):1197-1207. doi:10.1053/j.gastro.2006.08.012

66. Drover VA, Ajmal M, Nassir F, et al. CD36 deficiency impairs intestinal lipid secretion and clearance of chylomicrons from the blood. *J Clin Invest*. 2005;115(5):1290-1297. doi:10.1172/JCI21514

67. Drover VA, Nguyen D V, Bastie CC, et al. CD36 mediates both cellular uptake of very long chain fatty acids and their intestinal absorption in mice. *J Biol Chem*. 2008;283(19):13108-13115. doi:10.1074/jbc.M708086200

68. Lobo M V, Huerta L, Ruiz-Velasco N, et al. Localization of the lipid receptors CD36 and CLA-1/SR-BI in the human gastrointestinal tract: towards the identification of receptors mediating the intestinal absorption of dietary lipids. *J Histochem Cytochem*. 2001;49(10):1253-1260. doi:10.1177/002215540104901007

69. Cai SF, Kirby RJ, Howles PN, Hui DY. Differentiation-dependent expression and localization of the class B type I scavenger receptor in intestine. *J Lipid Res*. 2001;42(6):902-909.

70. Kiens B, Kristiansen S, Jensen P, Richter EA, Turcotte LP. Membrane associated fatty acid binding protein (FABPpm) in human skeletal muscle is increased by endurance training. *Biochem Biophys Res Commun*. 1997;231(2):463-465. doi:10.1006/bbrc.1997.6118

71. Turcotte LP, Srivastava AK, Chiasson JL. Fasting increases plasma membrane fatty acid-binding protein (FABP(PM)) in red skeletal muscle. *Mol Cell Biochem*. 1997;166(1-2):153-158.

72. Murota K, Matsui N, Kawada T, Takahashi N, Fushuki T. Inhibitory effect of monoacylglycerol on fatty acid uptake into rat intestinal epithelial cells. *Biosci Biotechnol Biochem*. 2001;65(6):1441-1443. doi:10.1271/bbb.65.1441

73. Richard VR, Beach A, Piano A, et al. Mechanism of liponecrosis, a distinct mode of programmed cell death. *Cell Cycle*. 2014;13(23):3707-3726. doi:10.4161/15384101.2014.965003

74. Rockenfeller P, Ring J, Muschett V, et al. Fatty acids trigger mitochondrion-dependent necrosis. *Cell Cycle*. 2010;9(14):2836-2842. doi:10.4161/cc.9.14.12267

75. Listenberger LL, Ory DS, Schaffer JE. Palmitate-induced apoptosis can occur through a ceramide-independent pathway. *J Biol Chem*. 2001;276(18):14890-14895. doi:10.1074/jbc.M010286200

76. Mashek DG, Li LO, Coleman RA. Rat long-chain acyl-CoA synthetase mRNA, protein, and activity vary in tissue distribution and in response to diet. *J Lipid Res*. 2006;47(9):2004-2010. doi:10.1194/jlr.M600150-JLR200

77. Milger K, Herrmann T, Becker C, et al. Cellular uptake of fatty acids driven by the ER-localized acyl-CoA synthetase FATP4. *J Cell Sci*. 2006;119(Pt 22):4678-4688. doi:10.1242/jcs.03280

78. Cao J, Hawkins E, Brozinick J, et al. A predominant role of acyl-CoA:monoacylglycerol acyltransferase-2 in dietary fat absorption implicated by tissue distribution, subcellular localization, and up-regulation by high fat diet. *J Biol Chem*. 2004;279(18):18878-18886. doi:10.1074/jbc.M313272200

79. Yen C-LE, Nelson DW, Yen M-I. Intestinal triacylglycerol synthesis in fat absorption and systemic energy metabolism. *J Lipid Res*. 2015;56(3):489-501. doi:10.1194/jlr.R052902

80. Buhman KK, Smith SJ, Stone SJ, et al. DGAT1 is not essential for intestinal triacylglycerol absorption or chylomicron synthesis. *J Biol Chem*. 2002;277(28):25474-25479. doi:10.1074/jbc.M202013200

81. Shi Y, Cheng D. Beyond triglyceride synthesis: the dynamic functional roles of MGAT and DGAT enzymes in energy metabolism. *Am J Physiol Endocrinol Metab*. 2009;297(1):E10-8. doi:10.1152/ajpendo.90949.2008

82. Yen C-LE, Cheong M-L, Grueter C, et al. Deficiency of the intestinal enzyme acyl CoA:monoacylglycerol acyltransferase-2 protects mice from metabolic disorders induced by high-fat feeding. *Nat Med*. 2009;15(4):442-446. doi:10.1038/nm.1937

83. Pan X, Hussain MM. Gut triglyceride production. *Biochim Biophys Acta*. 2012;1821(5):727-735. doi:10.1016/j.bbalip.2011.09.013

84. Takeuchi K, Reue K. Biochemistry, physiology, and genetics of GPAT, AGPAT, and lipin enzymes in triglyceride synthesis. *Am J Physiol Endocrinol Metab*. 2009;296(6):E1195-209. doi:10.1152/ajpendo.90958.2008

85. Jamdar SC, Cao WF. Triacylglycerol biosynthetic enzymes in lean and obese Zucker rats. *Biochim Biophys Acta*. 1995;1255(3):237-243. doi:10.1016/0005-2760(94)00217-m

86. Beilstein F, Carriere V, Leturque A, Demignot S. Characteristics and functions of lipid droplets and associated proteins in enterocytes. *Exp Cell Res*. 2016;340(2):172-179. doi:10.1016/j.yexcr.2015.09.018

87. Demignot S, Beilstein F, Morel E. Triglyceride-rich lipoproteins and cytosolic lipid droplets in enterocytes: key players in intestinal physiology and metabolic disorders. *Biochimie*. 2014;96:48-55. doi:10.1016/j.biochi.2013.07.009

88. Auclair N, Melbouci L, St-Pierre D, Levy E. Gastrointestinal factors regulating lipid droplet formation in the intestine. *Exp Cell Res*. 2018;363(1):1-14. doi:10.1016/j.yexcr.2017.12.031

89. Wang B, Rong X, Duerr MA, et al. Intestinal Phospholipid Remodeling Is Required for Dietary-Lipid Uptake and Survival on a High-Fat Diet. *Cell Metab*. 2016;23(3):492-504. doi:10.1016/j.cmet.2016.01.001

90. Hashidate-Yoshida T, Harayama T, Hishikawa D, et al. Fatty acid remodeling by LPCAT3 enriches arachidonate in phospholipid membranes and regulates triglyceride transport. *Elife*. 2015;4. doi:10.7554/eLife.06328

91. Hong SH, Ahmadian M, Yu RT, Atkins AR, Downes M, Evans RM. Nuclear receptors and metabolism: From feast to famine. *Diabetologia*. 2014;57(5):860-867. doi:10.1007/s00125-014-3209-9

92. Naughton SS, Mathai ML, Hryciw DH, McAinch AJ. Fatty acid modulation of the endocannabinoid system and the effect on food intake and metabolism. *Int J Endocrinol*. 2013;2013. doi:10.1155/2013/361895

93. Demuth DG, Molleman A. Cannabinoid signalling. *Life Sci*. 2006;78(6):549-563. doi:10.1016/j.lfs.2005.05.055

94. Margolskee RF, Dyer J, Kokrashvili Z, et al. T1R3 and gustducin in gut sense sugars to regulate expression of Na+-glucose cotransporter 1. *Proc Natl Acad Sci U S A*. 2007;104(38):15075-15080. doi:10.1073/pnas.0706678104

95. Overton HA, Fyfe MCT, Reynet C. GPR119, a novel G protein-coupled receptor target for the treatment of type 2 diabetes and obesity. *Br J Pharmacol*. 2008;153 Suppl(October 2007):S76-81. doi:10.1038/sj.bjp.0707529

96. Mishra AK, Dubey V, Ghosh AR. Obesity: An overview of possible role(s) of gut hormones, lipid sensing and gut microbiota. *Metabolism*. 2016;65(1):48-65. doi:10.1016/j.metabol.2015.10.008

97. Gribble FM, Reimann F. Enteroendocrine Cells: Chemosensors in the Intestinal Epithelium. *Annu Rev Physiol*. 2016;78:277-299. doi:10.1146/annurev-physiol-021115-105439

98. Begg DP, Woods SC. The endocrinology of food intake. *Nat Rev Endocrinol*. 2013;9(10):584-597. doi:10.1038/nrendo.2013.136

99. Egerod KL, Engelstoft MS, Grunddal K V, et al. A major lineage of enteroendocrine cells coexpress CCK, secretin, GIP, GLP-1, PYY, and neurotensin but not somatostatin. *Endocrinology*. 2012;153(12):5782-5795. doi:10.1210/en.2012-1595

100. Svendsen B, Pedersen J, Albrechtsen NJW, et al. An analysis of cosecretion and coexpression of gut hormones from male rat proximal and distal small intestine. *Endocrinology*. 2015;156(3):847-857. doi:10.1210/en.2014-1710

101. Adriaenssens A, Lam BYH, Billing L, et al. A Transcriptome-Led Exploration of Molecular Mechanisms Regulating Somatostatin-Producing D-Cells in the Gastric Epithelium. *Endocrinology*. 2015;156(11):3924-3936. doi:10.1210/en.2015-1301

102. Grunddal K V, Ratner CF, Svendsen B, et al. Neurotensin Is Coexpressed, Coreleased, and Acts Together With GLP-1 and PYY in Enteroendocrine Control of Metabolism. *Endocrinology*. 2016;157(1):176-194. doi:10.1210/en.2015-1600

103. Svendsen B, Pais R, Engelstoft MS, et al. GLP1- and GIP-producing cells rarely overlap and differ by bombesin receptor-2 expression and responsiveness. *J Endocrinol*. 2016;228(1):39-48. doi:10.1530/JOE-15-0247

104. Habib AM, Richards P, Cairns LS, et al. Overlap of endocrine hormone expression in the mouse intestine revealed by transcriptional profiling and flow cytometry. *Endocrinology*. 2012;153(7):3054-3065. doi:10.1210/en.2011-2170

105. Hallden G, Aponte GW. Evidence for a role of the gut hormone PYY in the regulation of intestinal fatty acid-binding protein transcripts in differentiated subpopulations of intestinal epithelial cell hybrids. *J Biol Chem*. 1997;272(19):12591-12600. doi:10.1074/jbc.272.19.12591

106. Mellitzer G, Beucher A, Lobstein V, et al. Loss of enteroendocrine cells in mice alters lipid absorption and glucose homeostasis and impairs postnatal survival. *J Clin Invest*. 2010;120(5):1708-1721. doi:10.1172/JCI40794

107. Breit S, Kupferberg A, Rogler G, Hasler G. Vagus Nerve as Modulator of the Brain-Gut Axis in Psychiatric and Inflammatory Disorders. *Front psychiatry*. 2018;9:44. doi:10.3389/fpsyt.2018.00044

108. Wren AM, Seal LJ, Cohen MA, et al. Ghrelin enhances appetite and increases food intake in humans. *J Clin Endocrinol Metab*. 2001;86(12):5992. doi:10.1210/jcem.86.12.8111

109. Alamri BN, Shin K, Chappe V, Anini Y. The role of ghrelin in the regulation of glucose homeostasis. *Horm Mol Biol Clin Investig*. 2016;26(1):3-11. doi:10.1515/hmbci-2016-0018

110. Glatz JFC, Luiken JJFP. Fatty acids in cell signaling: Historical perspective and future outlook. *Prostaglandins Leukot Essent Fat Acids*. 2015;92:57-62. doi:10.1016/j.plefa.2014.02.007

111. Gillum MP, Zhang D, Zhang X-M, et al. N-acylphosphatidylethanolamine, a gut- derived circulating factor induced by fat ingestion, inhibits food intake. *Cell*. 2008;135(5):813-824. doi:10.1016/j.cell.2008.10.043

112. Kersten S. Integrated physiology and systems biology of PPARα. *Mol Metab*. 2014;3(4):354-371. doi:10.1016/j.molmet.2014.02.002

113. Newberry EP, Kennedy SM, Xie Y, et al. Decreased body weight and hepatic steatosis with altered fatty acid ethanolamide metabolism in aged L-Fabp -/- mice. *J Lipid Res*. 2012;53(4):744-754. doi:10.1194/jlr.M020966

114. Schwartz GJ, Fu J, Astarita G, et al. The lipid messenger OEA links dietary fat intake to satiety. *Cell Metab*. 2008;8(4):281-288. doi:10.1016/j.cmet.2008.08.005

115. Cristino L, Becker T, Di Marzo V. Endocannabinoids and energy homeostasis: An update. *Biofactors*. 2014:1-9. doi:10.1002/biof.1168

116. Silvestri C, Di Marzo V. The endocannabinoid system in energy homeostasis and the etiopathology of metabolic disorders. *Cell Metab*. 2013;17(4):475-490. doi:10.1016/j.cmet.2013.03.001

117. Izzo AA, Piscitelli F, Capasso R, et al. Peripheral endocannabinoid dysregulation in obesity: Relation to intestinal motility and energy processing induced by food deprivation and re-feeding. *Br J Pharmacol*. 2009;158(2):451-461. doi:10.1111/j.1476-5381.2009.00183.x

118. Vianna CR, Donato JJ, Rossi J, et al. Cannabinoid receptor 1 in the vagus nerve is dispensable for body weight homeostasis but required for normal gastrointestinal motility. *J Neurosci*. 2012;32(30):10331-10337. doi:10.1523/JNEUROSCI.4507-11.2012

119. Colombo G, Agabio R, Lobina C, Reali R, Gessa GL. Cannabinoid modulation of intestinal propulsion in mice. *Eur J Pharmacol*. 1998;344(1):67-69. doi:10.1016/s0014-2999(97)01555-0

120. Yuece B, Sibaev A, Broedl U, et al. Cannabinoid type 1 receptor modulates intestinal propulsion by an attenuation of intestinal motor responses within the myenteric part of the peristaltic reflex. *Neurogastroenterol Motil*. 2007;19:744-753. doi:10.1111/j.1365-2982.2007.00975.x

121. Cardinal P, Bellocchio L, Clark S, et al. Hypothalamic CB1 cannabinoid receptors regulate energy balance in mice. *Endocrinology*. 2012;153(9):4136-4143. doi:10.1210/en.2012-1405

122. Watkins B a., Kim J. The endocannabinoid system: directing eating behavior and macronutrient metabolism. *Front Psychol*. 2015;5(January):1-10. doi:10.3389/fpsyg.2014.01506

123. DiPatrizio N V., Joslin A, Jung KM, Piomelli D. Endocannabinoid signaling in the gut mediates preference for dietary unsaturated fats. *FASEB J*. 2013;27(6):2513-2520. doi:10.1096/fj.13-227587

124. Ockner RK, Manning JA, Poppenhausen RB, Ho WKL. A Binding Protein for Fatty Acids in Cytosol of Intestinal Mucosa, Liver, Myocardium, and Other Tissues. *Science (80-)*. 1972;177(4043):56 LP - 58.

125. Ockner RKRK, Manning JA. Fatty acid-binding protein in small intestine. Identification, isolation, and evidence for its role in cellular fatty acid transport. *J Clin Invest*. 1974;54(2):326-338. doi:10.1172/JCI107768

126. Storch J, Thumser AE. Tissue-specific functions in the fatty acid-binding protein family. *J Biol Chem*. 2010;285(43):32679-32683. doi:10.1074/jbc.R110.135210

127. Napoli JL. *Functions of Intracellular Retinoid Binding-Proteins*.; 2016. doi:10.1007/978-94-024-0945-1

128. Lagakos WS, Guan X, Ho S-Y, et al. Liver fatty acid-binding protein binds monoacylglycerol in vitro and in mouse liver cytosol. *J Biol Chem*. 2013;288(27):19805-19815. doi:10.1074/jbc.M113.473579

129. Kaczocha M, Glaser ST, Deutsch DG. Identification of intracellular carriers for the endocannabinoid anandamide. *Proc Natl Acad Sci U S A*. 2009;106(15):6375-6380. doi:10.1073/pnas.0901515106

130. Kaczocha M, Vivieca S, Sun J, Glaser ST, Deutsch DG. Fatty acid-binding proteins transport N-acylethanolamines to nuclear receptors and are targets of endocannabinoid transport inhibitors. *J Biol Chem*. 2012;287(5):3415-3424. doi:10.1074/jbc.M111.304907

131. Kaczocha M, Glaser ST, Maher T, et al. Fatty acid binding protein deletion suppresses inflammatory pain through endocannabinoid/N-acylethanolamine-dependent mechanisms. *Mol Pain*. 2015;11:52. doi:10.1186/s12990-015-0056-8

132. Martin GG, Chung S, Landrock D, et al. Fabp-1 gene ablation impacts brain endocannabinoid system in male mice. *J Neurochem*. 2016. doi:10.1111/jnc.13664

133. Chon SH, Douglass JD, Zhou YX, et al. Over-Expression of Monoacylglycerol Lipase (MGL) in Small Intestine Alters Endocannabinoid Levels and Whole Body Energy Balance, Resulting in Obesity. *PLoS One*. 2012;7(8):1-12. doi:10.1371/journal.pone.0043962

134. Douglass JD, Zhou YX, Wu A, et al. Global deletion of monoacylglycerol lipase in mice delays lipid absorption and alters energy homeostasis and diet-induced obesity. *J Lipid Res.* 2015;56:jlr.M058586-. doi:10.1194/jlr.M058586

135. Levy E, Ménard D, Delvin E, et al. Localization , function and regulation of the two intestinal fatty acid-binding protein types. *Histochem Cell Biol.* 2009:351-367. doi:10.1007/s00418-009-0608-y

136. Pelsers MMAL, Namiot Z, Kisielewski W, et al. Intestinal-type and liver-type fatty acid-binding protein in the intestine. Tissue distribution and clinical utility. *Clin Biochem.* 2003;36(7):529-535. doi:10.1016/S0009-9120(03)00096-1

137. Bass NM, Manning JA, Ockner RK, Gordon JI, Seetharam S, Alpers DH. Regulation of the biosynthesis of two distinct fatty acid-binding proteins in rat liver and intestine. Influences of sex difference and of clofibrate. *J Biol Chem.* 1985;260(3):1432-1436.

138. Reboul E. Absorption of Vitamin A and Carotenoids by the Enterocyte: Focus on Transport Proteins. 2013:3563-3581. doi:10.3390/nu5093563

139. Zimmerman A, van Moerkerk H, Veerkamp J. Ligand specificity and conformational stability of human fatty acid-binding proteins. *Int J Biochem Cell Biol.* 2001;33(9):865-876. doi:10.1016/S1357-2725(01)00070-X

140. Miller KR, Cistola DP. Titration calorimetry as a binding assay for lipid-binding proteins. *Mol Cell Biochem.* 1993;123(1-2):29-37.

141. Fujita M, Fujii H, Kanda T, Sato E, Hatakeyama K, Ono T. Molecular cloning, expression, and characterization of a human intestinal 15-kDa protein. *Eur J Biochem.* 1995;233(2):406-413.

142. Sacchettini JC, Hauft SM, Van Camp SL, Cistola DP, Gordon JI. Developmental and structural studies of an intracellular lipid binding protein expressed in the ileal epithelium. *J Biol Chem.* 1990;265(31):19199-19207.

143. Crow JA, Ong DE. Cell-specific immunohistochemical localization of a cellular retinol-binding protein (type two) in the small intestine of rat. *Proc Natl Acad Sci U S A.* 1985;82(14):4707-4711. doi:10.1073/pnas.82.14.4707

144. Richieri GV, Ogata RT, Kleinfeld AM. Equilibrium Constants for the Binding of Fatty Acids with Fatty Acid-binding Proteins from Adipocyte, Intestine, Heart, and Liver Measured with the Fluorescent Probe ADIFAB. *J Biol Chem.* 1994;269(39):23918-23930.

145. Richieri G V, Ogata RT, Zimmerman AW, Veerkamp JH, Kleinfeld AM. Fatty acid binding proteins from different tissues show distinct patterns of fatty acid interactions. *Biochemistry.* 2000;39(24):7197-7204. doi:10.1021/bi000314z

146. Wolfrum, Borchers, Sacchettini, Spener. Binding of fatty acids and peroxisome proliferators to orthologous fatty acid binding proteins from human, murine, and bovine liver. *Biochemistry.* 2000;39(46):14363.

147. Hsu KT, Storch J. Fatty Acid Transfer from Liver and Intestinal Fatty Acid-binding Proteins to Membranes Occurs by Different Mechanisms. *J Biol Chem.* 1996;271(23):13317-13323. doi:10.1074/jbc.271.23.13317

148. Alpers DH, Bass NM, Engle M., DeSchryver-Kecskemeti K. Intestinal fatty acid binding protein may favor differential apical fatty acid binding in the intestine. *BBA*. 2000;1483(3):352-362.

149. Siddiqi S, Saleem U, Abumrad NA, et al. A novel multiprotein complex is required to generate the prechylomicron transport vesicle from intestinal ER. *J Lipid Res*. 2010;51(7):1918-1928. doi:10.1194/jlr.M005611

150. Mansbach CM 2nd, Siddiqi S. Control of chylomicron export from the intestine. *Am J Physiol Gastrointest Liver Physiol*. 2016;310(9):G659-68. doi:10.1152/ajpgi.00228.2015

151. Neeli I, Siddiqi SA, Siddiqi S, et al. Liver fatty acid-binding protein initiates budding of pre-chylomicron transport vesicles from intestinal endoplasmic reticulum. *J Biol Chem*. 2007;282(25):17974-17984. doi:10.1074/jbc.M610765200

152. Guzmán C, Benet M, Pisonero-Vaquero S, et al. The human liver fatty acid binding protein (FABP1) gene is activated by FOXA1 and PPARα; And repressed by C/EBPα: Implications in FABP1 down-regulation in nonalcoholic fatty liver disease. *Biochim Biophys Acta - Mol Cell Biol Lipids*. 2013;1831(4):803-818. doi:10.1016/j.bbalip.2012.12.014

153. Huang H, Starodub O, McIntosh A, Kier AB, Schroeder F. Liver fatty acid-binding protein targets fatty acids to the nucleus. Real time confocal and multiphoton fluorescence imaging in living cells. *J Biol Chem*. 2002;277(32):29139-29151. doi:10.1074/jbc.M202923200

154. McIntosh AL, Atshaves BP, Hostetler HA, et al. Liver type fatty acid binding protein (L-FABP) gene ablation reduces nuclear ligand distribution and peroxisome proliferator-activated receptor-α activity in cultured primary hepatocytes. *Arch Biochem Biophys*. 2009;485(2):160-173. doi:10.1016/j.abb.2009.03.004

155. Hostetler H a, McIntosh AL, Atshaves BP, et al. L-FABP directly interacts with PPARalpha in cultured primary hepatocytes. *J Lipid Res*. 2009;50(8):1663-1675. doi:10.1194/jlr.M900058-JLR200

156. Wolfrum C, Borrmann CM, Borchers T, Spener F. Fatty acids and hypolipidemic drugs regulate peroxisome proliferator-activated receptors - and -mediated gene expression via liver fatty acid binding protein: A signaling path to the nucleus. *Proc Natl Acad Sci*. 2001;98(5):2323-2328. doi:10.1073/pnas.051619898

157. Hughes MLR, Liu B, Halls ML, et al. Fatty acid-binding proteins 1 and 2 differentially modulate the activation of peroxisome proliferator-activated receptor ?? in a ligand-selective manner. *J Biol Chem*. 2015;290(22):13895-13906. doi:10.1074/jbc.M114.605998

158. McIntosh AL, Petrescu AD, Hostetler HA, Kier AB, Schroeder F. Liver-type fatty acid binding protein interacts with hepatocyte nuclear factor 4?? *FEBS Lett*. 2013;587(23):3787-3791. doi:10.1016/j.febslet.2013.09.043

159. Roman AKS, Aronson BE, Krasinski SD, Shivdasani RA, Verzi MP. Transcription Factors GATA4 and HNF4A Control Distinct Aspects of Intestinal Homeostasis in Conjunction with Transcription Factor CDX2 * □. *J Biol Chem*. 2015;290(3):1850-1860. doi:10.1074/jbc.M114.620211

160. McMullen PD, Bhattacharya S, Woods CG, et al. A map of the PPAR?? transcription regulatory network for primary human hepatocytes. *Chem Biol Interact*. 2014;209(1):14-24. doi:10.1016/j.cbi.2013.11.006

161. Erol E, Kumar LS, Cline GW, Shulman GI, Kelly DP, Binas B. Liver fatty acid-binding protein is required for high rates of hepatic fatty acid oxidation but not for the action of PPAR-alpha in fasting mice. *Faseb J*. 2003;17:347-349. doi:10.1096/fj.03-0330fje

162. Martin GG, Huang H, Atshaves BP, Binas B, Schroeder F. Ablation of the liver fatty acid binding protein gene decreases fatty acyl CoA binding capacity and alters fatty acyl CoA pool distribution in mouse liver. *Biochemistry*. 2003;42(39):11520-11532. doi:10.1021/bi0346749

163. Mallordy A, Poirier H, Besnard P, Niot I, Carlier H. Evidence for transcriptional induction of the liver fatty-acid-binding-protein gene by bezafibrate in the small intestine. *Eur J Biochem*. 1995;227(3):801-807.

164. Poirier H, Niot I, Degrace P, Monnot MC, Bernard A, Besnard P. Fatty acid regulation of fatty acid-binding protein expression in the small intestine. *Am J Physiol*. 1997;273(2 Pt 1):G289-95. doi:10.1152/ajpgi.1997.273.2.G289

165. Malewiak MI, Bass NM, Griglio S, Ockner RK. Influence of genetic obesity and of fat-feeding on hepatic FABP concentration and activity. *Int J Obes*. 1988;12(6):543-546.

166. Ockner RK, Burnett DA, Lysenko N, Manning JA. Sex differences in long chain fatty acid utilization and fatty acid binding protein concentration in rat liver. *J Clin Invest*. 1979;64(1):172-181. doi:10.1172/JCI109437

167. Ockner RK, Lysenko N, Manning JA, Monroe SE, Burnett DA. Sex steroid modulation of fatty acid utilization and fatty acid binding protein concentration in rat liver. *J Clin Invest*. 1980;65(5):1013-1023. doi:10.1172/JCI109753

168. McIntosh AL, Huang H, Storey SM, et al. Human FABP1 T94A variant impacts fatty acid metabolism and PPAR-α activation in cultured human female hepatocytes. *Am J Physiol Gastrointest Liver Physiol*. 2014;307(2):G164-76. doi:10.1152/ajpgi.00369.2013

169. Schroeder F, McIntosh AL, Martin GG, et al. Fatty Acid Binding Protein-1 (FABP1) and the Human FABP1 T94A Variant: Roles in the Endocannabinoid System and Dyslipidemias. *Lipids*. 2016;51(6):655-676. doi:10.1007/s11745-016-4155-8

170. Robitaille J, Brouillette C, Lemieux S, Perusse L, Gaudet D, Vohl MC. Plasma concentrations of apolipoprotein B are modulated by a gene--diet interaction effect between the LFABP T94A polymorphism and dietary fat intake in French-Canadian men. *Mol Genet Metab*. 2004;82(4):296-303. doi:10.1016/j.ymgme.2004.06.002

171. Brouillette C, Bosse Y, Perusse L, Gaudet D, Vohl M-C. Effect of liver fatty acid binding protein (FABP) T94A missense mutation on plasma lipoprotein responsiveness to treatment with fenofibrate. *J Hum Genet*. 2004;49(8):424-432. doi:10.1007/s10038-004-0171-2

172. Fisher E, Weikert C, Klapper M, et al. L-FABP T94A is associated with fasting triglycerides and LDL-cholesterol in women. *Mol Genet Metab*. 2007;91(3):278-284. doi:10.1016/j.ymgme.2007.03.002

173. Schroeder F, McIntosh AL, Martin GG, et al. Fatty Acid Binding Protein-1 (FABP1) and the Human FABP1 T94A Variant: Roles in the Endocannabinoid System and Dyslipidemias. *Lipids.* 2016;51(6):655-676. doi:10.1007/s11745-016-4155-8

174. Gao N, Qu X, Yan J, Huang Q, Yuan H-Y, Ouyang D-S. L-FABP T94A decreased fatty acid uptake and altered hepatic triglyceride and cholesterol accumulation in Chang liver cells stably transfected with L-FABP. *Mol Cell Biochem.* 2010;345(1-2):207-214. doi:10.1007/s11010-010-0574-7

175. Lowe JB, Sacchettini JC, Laposata M, McQuillan JJ, Gordon JI. Expression of rat intestinal fatty acid-binding protein in Escherichia coli. Purification and comparison of ligand binding characteristics with that of Escherichia coli-derived rat liver fatty acid-binding protein. *J Biol Chem.* 1987;262(12):5931-5937.

176. Besnard P, Niot I, Poirier H, Clement L, Bernard A. New insights into the fatty acid-binding protein (FABP) family in the small intestine. *Mol Cell Biochem.* 2002;239(1-2):139-147.

177. Baier LJ, Sacchettini JC, Knowler WC, et al. An amino acid substitution in the human intestinal fatty acid binding protein is associated with increased fatty acid binding, increased fat oxidation, and insulin resistance. *J Clin Invest.* 1995;95(3):1281-1287. doi:10.1172/JCI117778

178. Storch J, Veerkamp JH, Hsu K-T. Similar mechanisms of fatty acid transfer from human anal rodent fatty acid-binding proteins to membranes: liver, intestine, heart muscle, and adipose tissue FABPs. *Mol Cell Biochem.* 2002;239(1-2):25-33.

179. De Luis DA, Gonzalez Sagrado M, Aller R, Izaola O, Conde R, De la Fuente B. Influence of Ala54Thr polymorphism of fatty acid-binding protein 2 on insulin resistance and adipocytokines in patients with diabetes mellitus type 2. *Eur Rev Med Pharmacol Sci.* 2010;14(2):89-95.

180. Khattab SA, Abo-Elmatty DM, Ghattas MH, Mesbah NM, Mehanna ET. Intestinal fatty acid binding protein Ala54Thr polymorphism is associated with peripheral atherosclerosis combined with type 2 diabetes mellitus. *J Diabetes.* 2017;9(9):821-826. doi:10.1111/1753-0407.12496

181. Chamberlain AM, Schreiner PJ, Fornage M, Loria CM, Siscovick D, Boerwinkle E. Ala54Thr polymorphism of the fatty acid binding protein 2 gene and saturated fat intake in relation to lipid levels and insulin resistance: the Coronary Artery Risk Development in Young Adults (CARDIA) study. *Metabolism.* 2009;58(9):1222-1228. doi:10.1016/j.metabol.2009.04.007

182. Levy E, Menard D, Delvin E, et al. The polymorphism at codon 54 of the FABP2 gene increases fat absorption in human intestinal explants. *J Biol Chem.* 2001;276(43):39679-39684. doi:10.1074/jbc.M105713200

183. Baier LJ, Bogardus C, Sacchettini JC. A polymorphism in the human intestinal fatty acid binding protein alters fatty acid transport across Caco-2 cells. *J Biol Chem.* 1996;271(18):10892-10896. doi:10.1074/jbc.271.18.10892

184. Murphy EJ, Prows DR, Jefferson JR, Schroeder F. Liver fatty acid-binding protein expression in transfected fibroblasts stimulates fatty acid uptake and metabolism. *Biochim Biophys Acta.* 1996;1301:191-198.

185. Newberry EP, Xie Y, Kennedy S, et al. Decreased Hepatic Triglyceride Accumulation and Altered Fatty Acid Uptake in Mice with Deletion of the Liver Fatty Acid-binding Protein Gene. *J Biol Chem.* 2003;278(51):51664-51672. doi:10.1074/jbc.M309377200

186. Newberry EP, Kennedy S, Xie Y, et al. Phenotypic divergence in two lines of *L-Fabp* $^{-/-}$ mice reflects substrain differences and environmental modifiers. *Am J Physiol - Gastrointest Liver Physiol.* 2015;309(8):G648-G661. doi:10.1152/ajpgi.00170.2015

187. Newberry EP, Xie Y, Kennedy SM, Luo J, Davidson NO. Protection against Western diet-induced obesity and hepatic steatosis in liver fatty acid-binding protein knockout mice. *Hepatology.* 2006;44(5):1191-1205. doi:10.1002/hep.21369

188. Martin GG, Atshaves BP, McIntosh AL, Mackie JT, Kier AB, Schroeder F. Liver fatty acid-binding protein gene ablated female mice exhibit increased age dependent obesity. *J Nutr.* 2008;138(10):1859-1865.

189. Atshaves BP, Martin GG, Hostetler HA, McIntosh AL, Kier AB, Schroeder F. Liver fatty acid-binding protein and obesity. *J Nutr Biochem.* 2010;21(11):1015-1032. doi:10.1016/j.jnutbio.2010.01.005

190. Atshaves BP, McIntosh AL, Strorey SM, Landrock KK, Kier AB, Schroeder F. High Dietary Fat Exacrbates Weigth Gain and Obesity in Female Liver Fatty Acid Binding Protein Gene-Ablated Mice. *Lipids.* 2010;45(2):97-110. doi:10.1038/jid.2014.371

191. Vassileva G, Huwyler L, Poirier K, Agellon LB, Toth MJ. The intestinal fatty acid binding protein is not essential for dietary fat absorption in mice. 2000;14(13):2040-2046.

192. Newberry EP, Kennedy SM, Xie Y, et al. Diet-induced obesity and hepatic steatosis in L-Fabp − / − mice is abrogated with SF , but not PUFA , feeding and attenuated after cholesterol supplementation Diet-induced obesity and hepatic steatosis in L-Fabp ɤ / ɤ mice is abrogated with SF , but not P. 2008;(November 2007). doi:10.1152/ajpgi.00377.2007

193. Douglass JD, Malik N, Chon S, et al. Intestinal mucosal triacylglycerol accumulation secondary to decreased lipid secretion in obese and high fat fed mice. 2012;3(February):1-8. doi:10.3389/fphys.2012.00025

194. Xu H, Gajda A, Zhou YX, Fatima A, Agellon LB, Storch J. Increased Endurance Exercise Capacity Secondary to Liver Fatty Acid-Binding Protein Ablation. *FASEB J.* 2016;30(1_supplement):1132.8-1132.8. doi:10.1096/fasebj.30.1_supplement.1132.8

195. Primeau V, Coderre L, Karelis a D, et al. Characterizing the profile of obese patients who are metabolically healthy. *Int J Obes (Lond).* 2011;35(7):971-981. doi:10.1038/ijo.2010.216

196. Gonçalves CG, Glade MJ, Meguid MM. Metabolically healthy obese individuals: Key protective factors. *Nutrition.* 2016;32(1):14-20. doi:10.1016/j.nut.2015.07.010

197. Wang H, Yang H, Shivalila CS, et al. One-step generation of mice carrying mutations in multiple genes by CRISPR/Cas-mediated genome engineering. *Cell.* 2013;153(4):910-918. doi:10.1016/j.cell.2013.04.025

198. Seruggia D, Montoliu L. The new CRISPR–Cas system: RNA-guided genome engineering to efficiently produce any desired genetic alteration in animals. *Transgenic Res.* 2014;23(5):707-716. doi:10.1007/s11248-014-9823-y

199. Horii T, Morita S, Kimura M, Terawaki N, Shibutani M, Hatada I. Efficient generation of conditional knockout mice via sequential introduction of lox sites. *Sci Rep.* 2017;7(1):7891. doi:10.1038/s41598-017-08496-8

200. Zhou W, Deiters A. Conditional Control of CRISPR/Cas9 Function. *Angew Chemie - Int Ed.* 2016;55(18):5394-5399. doi:10.1002/anie.201511441

201. Jinek M, Chylinski K, Fonfara I, Hauer M, Doudna JA, Charpentier E. A Programmable Dual-RNA – Guided DNA Endonuclease in Adaptive Bacterial Immunity. *Science (80-).* 2012;337(August):816-822. doi:10.1126/science.1225829

202. Sauer B. Inducible gene targeting in mice using the Cre/lox system. *Methods.* 1998;14(4):381-392. doi:10.1006/meth.1998.0593

203. Garcia-Otin AL, Guillou F. Mammalian genome targeting using site-specific recombinases. *Front Biosci.* 2006;11:1108-1136.

204. Singh P, Schimenti JC, Bolcun-Filas E. A mouse geneticist???s practical guide to CRISPR applications. *Genetics.* 2015;199(1):1-15. doi:10.1534/genetics.114.169771

205. The Jackson Laboratory. B6.Cg-Tg(Vil1-cre)997Gum/J- Mouse Strain Datasheet-004586. 2018.

206. McLean JA, Tobin G. Animal and human calorimetry. 1987;(April):338. doi:10.1016/0007-1935(89)90021-3

207. Tanner CB, Madsen SR, Hallowell DM, et al. Mitochondrial and performance adaptations to exercise training in mice lacking skeletal muscle LKB1. *Am J Physiol Endocrinol Metab.* 2013;305(8):E1018-29. doi:10.1152/ajpendo.00227.2013

208. Ma X, Hamadeh MJ, Christie BR, Foster JA, Tarnopolsky MA. Impact of treadmill running and sex on hippocampal neurogenesis in the mouse model of amyotrophic lateral sclerosis. *PLoS One.* 2012;7(4):e36048. doi:10.1371/journal.pone.0036048

209. Bradford MM. A rapid and sensitive method for the quantitation of microgram quantities of protein utilizing the principle of protein-dye binding. *Anal Biochem.* 1976;72(1-2):248-254. doi:10.1016/0003-2697(76)90527-3

210. Xu H, Gajda AM, Zhou YX, et al. Muscle metabolic reprogramming underlies the resistance to high fat feeding-induced decline in exercise capacity in Liver Fatty Acid-Binding Protein null mice. *J Biol Chem.*

211. Chen J, Guo Y, Gui Y, Xu D. Physical exercise, gut, gut microbiota, and atherosclerotic cardiovascular diseases. *Lipids Health Dis.* 2018;17(1):17. doi:10.1186/s12944-017-0653-9

212. Cook MD, Allen JM, Pence BD, et al. Exercise and gut immune function: evidence of alterations in colon immune cell homeostasis and microbiome characteristics with exercise training. *Immunol Cell Biol.* 2016;94(2):158-163. doi:10.1038/icb.2015.108

213. Clark A, Mach N. The Crosstalk between the Gut Microbiota and Mitochondria during Exercise. *Front Physiol.* 2017;8:319. doi:10.3389/fphys.2017.00319

214. Bleau C, Karelis AD, St-Pierre DH, Lamontagne L. Crosstalk between intestinal microbiota, adipose tissue and skeletal muscle as an early event in systemic low-grade inflammation and the development of obesity and diabetes. *Diabetes Metab Res Rev*. 2015;31(6):545-561. doi:10.1002/dmrr.2617

215. Mathison R, Ho W, Pittman QJ, Davison JS, Sharkey KA. Effects of cannabinoid receptor-2 activation on accelerated gastrointestinal transit in lipopolysaccharide-treated rats. *Br J Pharmacol*. 2004;142(8):1247-1254. doi:10.1038/sj.bjp.0705889

216. Woting A, Blaut M. Small Intestinal Permeability and Gut-Transit Time Determined with Low and High Molecular Weight Fluorescein Isothiocyanate-Dextrans in C3H Mice. *Nutrients*. 2018;10(6). doi:10.3390/nu10060685

217. Newberry EP, Kennedy SM, Xie Y, Luo J, Davidson NO. Diet-induced alterations in intestinal and extrahepatic lipid metabolism in liver fatty acid binding protein knockout mice. *Mol Cell Biochem*. 2009;326(1-2):79-86. doi:10.1007/s11010-008-0002-4

218. Nikonorova IA, Mirek ET, Signore CC, Goudie MP, Wek RC, Anthony TG. Time-resolved analysis of amino acid stress identifies eIF2 phosphorylation as necessary to inhibit mTORC1 activity in liver. *J Biol Chem*. 2018;293(14):5005-5015. doi:10.1074/jbc.RA117.001625

219. Folch J, Lees M, Sloane GH. A simple method for the isolation and purification of total lipides from animal tissues. 1957;226(1):497-509.

220. Nelson DW, Gao Y, Yen MI, Yen CLE. Intestine-specific deletion of acyl-CoA:Monoacylglycerol Acyltransferase (MGAT) 2 protects mice from diet-induced obesity and glucose intolerance. *J Biol Chem*. 2014;289(25):17338-17349. doi:10.1074/jbc.M114.555961

221. Nagakura Y, Naitoh Y, Kamato T, Yamano M, Miyata K. Compounds possessing 5 -. 1996;311:67-72.

222. Kelly JR, Borre Y, Brien CO, et al. Transferring the blues : Depression-associated gut microbiota induces neurobehavioural changes in the rat. *J Psychiatr Res*. 2016;82:109-118. doi:10.1016/j.jpsychires.2016.07.019

223. Bonaz B, Sinniger V. Vagal tone : effects on sensitivity , motility , and inflammation. 2016:455-462. doi:10.1111/nmo.12817

224. Kaser a, Blumberg RS. Endoplasmic reticulum stress in the intestinal epithelium and inflammatory bowel disease. *Semin Immunol*. 2009;21(3):156-163. doi:S1044-5323(09)00006-2 [pii]\r10.1016/j.smim.2009.01.001

225. Kaser A, Blumberg RS. Endoplasmic reticulum stress and intestinal inflammation. *Mucosal Immunol*. 2010;3(1):11-16. doi:10.1038/mi.2009.122

226. Partosoedarso ER, Abrahams TP, Scullion RT, Moerschbaecher JM, Hornby PJ. Cannabinoid1 receptor in the dorsal vagal complex modulates lower oesophageal sphincter relaxation in ferrets. 2003:149-158. doi:10.1113/jphysiol.2003.042242

227. Izzo AA, Sharkey KA. Cannabinoids and the gut: New developments and emerging concepts. *Pharmacol Ther*. 2010;126(1):21-38. doi:10.1016/j.pharmthera.2009.12.005

228. Sibaev A, Yuce B, Kemmer M, et al. Cannabinoid-1 (CB 1) receptors regulate colonic propulsion by acting at motor neurons within the ascending motor pathways in mouse colon. *Am J Gastrointest Liver Physiol*. 2009;1(296):119-128. doi:10.1152/ajpgi.90274.2008.

229. Wang J, Ueda N. Biology of endocannabinoid synthesis system. *Prostaglandins Other Lipid Mediat*. 2009;89(3-4):112-119. doi:10.1016/j.prostaglandins.2008.12.002

230. Heinemann A, Shahbazian A, Holzer P. Cannabinoid inhibition of guinea-pig intestinal peristalsis via inhibition of excitatory and activation of inhibitory neural pathways. *Neuropharmacology*. 1999;38:1289-1297.

231. Izzo AA, Mascolo N, Pinto L, Capasso R, Capasso F. The role of cannabinoid receptors in intestinal motility , defaecation and diarrhoea in rats. 1999:37-42.

232. Agellon LB, Li L, Luong L, Uwiera RRE. Adaptations to the loss of intestinal fatty acid binding protein in mice. 2006:159-166. doi:10.1007/s11010-005-9042-1

233. Tomas J, Brenner C, Sansonetti PJ. Biochimie Impact of high-fat diet on the intestinal microbiota and small intestinal physiology before and after the onset of obesity. 2017:1-10. doi:10.1016/j.biochi.2017.05.019

234. Chassaing B, Miles-Brown J, Pellizzon M, et al. Lack of soluble fiber drives diet-induced adiposity in mice. *Am J Physiol - Gastrointest Liver Physiol*. 2015;309(7):G528-G541. doi:10.1152/ajpgi.00172.2015

235. Moreira APB, Texeira TFS, Ferreira AB, Do Carmo Gouveia Peluzio M, De Cássia Gonçalves Alfenas R. Influence of a high-fat diet on gut microbiota, intestinal permeability and metabolic endotoxaemia. *Br J Nutr*. 2012;108(5):801-809. doi:10.1017/S0007114512001213

236. Escaffit F, Boudreau F, Beaulieu JF. Differential expression of claudin-2 along the human intestine: Implication of GATA-4 in the maintenance of claudin-2 in differentiating cells. *J Cell Physiol*. 2005;203(1):15-26. doi:10.1002/jcp.20189

237. Al-Sadi R, Ye D, Boivin M, et al. Interleukin-6 modulation of intestinal epithelial tight junction permeability is mediated by JNK pathway. *PLoS One*. 2014;9(3). doi:10.1371/journal.pone.0085345

238. Bottasso Arias NM, García M, Bondar C, et al. Expression Pattern of Fatty Acid Binding Proteins in Celiac Disease Enteropathy. *Mediators Inflamm*. 2015;2015:1-11. doi:10.1155/2015/738563

239. Tye-din JA, Galipeau HJ, Agardh D. Celiac Disease : A Review of Current Concepts in Pathogenesis , Prevention , and Novel Therapies. *Front Pediatr*. 2018;6(November):1-19. doi:10.3389/fped.2018.00350

240. Owens SR, Greenson JK. The pathology of malabsorption: Current concepts. *Histopathology*. 2007;50(1):64-82. doi:10.1111/j.1365-2559.2006.02547.x

241. Johansson ME V, Phillipson M, Petersson J, Velcich A, Holm L, Hansson GC. The inner of the two Muc2 mucin-dependent mucus layers in colon is devoid of bacteria. *PNAS*. 2008;105(39):15064-15069.

242. Van Der Sluis M, De Koning BAE, De Bruijn ACJ., et al. Muc2-Deficient Mice Spontaneously Develop Colitis, Indicating That Muc2 Is Critical for Colonic Protection. *Gastroenterology*. 2006;131:117-129. doi:10.1053/j.gastro.2006.04.020

243. Younce C, Kolattukudy P. MCP-1 causes cardiomyoblast death via autophagy resulting from ER stress caused by oxidative stress generated by inducing a novel zinc-finger protein, MCPIP. *Biochem J*. 2010;426(1):43-53. doi:10.1042/BJ20090976

244. Yu Y, Zhang L, Liu Q, Tang L, Sun H, Guo H. Endoplasmic reticulum stress preconditioning antagonizes low-density lipoprotein-induced inflammation in human mesangial cells through upregulation of XBP1 and suppression of the IRE1α/IKK/NF-B pathway. *Mol Med Rep*. 2015;11(3):2048-2054. doi:10.3892/mmr.2014.2960

245. Kolattukudy PE, Niu J. Inflammation, endoplasmic reticulum stress, autophagy, and the monocyte chemoattractant protein-1/CCR2 pathway. *Circ Res*. 2012;110(1):174-189. doi:10.1161/CIRCRESAHA.111.243212

246. Chen J, Guo Y, Zeng W, et al. ER stress triggers MCP-1 expression through SET7/9-induced histone methylation in the kidneys of db/db mice. *Am J Physiol Renal Physiol*. 2014;306(8):F916-25. doi:10.1152/ajprenal.00697.2012

247. Rasheed Z, Haqqi TM. Endoplasmic reticulum stress induces the expression of COX-2 through activation of eIF2alpha, p38-MAPK and NF-kappaB in advanced glycation end products stimulated human chondrocytes. *Biochim Biophys Acta*. 2012;1823(12):2179-2189. doi:10.1016/j.bbamcr.2012.08.021

248. Hung J-H, Su I-J, Lei H-Y, et al. Endoplasmic reticulum stress stimulates the expression of cyclooxygenase-2 through activation of NF-kappaB and pp38 mitogen-activated protein kinase. *J Biol Chem*. 2004;279(45):46384-46392. doi:10.1074/jbc.M403568200

249. Guo F, Lin EA, Liu P, Lin J, Liu C. XBP1U inhibits the XBP1S-mediated upregulation of the iNOS gene expression in mammalian ER stress response. *Cell Signal*. 2010;22(12):1818-1828. doi:10.1016/j.cellsig.2010.07.006

250. Hsieh Y-H, Su I-J, Lei H-Y, Lai M-D, Chang W-W, Huang W. Differential endoplasmic reticulum stress signaling pathways mediated by iNOS. *Biochem Biophys Res Commun*. 2007;359(3):643-648. doi:10.1016/j.bbrc.2007.05.154

251. Kitiphongspattana K, Khan TA, Ishii-Schrade K, Roe MW, Philipson LH, Gaskins HR. Protective role for nitric oxide during the endoplasmic reticulum stress response in pancreatic beta-cells. *Am J Physiol Endocrinol Metab*. 2007;292(6):E1543-54. doi:10.1152/ajpendo.00620.2006

252. Ma D, Li S, Molusky MM, Lin JD. Circadian autophagy rhythm: A link between clock and metabolism? *Trends Endocrinol Metab*. 2012;23(7):319-325. doi:10.1016/j.tem.2012.03.004

253. Bass J, Takahashi JS. Circadian integration of metabolism and energetics. *Science*. 2010;330(6009):1349-1354. doi:10.1126/science.1195027

254. Maillo C, Martin J, Sebastian D, et al. Circadian- and UPR-dependent control of CPEB4 mediates a translational response to counteract hepatic steatosis under ER stress. *Nat Cell Biol*. 2017;19(2):94-105. doi:10.1038/ncb3461

255. Kaser A, Lee A, Franke A, Glickman J. XBP1 links ER stress to intestinal inflammation and confers genetic risk for human inflammatory bowel disease. *Cell.* 2008;134(5):743-756. doi:10.1016/j.cell.2008.07.021.XBP1

256. Williams JM, Duckworth CA, Burkitt MD, Watson AJM, Campbell BJ, Pritchard DM. Epithelial cell shedding and barrier function: a matter of life and death at the small intestinal villus tip. *Vet Pathol.* 2015;52(3):445-455. doi:10.1177/0300985814559404

257. Blander JM. Death in the intestinal epithelium-basic biology and implications for inflammatory bowel disease. *FEBS J.* 2016;283(14):2720-2730. doi:10.1111/febs.13771

258. Petrescu AD, Huang H, Martin GG, et al. Impact of L-FABP and glucose on polyunsaturated fatty acid induction of PPARα-regulated β-oxidative enzymes. *Am J Physiol Gastrointest Liver Physiol.* 2013;304:G241-56. doi:10.1152/ajpgi.00334.2012

259. den Besten G, van Eunen K, Groen AK, Venema K, Reijngoud D-J, Bakker BM. The role of short-chain fatty acids in the interplay between diet, gut microbiota, and host energy metabolism. *J Lipid Res.* 2013;54(9):2325-2340. doi:10.1194/jlr.R036012

260. Bar F, Bochmann W, Widok A, et al. Mitochondrial gene polymorphisms that protect mice from colitis. *Gastroenterology.* 2013;145(5):1055-1063.e3. doi:10.1053/j.gastro.2013.07.015

261. Circu ML, Aw TY. Intestinal redox biology and oxidative stress. *Semin Cell Dev Biol.* 2012;23(7):729-737. doi:10.1016/j.semcdb.2012.03.014

262. Mottawea W, Chiang C-K, Muhlbauer M, et al. Altered intestinal microbiota-host mitochondria crosstalk in new onset Crohn's disease. *Nat Commun.* 2016;7:13419. doi:10.1038/ncomms13419

263. Douris N, Kojima S, Pan X, et al. Nocturnin regulates circadian trafficking of dietary lipid in intestinal enterocytes. *Curr Biol.* 2011;21(16):1347-1355. doi:10.1016/j.cub.2011.07.018

264. Hussain MM, Pan X. Clock genes, intestinal transport and plasma lipid homeostasis. *Trends Endocrinol Metab.* 2009;20(4):177-185. doi:10.1016/j.tem.2009.01.001

265. Wright KL, Duncan M, Sharkey KA. Cannabinoid CB2 receptors in the gastrointestinal tract: a regulatory system in states of inflammation. *Br J Pharmacol.* 2008;153(2):263-270. doi:0707486 [pii]\r10.1038/sj.bjp.0707486

266. Hornby PJ, Prouty SM. Involvement of cannabinoid receptors in gut motility and visceral perception. *Br J Pharmacol.* 2004;141(8):1335-1345. doi:10.1038/sj.bjp.0705783

267. Furuhashi M, Hotamisligil GS. Fatty acid-binding proteins: role in metabolic diseases and potential as drug targets. *Nat Rev Drug Discov.* 2008;7(6):489-503. doi:10.1038/nrd2589

268. Velkov T. Interactions between Human Liver Fatty Acid Binding Protein and Peroxisome Proliferator Activated Receptor Selective Drugs. *PPAR Res.* 2013;2013:17-19. doi:http://dx.doi.org/10.1155/2013/938401

269. Richmond CA, Breault DT. Regulation of Gene Expression in the Intestinal Epithelium. *Prog Mol Biol Transl Sci.* 2010;96:207-229. doi:10.1016/B978-0-12-381280-3.00009-9.REGULATION

270. Watanabe K, Hoshi N, Tsuura Y, et al. Immunohistochemical distribution of intestinal 15 kDa protein in human tissues. *Arch Histol Cytol.* 1995;58(3):303-306.

271. Lucke C, Zhang F, Ruterjans H, Hamilton JA, Sacchettini JC. Flexibility is a likely determinant of binding specificity in the case of ileal lipid binding protein. *Structure.* 1996;4(7):785-800.

272. Kim Y-K, Wassef L, Hamberger L, et al. Retinyl ester formation by lecithin: retinol acyltransferase is a key regulator of retinoid homeostasis in mouse embryogenesis. *J Biol Chem.* 2008;283(9):5611-5621. doi:10.1074/jbc.M708885200

273. McCullough FS, Northrop-Clewes CA, Thurnham DI. The effect of vitamin A on epithelial integrity. *Proc Nutr Soc.* 1999;58(2):289-293.

274. Goncalves A, Roi S, Nowicki M, et al. Fat-soluble vitamin intestinal absorption: absorption sites in the intestine and interactions for absorption. *Food Chem.* 2015;172:155-160. doi:10.1016/j.foodchem.2014.09.021

275. Byrne SMO, Blaner WS. Retinol and retinyl esters : biochemistry and physiology. 2013;54:1731-1743. doi:10.1194/jlr.R037648

276. Ables GP, Jian K, Yang Z, et al. Intestinal DGAT1 defi ciency reduces postprandial triglyceride and retinyl ester excursions by inhibiting chylomicron secretion and delaying gastric emptying. 2012;53. doi:10.1194/jlr.M029041

277. Mezaki Y, Fujimi TJ, Senoo H, Matsuura T. The coordinated action of lecithin:retinol acyltransferase and cellular retinol-binding proteins for regulation of vitamin A esterification. *Med Hypotheses.* 2016;88:60-62. doi:10.1016/j.mehy.2016.01.013

278. Bando Y, Yamamoto M, Sakiyama K, Sakashita H. Retinoic acid regulates cell - shape and - death of E - FABP (FABP5)- immunoreactive septoclasts in the growth plate cartilage of mice. *Histochem Cell Biol.* 2017;148(3):229-238. doi:10.1007/s00418-017-1578-0

279. di Masi A, Leboffe L, De Marinis E, et al. Retinoic acid receptors: from molecular mechanisms to cancer therapy. *Mol Aspects Med.* 2015;41:1-115. doi:10.1016/j.mam.2014.12.003

280. D PDP, D YTP, D YYP, D WWP. Expression of retinoic acid receptors in intestinal mucosa and the effect of vitamin A on mucosal immunity. *Nutrition.* 2010;26(7-8):740-745. doi:10.1016/j.nut.2009.08.011

281. Zhang R, Wang Y, Li R, Chen G. Transcriptional Factors Mediating Retinoic Acid Signals in the Control of Energy Metabolism. 2015:14210-14244. doi:10.3390/ijms160614210

282. Mendelsohn C, Larkin S, Mark M, et al. RAR beta isoforms: distinct transcriptional control by retinoic acid and specific spatial patterns of promoter activity during mouse embryonic development. *Mech Dev.* 1994;45(3):227-241.

283. Li Y, Gao Y, Cui T, et al. Retinoic Acid Facilitates Toll-Like Receptor 4 Expression to Improve Intestinal Barrier Function through Retinoic Acid Receptor Beta. *Cell Physiol Biochem.* 2017;42(4):1390-1406. doi:10.1159/000479203

284. Fan X, Liu S, Liu G, Zhao J, Jiao H. Vitamin A Deficiency Impairs Mucin Expression and Suppresses the Mucosal Immune Function of the Respiratory Tract in Chicks. 2015:1-16. doi:10.1371/journal.pone.0139131

285. Kochansky CJ, Lyman MJ, Fauty SE, Vlasakova K, D'mello AP. Administration of Fenofibrate Markedly Elevates Fabp3 in Rat Liver and Plasma and Confounds Its Use as a Preclinical Biomarker of Cardiac and Muscle Toxicity. *Lipids*. 2018;53(10):947-960. doi:10.1002/lipd.12110

286. Owada Y. Fatty acid binding protein: localization and functional significance in the brain. *Tohoku J Exp Med*. 2008;214(3):213-220. doi:10.1620/tjem.214.213

287. Rajan N, Blaner WS, Soprano DR, Suhara A, Goodman DS. Cellular retinol-binding protein messenger RNA levels in normal and retinoid-deficient rats. *J Lipid Res*. 1990;31(5):821-829.

288. Evans RM, Mangelsdorf DJ. Nuclear receptors, RXR, and the big bang. *Cell*. 2014;157(1):255-266. doi:10.1016/j.cell.2014.03.012

289. Xueping E, Zhang L, Lu J, et al. Increased Neonatal Mortality in Mice Lacking Cellular Retinol-binding Protein II *. 2002;277(39):36617-36623. doi:10.1074/jbc.M205519200

290. He Y, Yang X, Wang H, et al. Solution-state molecular structure of apo and oleate-liganded liver fatty acid-binding protein. *Biochemistry*. 2007;46(44):12543-12556. doi:10.1021/bi701092r

291. Balendiran GK, Schnutgen F, Scapin G, et al. Crystal structure and thermodynamic analysis of human brain fatty acid-binding protein. *J Biol Chem*. 2000;275(35):27045-27054. doi:10.1074/jbc.M003001200

292. Lu J, Cistola DP, Li E. Two homologous rat cellular retinol-binding proteins differ in local conformational flexibility. *J Mol Biol*. 2003;330(4):799-812. doi:10.1016/s0022-2836(03)00629-6

293. Wang Q, Rizk S, Bernard C, et al. Protocols and pitfalls in obtaining fatty acid-binding proteins for biophysical studies of ligand-protein and protein-protein interactions. *Biochem Biophys reports*. 2017;10:318-324. doi:10.1016/j.bbrep.2017.05.001

294. Karshikoff A, Nilsson L, Ladenstein R. Rigidity versus flexibility : the dilemma of understanding protein thermal stability. 2015;282:3899-3917. doi:10.1111/febs.13343

295. Vihinen M. Relationship of protein flexibility to thermostability. *Protein Eng*. 1987;1(6):477-480.

296. Ía MAR, Celej S, Montich GG, Fidelio GD. Protein stability induced by ligand binding correlates with changes in protein flexibility. *Protein Sci*. 2003;12:1496–1506. doi:10.1110/ps.0240003.strated

297. van der Lee R, Lang B, Kruse K, et al. Intrinsically disordered segments affect protein half-life in the cell and during evolution. *Cell Rep*. 2014;8(6):1832-1844. doi:10.1016/j.celrep.2014.07.055

298. Depuydt G, Shanmugam N, Rasulova M, Dhondt I, Braeckman BP. Increased Protein Stability and Decreased Protein Turnover in the Caenorhabditis elegans Ins/IGF-1 daf-2 Mutant. *J Gerontol A Biol Sci Med Sci*. 2016;71(12):1553-1559. doi:10.1093/gerona/glv221

299. Parsell DA, Sauer RT. The structural stability of a protein is an important determinant of its proteolytic susceptibility in Escherichia coli. *J Biol Chem*. 1989;264(13):7590-7595.

300. Asher G, Shaul Y. p53 proteasomal degradation: poly-ubiquitination is not the whole story. *Cell Cycle*. 2005;4(8):1015-1018. doi:10.4161/cc.4.8.1900

301. Asher G, Reuven N, Shaul Y. 20S proteasomes and protein degradation "by default". *Bioessays*. 2006;28(8):844-849. doi:10.1002/bies.20447

302. Rape M, Jentsch S. Taking a bite: proteasomal protein processing. *Nat Cell Biol*. 2002;4(5):E113-6. doi:10.1038/ncb0502-e113

303. Zhou X, Yang P-C. MicroRNA: a small molecule with a big biological impact. *MicroRNA (Shariqah, United Arab Emirates)*. 2012;1(1):1.

304. Bartel DP. MicroRNAs: genomics, biogenesis, mechanism, and function. *Cell*. 2004;116(2):281-297. doi:10.1016/s0092-8674(04)00045-5

305. Quadro L, Gamble M V, Vogel S, et al. Retinol and retinol-binding protein: gut integrity and circulating immunoglobulins. *J Infect Dis*. 2000;182 Suppl:S97-S102. doi:10.1086/315920

306. Quadro L, Blaner WS, Hamberger L, et al. The role of extrahepatic retinol binding protein in the mobilization of retinoid stores. 2004;45:1975-1982. doi:10.1194/jlr.M400137-JLR200

307. Napoli JL. Pharmacology & Therapeutics Cellular retinoid binding-proteins , CRBP , CRABP , FABP5 : Effects on retinoid metabolism , function and related diseases. *Pharmacol Ther*. 2017;173:19-33. doi:10.1016/j.pharmthera.2017.01.004

308. Wright K, Rooney N, Feeney M, et al. Differential expression of cannabinoid receptors in the human colon: Cannabinoids promote epithelial wound healing. *Gastroenterology*. 2005;129(2):437-453. doi:10.1016/j.gastro.2005.05.026

309. Lee Y, Jo J, Chung HY, Pothoulakis C, Im E. Endocannabinoids in the gastrointestinal tract. *Am J Physiol Gastrointest Liver Physiol*. 2016;311(4):G655-G666. doi:10.1152/ajpgi.00294.2015